EXTREMELY LOW FREQUENCY MAGNETIC FIELD SHIELDING IN LARGE OFFICE BUILDING

BY Kong Siu Kuen Sammy
September, 1999

A dissertation submitted to The Hong Kong Polytechnic University in accordance with the regulation for the Degree of Master of Philosophy

Abstract of thesis entitled
'Extremely Low Frequency Magnetic Field Shielding in Large Office Building'
submitted by Kong Siu Kuen Sammy
for the degree of Master of Philosophy
at The Hong Kong Polytechnic University in September 1999

ABSTRACT

Recently the extremely low frequency (ELF) magnetic field environment inside buildings has been the subject of greater attention. This is because of the concerns over actual or potential ELF magnetic field interference and possible associated health hazard.

In response to these concerns, this project has examined the mitigation of magnetic fields in office buildings, with the focus on the ELF magnetic shielding. Until now, there is no standards or other known methods given in literature for designing a shield in buildings. The objectives of the thesis are to characterize two major types of commercial shields, metallic trunking and planar sheets, and to develop semi-empirical formulas for design purposes through experiment measurements and numerical analysis. This thesis includes the discussions on these issues as well as on the electromagnetic environment in buildings, the associated EMI problems, ELF magnetic field shielding theory, and consideration of their application in buildings.

The study began with an investigation into the magnetic environment in office buildings. Various magnetic field sources and possible mitigation methods have been identified. It is found that shielding is considering as one of the most

efficient methods to mitigate any unwanted fields. In office buildings, two different types of shields can be employed: planar shield and rectangular shield (trunking). The planar shield refers to the use of flat metallic sheets. It can be used for shielding large sources, such as a transformer room, or for mitigation in an affected room. Metallic trunking can be used for shielding line sources, such as, heavy current-carrying cables or busbars (sometimes referred to the busduct).

A large amount of experimental works and computer simulations have been carried out to study shielding characteristics of both rectangular shields and planar shields. For the trunking type shield, a set of semi-empirical formulas for shielding effectiveness against shield size, thickness, and material were derived for different trunking types that are commonly used in buildings in Hong Kong. These formulas were obtained by using numerical simulation software and with verification using experimental data. They describe the shielding phenomenon in trunking and provide an easier way to estimate shielding effectiveness of the trunking.

The characteristics of the planar shields were also investigated in great detail through both numerical analysis and experimental measurements. Practical issues, such as the leakage at the seam position were also investigated.

In the past, the shielding performance of the applied shield can only be estimated roughly. However, with the semi-empirical formulas provided in this thesis, the prediction of the shielding effectiveness for trunking shield design is possible. It can overcome the burden in shielding design. On the other hand, the shielding characteristics of the finite planar shield that are related to the real practice were

addressed in the thesis. With these findings, the electrical engineers can design the shield more efficiently. The design procedure is simplified and the cost-effective shield design is feasible. The ELF magnetic fields inside a building can be effectively mitigated, and the compatible electromagnetic environment in the building can be ensured.

ACKNOWLEDGEMENT

I wish to express my most sincere gratitude to my supervisors Professor John Burnett and Dr. Yaping Du for their keen enthusiasm, constant guidance and help through the course of this work. Their suggestions, comments, and advice helped considerably in the development of the work presented here.

My thanks are also due to Mr. Fu Zhengcai and Mr. Zhou Jimin for their help in the experimental work. Last but not least, thank you for my parents and my girl friend, Jessica, for their endless supports.

TABLE OF CONTENT

CONTENT

LIST OF FIGURES

LIST OF TABLES

APPENDIX

NOMENCLATURE

μ, μ_r, μ_o	Permeability, Relative Permeability and Permeability of free space
σ, σ_r	Conductivity and Relative Conductivity
SE	Shielding Effectiveness
I	Current
δ	Skin Depth
λ	Wavelength
f	Frequency
$\boldsymbol{B}$	Magnetic Flux Density
W	Width of Rectangular Shield
h	Height of Rectangular Shield
L	Side Length of a Square Shield
r_s	Shield Radius
r_{eq}	Equivalent Radius
S_h	Size Coefficient
d	Separation of Conductor
t	Shield Thickness
m	Magnetic Dipole Moment
R	Distance from Source to Observation Point
l	length of current filament
$\boldsymbol{H}$	Magnetic Field Strength
$\boldsymbol{E}$	Electric Field Strength
R_{dB}	Reflection Loss
A_{dB}	Absorption Loss
B_{dB}	Multiple reflection correction term

CHAPTER 1 INTRODUCTION

In Hong Kong, as in many major cities, high rise, air-conditioned commercial buildings are important assets to economic activity. These kinds of buildings draw very large amounts of power and consume significant amounts of energy. To achieve the ever-increasing demand on power and energy, it is necessary to install large capacity electrical distribution systems and equipment. The increase of the scale and complexity of the system and equipment makes the electromagnetic environment in commercial buildings worse.

In recent years the electromagnetic environment inside buildings has received greater attention than previously. This attention is not only focused on the high frequency or radio frequency (RF) electromagnetic field, the magnetic field at extremely-low frequency (ELF) is also of concern. This is because of concerns over the possible health hazards associated with ELF magnetic fields [1-3], and the actual or potential ELF magnetic field interference with sensitive equipment, such as video display units (VDUs) [4-6].

The ELF electromagnetic field in buildings is associated with the delivery of the electricity. Therefore the electromagnetic fields alternates 50 times per second, which is in the ELF range (3-3000Hz). In the ELF range, the fields do not radiate, as they do for higher frequency fields like microwaves and radio waves. ELF electric and magnetic fields are not coupled or interrelated in the same way that they are at much higher frequencies. So it is more appropriate to refer to them as electric field and magnetic field rather than electromagnetic fields.

1.1 Associated Problems

ELF magnetic field interference can cause sensitive electronic equipment to malfunction or be permanently damaged. Recently, because of the magnetic emission is getting worse, there is an increasing trend of complaints about ELF interference in office buildings. Most of the problems reported are the instability on computer monitors. Several studies [7-9] show that such instability as jitter may appear in the monitor screen when the magnetic filed is as low as 10 mG. However, an ELF magnetic field over 20 mG is not uncommon in office areas. Such affected areas are generally located below or above the intermediate transformer floor, or near the electrical riser system, or large equipment. The ELF magnetic field may reach several hundreds milligauss as observed in some buildings. Some practical problems may be cited.

An extensive data processing system had been installed near a power distribution system that was not designed to minimize magnetic fields. Data tapes at one computer suite were stored at floor level and a main cable passing immediately below the floor caused data corruption of the tapes, resulting in lose of many hours of work [10]. Another example is where a major electronic company was close to completing the installation of very complex (and very expensive) microcircuit etching machines, but discovered that they would not work properly. The machines work to a very fine accuracy and a stray magnetic field was causing the etching beams to wobble. Unfortunately, nobody had realized the effect of the switch room for the building which was only 10m away from the affected equipment.

It was also reported that several computer monitors located in one part of an office floor suffered an image distortion, image waving and jittering on their screens. After

investigation, it was revealed that these monitors were subjected to ELF EMI. The external ELF magnetic field was generated from the intermediate transformer room on the floor below.

These examples illustrate that the poor installation planning or design and lack of awareness with regard to the ELF EMI in office buildings.

Another main concern about ELF magnetic field is the associated possible health hazards. The health hazards fear from the exposure to low-frequency electromagnetic fields have been under discussion since at least the end of the 1970s. Since then, numerous epidemiological and biological studies have been conducted worldwide [1-3]. The main apprehensions have concerned the risk of cancer, miscarriage, and so-called electrical hypersensitivity. However, the available evidence does not provide conclusive cause-and-effect relationship. The results presented by different research groups have sometimes been contradictory. Moreover, very little is known about the ways in which human beings are affected by ELF magnetic fields. Although none of the results of the research demonstrates a direct connection between health effects and extremely low frequency magnetic field, methods to reduce fields should be examined in the event that low frequency magnetic field does present a health hazard.

The interference issue caused by the ELF magnetic field inside a building is not usually considered in design, installation and maintenance of building electrical distribution systems. The lack of awareness leads to a not uncommon situation where the background level of magnetic fields in office area is higher than the susceptibility levels of sensitive business equipment. As the increasing demand for electricity in a

building is unavoidable, ELF EMI may be more serious in the future. Therefore, it is necessary to mitigate the ELF magnetic field to reduce the electromagnetic interference. As the objective of building services engineering is to provide a safe, comfortable and functional environment for occupants and equipment, the final goal is to achieve electromagnetic compatibility in office buildings.

1.2 Mitigation Techniques

There are some common ELF magnetic field mitigation techniques in practice. Obviously, the simplest measure is to increase the separation between the sources and the affected areas [11,36]. The magnetic field decays inversely with the square of the distance from the source for a single-phase circuit. Doubling the distance can leads to one fourth the field strength. In addition, portable electrical equipment that is found to cause interference can be moved away from the magnetic field producing equipment. However, relocating the affected equipment away from the source may not be always be practical to implement.

Another common method is rewiring the distribution system [11]. It includes the changing of phase configuration and reducing the spacing of the conductors. The ELF magnetic field is both a spatial vector and a temporal phasor. Therefore, the magnetic field produced by the distribution and the utilization circuits can be reduced by applying the optimal configuration of phase cables. For using three single core cables for three-phase configuration, the preferred arrangement of conductors is trefoil. A substantial reduction of the magnetic field due to a cancellation effect can be achieved by re-configuring a flat-array of four LV single core cables installed side by side, into trefoil arrangement with the neutral in the middle.

The spacing between the conductors is another important factor in determining the magnetic field generated by the conductors. The magnetic field generally decays linearly with reducing the spacing between the phase and neutral conductors. An example can be cited.

The tenant of a large building complained that computer monitors wavered unsteadily when running the Windows program [11]. It was suspected to be an interference problem. Two trial tests were performed. In the first trial, all lifts and power suppliers to the lift machine room were shut down. However, the problem still remained. The problem seemed to be solved in the second trial when the power for all the fluorescent luminaries on the premises were turned off. This shows that the interference source is related to the wiring system of the fluorescent luminaries. By closely examined the wiring system, the real problem was the large separation between the phase and neutral conductors. After the neutral conductors were routed in the same conduit as their phase conductors to reduce the conductors spacing, the magnetic field in the affected area was reduced significantly, and the wavering disappeared from the monitor's screens.

Generally, rewiring of the conductors is not easy to implement for an existing installation. Since this method mitigates the field by reducing the source magnetic field, the degree of mitigation may be limited. The magnetic environment may be still unsatisfactory after the mitigation work has been completed.

Magnetic shielding has been identified as one of the most effective mitigation measures. Unlike rewiring, it mitigates the magnetic field by altering the spatial distribution of the field. The designer can determine the desired degrees of mitigation

using different shield designs. Moreover, it is also applicable in an existing installation. It is the most effective of many available methods of mitigating ELF magnetic fields.

1.3 Magnetic Shielding in Practice

In fact, the major sources of this unwanted field are mainly the electrical distribution network and equipment. Transformers and the heavy current carrying conductors are the two main sources responsible for the ELF electromagnetic interference inside buildings. The single-core cable or busbars used for the transportation from the transformer in the intermediate floor can increase the magnitude of the ELF magnetic field in office areas right above or below, to hundreds times than of the other floors. Directed against the two major sources, two different types of shields can be employed in commercial buildings: planar shield and rectangular shield (trunking).

The planar shield refers to the metallic sheet. Several sheets are jointed to divide the shielded region from the sources. It is usually used for shielding larger sources such as, transformer rooms or the affected room. For example, for an affected room sited right besides a transformer room, a shield can be installed on the side facing the transformer. A shield on the ceiling or under floor can be also considered for the zone office area, if the transformer is located on an adjacent floor.

Rectangular metallic enclosure are frequently used to house cables or busbars in electrical installation systems. The main purpose is to provide mechanical protection However, the metal enclosure may also act as a shield for the enclosed conductors due to its metallic nature.

In the past, most of the research in electromagnetic shielding inside a building is related to the high frequency (above 100kHz) EMFs. There is relatively less research on the ELF magnetic field shielding. In 1930s, Levy [12] reported work on the ELF magnetic field shielding with infinite conductive plane sheets against circular coaxial cable. Following this, there were many studies on the ELF shielding problems on various kinds of sources, shapes of the shield, etc. A number of improvement works have been made over the years, such as the use of different materials, different magnetic field sources, and multiple layers. In all studies, the medium under consideration was homogeneous and linear. Kaden [13] and Du [14] presented approximate expressions for shielding effectiveness for spherical and cylindrical shields. Similar work has been carried out for infinite planar shields and closed-form expressions have been obtained [15]. These authors mainly used analytical methods, and the works were concentrated on the closed shield characteristics. That is the source region and the shielded region were completely divided by the shield. The goal of these studies was to calculate the penetration of fields through a homogeneous shield characterized by arbitrary scalar electrical constants.

However, this is not the case in real world. The planar shields may be in the form of open shield, such that the shield geometry does not completely separate the source and shielded region. For example, planar sheets must be finite in length. Furthermore, the material will not be homogeneous at the seam position. Actually, the field may leak through seams, holes or around the edges as well as penetrate it. Although closed form expressions for the shielding effectiveness of finite width planar shield have been developed by Olsen [15] and Du [16], the expressions are rather complex and difficult to apply in real situation. Moreover, the shield material

may not be linear. For example, galvanized iron (GI), a common shield material is a ferromagnetic material, shows a non-linearity with its permeability.

Complicated structures are generally evaluated by numerical calculation methods. For example, the vector potential can be solved by the finite-element method by using a finite element program, such as ACE [17]. The two-dimensional time-harmonic magnetic field in two-dimensional problems (for the model made up of different materials) can solved by the software OERSTED, which is based on the boundary element method [18].

Although the shield structure is similar to the cylindrical or the spherical shield, there is no analytic formula of shielding effectiveness for a rectangular shield (trunking). There has been little research about the shielding effect. The shielding performance of the trunking used in practice can only be estimated roughly. Therefore, it is necessary to study shielding prediction for shield design. Some design data may be needed to overcome the burden in shielding design. On the other hand, the shielding characteristics of the finite planar shield that are related to the real practice are not well known. It is necessary to characterize finite planar shielding. These findings can help to design cost-effective shields in buildings, and achieve better shielding performance.

1.4 Objectives

The aim of this project is to study the ELF magnetic field shielding in office building, the associated EMI problems and to achieve electromagnetic compatibility in office buildings. As the rectangular shield (trunking) have been identified as one of the major ELF shielding models, one of the objectives is to find out approximate equations to evaluate the shielding effectiveness of trunking with different size, material properties, etc. Moreover, the shielding characteristic and practical issues regarding design and installation are discussed, and the non-linear characteristic investigated through experiment. With these findings, engineers can know the shielding effectiveness of different trunking types used in practice. Then the engineer can select the most suitable trunking for shielding purposes.

The shielding equation for the cylindrical shield has already been derived [13]. To achieve the first objective, the shielding formula of the rectangular shield was approximated by the cylindrical shield equation times some specific coefficients, which are obtained through computer simulations. The model using in the simulation was validated by the laboratory experiment. With the aid of simulation results, a series of semi-empirical formulas of trunking can be obtained.

The second objective is the characterization of planar shield performance in real practice. Hence, the existing shield design can be improved. The characterization in real practice is different from the one derived in analytical. Also, the properties of the shield performance have not been understood entirely, and remain a large unexplored area. For example, the compensation of the seam, the leakages around the edge and the choice of material have different influence on the final shield result. With the

known characteristics in real practice, a planar shield can be designed to utilize its full potential, and achieve better shielding performance.

For the second objective, the characterization of the planar shield performance in real practice is mainly studied experimentally. And the simulation approach is used to identify the properties of the planar shield.

In the past, the shielding performance of the applied shield can only been estimated roughly. However, with the semi-empirical formulas provided in this thesis, the prediction of the shielding effectiveness for trunking shield design is possible. It can overcome the burden in shielding design. On the other hand, the shielding characteristics of the finite planar shield that are related to the real practice were addressed in the thesis. With these findings, the electrical engineers can design the shield more efficiently. The design procedure is simplified and the cost-effective shield design is feasible. The ELF magnetic fields inside building can be effectively mitigated.

There are totally eight chapters in this thesis. The second chapter discusses the magnetic environment in office building nowadays. It starts with the description of the typical features of the electrical installations in office buildings. Then, the sources of the ELF magnetic field inside the buildings associated to the electrical system are identified. The picture of the magnetic environment can be obtained through the discussion on the results of the magnetic field surveys in modern office buildings.

Different impacts of the ELF magnetic field are discussed in chapter three. The health issue and the exposure limits published by different authorities are also reviewed. Operation of sensitive electronic equipment, such as, video display units (VDUs) may be interfered by the external power frequency magnetic field. Magnetic flux density of 10mG will be enough to cause a detectable distortion for many of the computer monitors. There will be a deeper discussion about the ELF EMI in office buildings. The susceptibility of office appliance is discussed with the specific example being the VDUs.

Previously, magnetic shielding below 100 kHz is more difficult than for high frequency. It always requires very thick ferrous shields or high permeability materials to achieve. In chapter four, the shielding theory, especially in extremely low frequency is given full discussion. The low frequency magnetic field shielding mechanism is also introduced.

A rectangular shield has similar geometry structures to the square shield and cylindrical shield. Therefore, their shielding characteristic should be similar too. In chapter five, the shielding characteristic of the trunking used in practice is examined through theoretical analysis, numerical analysis and experiment measurements. Semi-empirical formulas have been derived to evaluate the shielding effectiveness of the metallic rectangular shield. With these formulas, the shielding effectiveness of the trunking in commercial can be estimated.

The shielding properties of a finite width planar shield in real practice are presented in chapter six. The shielding properties are discussed and verified by laboratory experiments and numerical calculation. The parameters associated with its design

include the source orientation, source to shield distance, leakage through the edges and the seam, and material.

The practical considerations about the two types of shields are addressed in chapter seven. It also discusses how it can be made compatible with real practice. Different design considerations are also discussed in this chapter.

CHAPTER 2 ELECTROMAGNETIC ENVIRONMENT IN BUILDINGS

In Hong Kong, buildings can be classified as industrial, commercial, domestic, composite and others. They may have different design types and different electrical devices may be installed. The majority of commercial buildings are the high-rise (it is defined as higher than 30m in Hong Kong) [19] office buildings. They are important assets to economy activity, but draw very large amounts of power and consume significant amounts of energy. The electrical installation in these buildings becomes increasingly complex, generally requires better quality than for industrial or domestic buildings. Since the sources of the ELF magnetic field are associated with the electrical distribution system, the electrical installation of office buildings is discussed first.

2.1 Electrical Installation

Electricity is generated at the power station which remote from the urban area. Since the power loads in commercial high-rise building are extremely high, power supply should be reliable. The electric supply companies usually feed the buildings by several 11kV underground cables from their distribution substation. These 11kV feeders then feed the building substation transformers. Distribution inside buildings is generally at low voltage (220V/380V, 50Hz). Transformers (typically 11/0.38kV, 1500kVA, three-phase core) are normally located at ground or basement level, but as the building height increases, they need to locate at intermediate and roof top level. Where buildings rise to fifty stories or more, the major loads centers of the building, like high-speed lift installations, are usually distributed at middle or high level of the buildings. Transformers are sometimes located at intermediate floors (between zoned office floors) to match the loads centers, to reduce energy loss and low-voltage drop.

Because of the limited space in the lift shafts used for the transportation of the transformer, single-phase units (typically 500kVA) may be used. Consequently, there are significant high current single-phase circuit connections between the transformers making up a three-phase unit. These transformers are connected to the main low-voltage (LV) switchboards in adjacent rooms via single core cables.

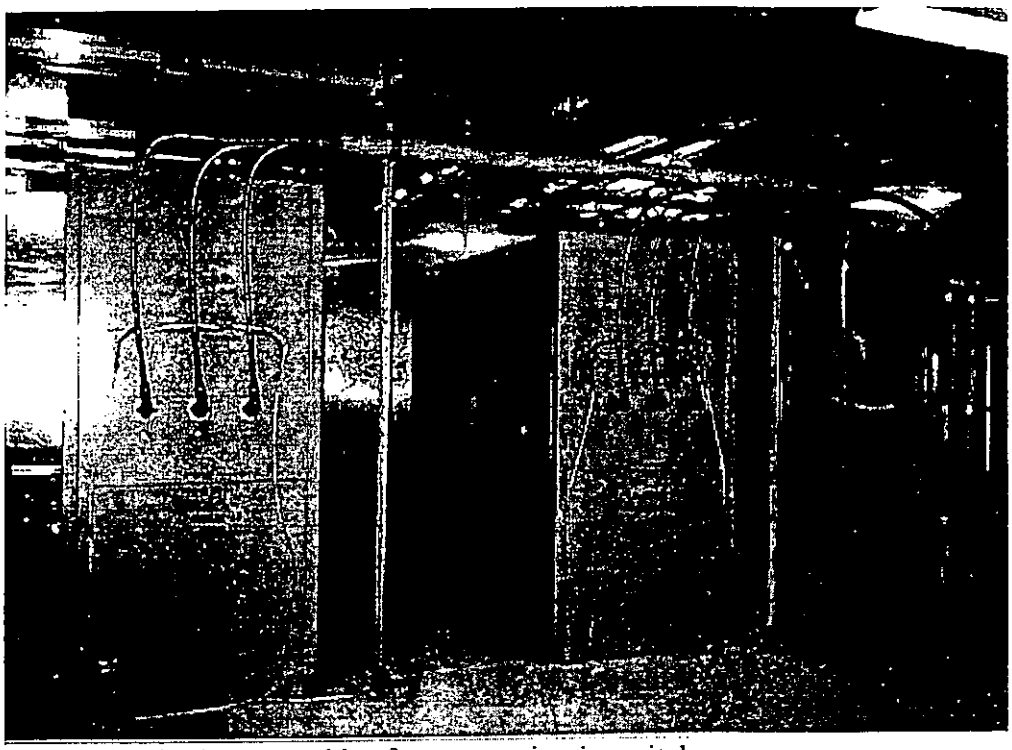

Figure 2.1 Single core-cables for connection in switch room

Risers are one of the main distribution elements. A building may contain numerous LV risers for air-conditioning, landlord services, tenant supplies, essential supplies, etc. Moreover, electrical supply to major loads such as the chiller plant and tenant loads is also by the heavy current risers. The usual method of main supply is to run conductors to the full height of the building and to provide convenient tapping-off points on each floor. A simplified electrical schematic diagram is shown in Fig.2.2. In practice, rising distribution is generally by power cables or busbars, and lengths over 100m was not uncommon in modern office buildings. Connections to individual loads, such as lighting equipment, socket outlets, fans, etc., is by smaller size wire. These wires are generally enclosed in the metallic or PVC trunking or conduit, and

installed in a false ceiling or under floor. Since the electrical distribution is over most of the area inside a commercial building, significant ELF magnetic field may be generated in vicinity if distribution conductors which carry heavy current.

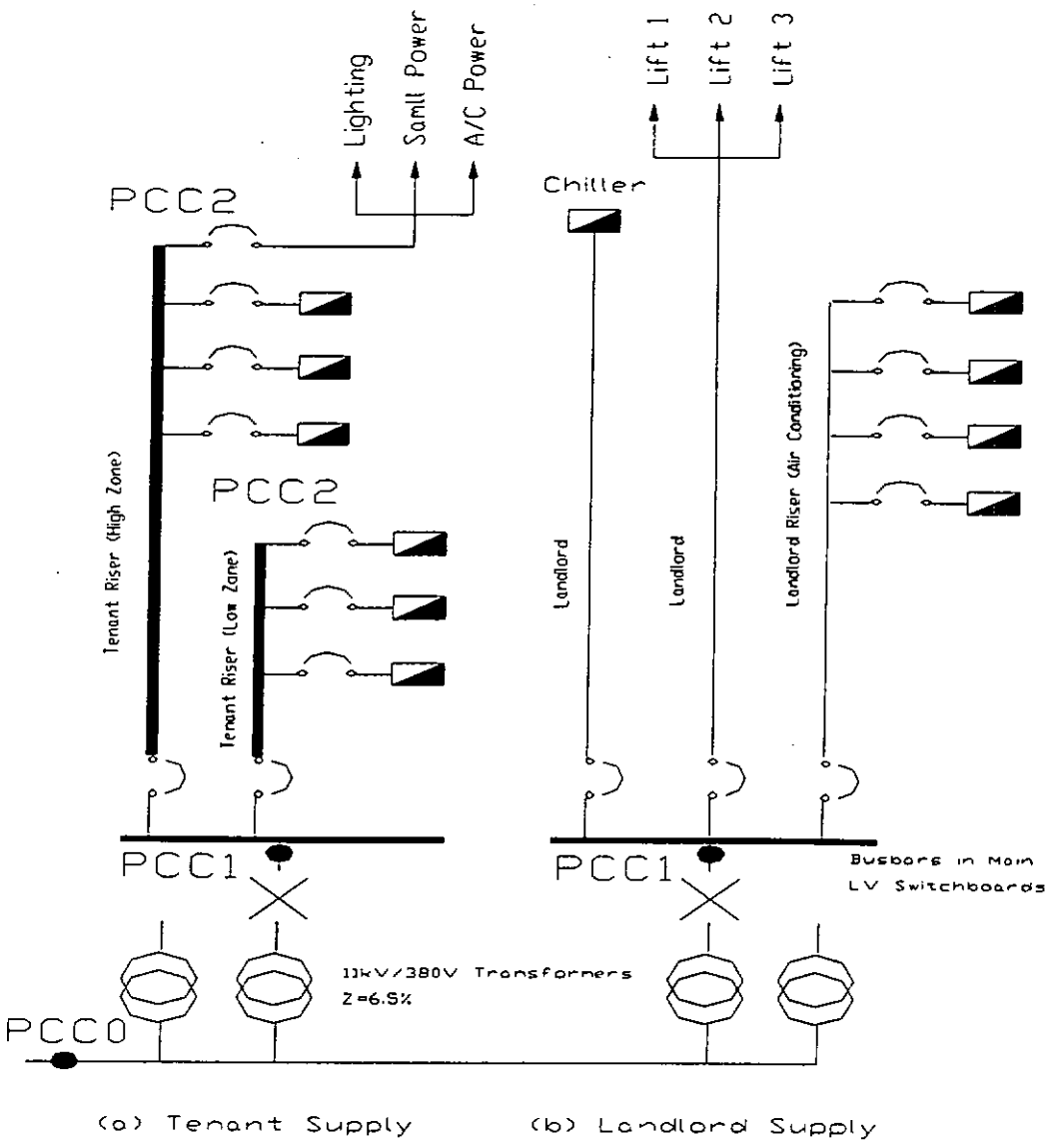

Fig.2.2 Simplified electrical schematic diagram

2.2 Sources of Magnetic Field

In commercial buildings, due to ever increasing electricity usage, substantial magnetic fields are generated in offices and other areas. Conductors and the

equipment carrying heavy current are identified as the major source in commercial buildings. The sources of magnetic field are as follows:

1. **Transformers** are installed in substations or transformer room, which are located on the ground floor or the floor in upper level of a building. Transformers usually have a metal enclosure. However, the connecting conductors may not be enclosed by the metal sheets, and will generate sufficient magnetic fields in the surrounding space. In general, transformers are connected to the main low-voltage (LV) switchboards in adjacent rooms via single-core cables. These heavy-current carrying cables will also create high level magnetic field in vicinity.

2. **HV and LV Switchboards** are usually located in substations or switch rooms. They also have a metal enclosure. Insides the switchboard, there are various type of switches, e.g. fused boxes, circuit breakers, push-button, etc. However, the copper busbars, the incoming and outgoing cables are identified as the major sources of the magnetic field, especially on the low voltage side. Large currents always flow on that side. Consequently, significant magnetic fields can be generated.

3. **Cables/ Busbars** comprise the main electrical distribution system in building. These distribution power lines are used to transmit power from transformer or switchboards to different load centers in the building. Since they carry heavy current, they are also identified as the major sources of magnetic field.

4. **End-user Equipment** such as motor-driven equipment (e.g., chiller, pumps, fan, AHU, etc.), lighting equipment, office appliances (computer monitors, printer, desk lamp, etc.) are another source of magnetic field. These equipment generate large localized magnetic fields as a point source, which decay to the ambient level meters away.

5. **Incidental Sources** such as metallic water or gas pipes, metallic air-condition ducts are another sources of magnetic fields. They may be intentionally used for earthing connections or may unintentionally carry a portion or substantial amount of neutral or earth currents. They provide multiple current paths through bolted or welded connections, or through metallic braces and bridging structures. As a result of these currents, magnetic fields may be produced. However, they are harder to locate and identify.

2.3 Modeling of Magnetic Field Sources

In general, the pattern of magnetic fields from these sources is rather complex. For estimation of the magnetic field generated by these equipment, the emission equipment can be modeled as point sources, while cables or busbars can be modeled as line sources since they are relatively long and run in parallel. In the following, the emissions from both point source and line source are discussed in detail.

2.3.1 Emission from the point source

A point source refers to a single or multiple loop of current that approximates a magnetic dipole [20]. (*A magnetic dipole is a current loop which dimension is small compared with the distance of the loop from the point of observation.*) The magnetic moment $\vec{m} = I\partial\bar{A}$ of the dipole is known as the magnetic dipole moment.

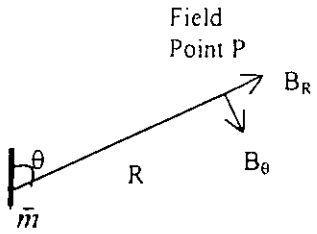

Fig. 2.3 Magnetic flux density due to a magnetic dipole

The magnetic flux density $\boldsymbol{B}$ due to a magnetic dipole at point P can be expressed as

$$\vec{B} = \frac{2\mu_o m\cos\theta}{4\pi R^3}\vec{R} + \frac{\mu_o m\sin\theta}{4\pi R^3}\vec{\theta} \qquad (2.1)$$

where R is the distance from the source to the observation point, A is the enclosed loop area of the magnetic dipole

According the equation (2.1), the magnetic fields diminish at a $1/R^3$ distance rate from the source. Among the magnetic sources in an office building, transformers, switchboard and end-user equipment can all be considered as a magnetic dipole. Since the decay rate is so rapid, these equipment always generate a large localized magnetic fields as a point source, which decay to ambient level meters away.

2.3.2 Emission from line sources

Emission from line sources can be calculated by the Biot-Savart's law. The Biot-Savart's law is an experiment law, it gives the magnetic field produced by a current distribution. In Fig. 2.4, the magnetic field flux density $\boldsymbol{B}$ at point P can be considered as the superposition of magnetic field produced by differential element *Idl*. Magnetic flux density due to the differential current element can be express as:

$$d\mathbf{B} = \frac{\mu_0}{4\pi}\frac{Id\boldsymbol{l}\times\boldsymbol{a}_R}{R^2} \qquad (2.2)$$

The total magnetic flux density is obtained by integrating (2.2) over the path of the current flow. It gives equation (2.3).

$$\boldsymbol{B} = \frac{\mu_0}{4\pi}\oint_l \frac{Idl \times \boldsymbol{a}_R}{R^2} \qquad (2.3)$$

where the units of B is tesla (T); l is a vector of the route of current filament; $\boldsymbol{a}_R$ is a unit vector from the integration point to the observation point; R is the distance from the integration point to the observation point.

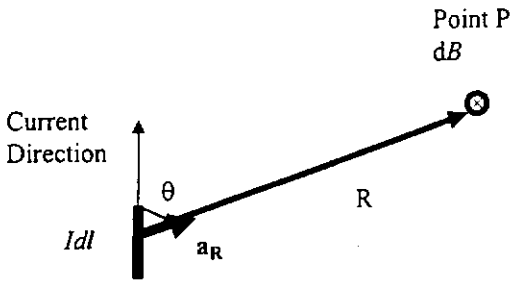

Fig 2.4 Magnetic flux density at P produced by current filament

Equation (2.2) and (2.3) are the mathematical forms of the Biot-Savart's law. In words, the Biot-Savart law states that due to a differential current *Idl*, the magnitude of the magnetic flux density at a point P is directly proportional to the product of the current I, the length of the current filament, *dl*, and the sine of the angle between the current element and the line joining the point P to the current element. But the flux density is inversely proportional to the square of the distance R between the point and the current element. The law further states that the direction of the magnetic flux density is normal to the plane containing ***dl*** and P, that is, into the paper. This normal is in the same direction as that of the cross product $Idl\mathbf{x}\boldsymbol{a}_R$, and the vectors ***dl***, $\mathbf{a}_R$ and ***dB*** form a right-handed coordinate system. [21].

The Biot-Savart's law can also be applied to the calculation of the magnetic field emissions for different combination of straight parallel conductors as follows:

2.3.2.1 Single conductor

By using the Biot-Savart's law, the magnetic field of a infinity long single conductor can be expressed as

$$B = \frac{\mu_0 I}{2\pi R} \qquad (2.4)$$

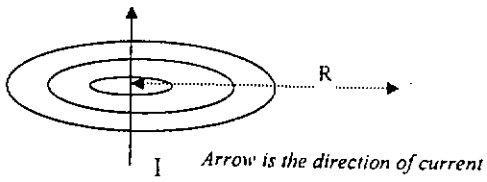

Fig. 2.5 Single conductor

2.3.2.2 Single-phase circuit

A single-phase circuit can be represented by an opposing current pair of dual conductors separating a small distance *d*. By using the superposition theorem, the magnetic field can be derived as follows:

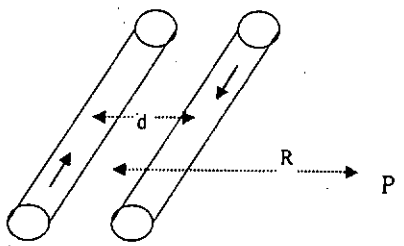

Fig.2.6 Two parallel conductors

At point P,

$$B = B_1 + B_2 = \frac{\mu_0 I}{2\pi(R - d/2)} - \frac{\mu_0 I}{2\pi(R + d/2)} = \frac{\mu_0 dI}{2\pi r^2 (1 - d^2/4R^2)}$$

In general, $R>>d$, we have $(1-d^2/4R^2)\approx 1$, so

$$B=\frac{\mu_0 dI}{2\pi R^2} \qquad (2.5)$$

2.3.2.3 Three-phase circuit

In Hong Kong, electric power is generated and distributed through three-phase AC transmission. In modeling, three-phase circuit can be represented by three conductors with a flat arrangement or with a trefoil arrangement, as illustrated in Fig 2.7 and 2.8. If each of the three-balanced phase voltages and currents are ideally 120 degrees apart, the magnetic field of the three-phase circuit with flat arrangement can be expressed as

$$B=\frac{\sqrt{3}\mu_0 Id}{2\pi R^2} \qquad (2.6)$$

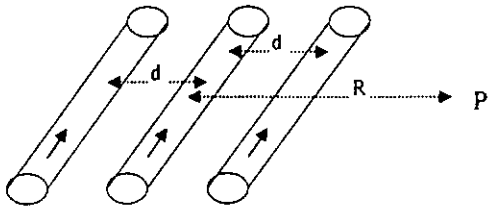

Fig.2.7 Conductors with flat arrangement

a) If the arrangement is in the trefoil form, the magnetic flux of the three-phase circuit is given by

$$B=\frac{\sqrt{6}\mu_0 Id}{4\pi R^2} \qquad (2.7)$$

where d is the spacing between conductors.

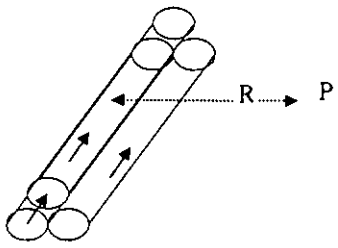

Fig.2.8 Conductors with trefoil arrangement

There is one requirement for all these equation is that the distance R to the observation point must be much greater than the conductor spacing d, i.e. $R >> d$. This requirement is always satisfied in practice.

From the equations above, we can observed that the magnetic flux density for a line source increase in proportion to the magnitude of the current, the conductor spacing, and decrease in proportion to the square of the distance from the conductor. By taking advantages on these features, certain degree of reduction of magnetic field generated can be obtained.

Among all the sources, transformers and the heavy current carrying conductors are mainly responsible for the ELF electromagnetic interference inside building. The magnetic surveys in the following will demonstrate the effect of these two major sources in real situation.

2.4 ELF Magnetic Field Survey

As discussed above, the ELF magnetic fields in offices have contributions from the current carrying conductors for distribution and from the office appliances. Obviously, the magnetic field from the former one will be predominate if the office area is near the electrical room or the distribution equipment. A numbers of site survey have been conducted to investigate the actual ELF magnetic field in large office buildings. Inside most of the office area, ELF magnetic field generally was lower than 1mG and a few mG near the office appliances (computer monitors printer, desk lamp, etc.) Throughout the office, fluorescent lights are perhaps the biggest contributors to the field among all the office appliances: the ceiling lights measured 5mG at about 2.5m from the floor, 1.5mG at 2m and 0.7mG at 1.8m

However, office appliances only generate large localized magnetic fields as a point source, which decay to the ambient level a few feet away. On the other hand, in the areas near the distribution conductors installed in the false ceiling or under floor, the ELF field may reached several hundreds mG at the ground and fell to 40-50 mG at the desk level.

Magnetic field site survey has also been performed on both lower and upper floors of the transformer room located in the intermediate level of a building. The findings from the site survey show that the most area right below the transformer room is exposed to a high magnetic field level (over 20mG), and a quite large amount of space is exposed to a magnetic field of over 100mG. On the upper floor, the distribution of magnetic field shows a similar pattern. Hence the transformer and the associated single-core cable is one of the major contributor of the high magnetic field.

In the transformer room, the magnitude of the magnetic field is much higher. It reaches several thousands mG near the transformer. Moreover, a single-phase transformer has a much higher values than the three-phase one. Along the single core cable connected to the adjacent switch room, comparable values can be obtained. At the switch room, the magnetic field is not as high as in the transformer room. It is usually at the range of several hundreds mG.

CHAPTER 3 IMPACT OF ELF MAGNETIC FIELDS

3.1 Health Issue

Health hazards feared from exposure to low-frequency electromagnetic fields have been under discussion since at least the end of the 1970s. The main apprehensions have concerned the risk of cancer, miscarriage, and so-called electrical hypersensitivity. The first study was carried in 1979, Wertheimer, N. and Leeper, E. [1] reported the results of an epidemiological studies on child deaths from cancer in Denver, Colorado. The results showed that child have a higher chance (2-3 times) of developing leukemia, lymphoma, or tumors of the nervous system if they lived near high-current wiring and its associated electromagnetic field.

Afterwards, numerous epidemiological and biological studies have, or being, conducted worldwide. However, the available evidences do not provide any conclusive cause-and-effect relationship. The results presented by different research groups have sometimes been contradictory. Moreover, we still know very little about the ways in which human beings are affected by the magnetic fields.

Although none of the results of the research demonstrate a direct connection between health effects and ELF magnetic field, we should research methods to reduce fields in the event any studies show that low frequency magnetic field present a health hazard.

In Sweden, the following precautionary principles are recommended by national authorities [22]: if measures generally reducing exposure can be taken at reasonable

expense and with reasonable consequence in all the aspects, an effort should be made to reduce fields radically deviating from what could be deemed normal in the environment concerned. Where new electrical installations and buildings are concerned, efforts should be made already at the planning stage to design and position them in such a way that exposure is limited.

In term of a health risk assessment, it is difficult to correlate precisely the internal tissue current densities with the external magnetic flux density. The statements given in table 3.1 can be made for magnetic flux densities of sinusoidal homogeneous fields that produce biological effects from whole-body exposure [23]:

Magnetic Field Strength	**Biological Effect**
Above 5 and up to 50G at 50/60 Hz	Minor biological effects have been reported
Above 50 and up to 500G at 50/60 Hz	There are well-established effects, including visual and nervous system effects
Above 500 and up to 5000G at 50/60 Hz	Stimulation of excitable tissue is observed and there are possible health hazards
Greater than 5000G at 50/60 Hz	Extra systoles and ventricular fibrillation can occur (acute health hazards)

Table 3.1 Biological Effect from whole body exposure to magnetic field

3.2 Exposure Limits

The International Non-ionizing radiation Committee of the International Radiation Protection Association (IRPA/INIRC) is a working group on non-ionizing radiation which examined the problems arising in the field of protection against the different types of non-ionizing radiation. The IRPA/INIRC, in cooperation with the World health Organization (WHO), has undertaken responsibility for the development of health criteria documents on non-ionizing radiation. Here are the interim standards they have issued against the ELF fields [24].

Occupational

Magnetic field: Continuous occupational exposure for the whole working day should be limited to magnetic flux densities not greater than 5 G. Short-term occupational for up to two hours per workday should not exceed a magnetic flux density of 50G. When restricted to the limbs, exposures limited to 250 G can be permitted.

General public

Members of the general public should not be exposed on a continuous basis to unperturbed rms magnetic flux densities exceeding 1G. This restriction applies to areas in which members of the general public might reasonably be expected to spend a substantial part of the day.

Exposures to magnetic flux densities between 1G and 10 G (rms) should be limited to a few hours per day. When necessary, exposures to magnetic flux densities in excess of 1 G should be limited to a few minutes per day.

A summary of the limits recommended for occupational and general public exposures to 50/60Hz magnetic field is given in Table 3.2

Guidelines for EMF Exposure		
International Commission on Non-Ionizing Radiation Protection		
Exposure--50/60 Hz	Electric field	Magnetic field
Occupational		
Whole working day Short-term* Limbs	10 kV/m 30 kV/m -	5 G (5,000 mG) 50 G (50,000 mG) 250 G (250,000 mG)
General Public		
Up to 24 hours per day	5 kV/m	1 G (1,000 mG)
Few hours per day	10 kV/m	10 G (10,000 mG)
* Whole-body exposure to magnetic fields up to 2 hours per day should not exceed 50G.		

Table 3.2 Guidelines for EMF exposure published by IRPA/WHO

Some countries have already adopted national electric and magnetic field exposure standards for ELF fields. Australia adopted the interim standards wholesale, and the Germany is drafting standards derived from the IRPA limits. The Russia and the United Kingdom derived national magnetic field limits from World Health organization guidelines.

The American Conference of Governmental Industrial hygienists (ACGIH) [25] has also developed voluntary occupational exposure guidelines for EMF exposure as shown in Table 3.3.

Other authorities have also developed magnetic field exposure limits. These data are often referred in evaluation of electromagnetic environments. The table 3.4 summarizes the limits of exposure to power frequency field recommended by several organizations in Europe.

Guidelines for EMF Exposure		
Threshold Limit Values for EMF Exposure American Conference of Governmental Industrial Hygienists		
Exposure--60 Hz	Electric field	Magnetic field
Occupational		
Occupational Levels should not exceed	25 kV/m* (from 0 to 100 Hz	10 G (10,000 mG)
Workers with cardiac pacemakers	1 kV/m or below	1 G (1,000 mG)

Table 3.3 Guidelines for EMF exposure published by ACGIH

Agency	Magnetic field
The National Radiological Protection Board (NRPB) (United Kingdom) [26]	16G
Verband Deutscher Elektrotechniker (VDE) (Germany) [27]	13.6G
European Prestandard, ENV 50166-1:1995 [28]	16G

Table 3.4 Exposure limits developed by other authorities

According to the section 2.4, the exposure limits is much larger than the level of magnetic field inside office. However, the level of magnetic field in the transformer room could reach a few thousand milligauss and comparable to the limits set in some standards. Workers in transformer room should pay attention to it. In the following, the ELF magnetic interference is discussed.

3.3 Electromagnetic Interference

Electromagnetic interference (EMI) is an electrical disturbance that may cause electronic equipment to malfunction, or be permanently damaged. Since the main power distribution systems are the main sources of the ELF magnetic fields. It may

cause ELF EMI if installed without considering their possible affect on sensitive equipment.

Currently there is no national or international provision for the ELF magnetic environment in office buildings regarding the interference. A value of 10mG is recommended by a local utility [29]. According to the IEC 1000-4-8[30], the levels of testing immunity of equipment used in six different environments are recommended. Two levels, 12.56mG and 37.6mG are applicable in buildings. In a derived standard [31], 12.56mG and 37.6mG are recommended as a generic immunity standard for residential, commercial and light industry. This standard is also applied in European EMC Directive (89/336/EEC). To achieve EMC in office buildings, the background level should not be higher than this corresponding immunity level of equipment. The minimal level (12.56mG) can be adopted as the maximum limit in ELF magnetic field level in office buildings.

A good design of electronic equipment should also have susceptibility larger than that value. However, manufacturers were not compulsory to pass the immunity tes specified in these standards. It is likely that some equipment will be susceptible t field below 12.56mG. In practice, most of the ELF EMI cases reported are related t the video displays units (VDUs). The computer monitor is the most easily affecte equipment by the power frequency magnetic field inside an office. Video displa units with cathode ray tube display systems may be affected by power frequenc magnetic fields in the form of image distortion. Recent studies [4-6] show th magnetic field 10mG could cause noticeable distortion in the screen of VDUs.

3.3.1 Physical Principle of CRT operation

VDUs display text and graphics by the action of a CRT, which projects an electron beam onto the phosphorous layer of the screen and a visible light emits in turn. If this electron beam is constantly shifted in horizontal and vertical direction then a visual pattern can be constructed on the screen. The picture that is seen on a screen is constructed from a large number of horizontal lines. Each such line is created by an electron beam, which is rapidly moving from one end of the screen to the other. When one line is completed the beam moves to the beginning of the line below. When the beam completes the last line of the screen, it moves back to the beginning of the top line. In modern CRT based computer screens, this process repeats itself 60 to 120 times per second (60 to 120 Hz). This cycling referred to as the refresh rate or vertical refresh rate. Since the beam must move back and forth horizontally right across the screen, tracing the screen from top to bottom, the horizontal frequency is very high (over 30kHz) while the vertical refresh rate is low.

During the movement the intensity of the beam is modulated by a video signal which is ultimately responsible for the visual images being displayed on the screen. The movement of the electron beam across the screen is the result of the interaction between the flow of the electrons in the beam and the magnetic field which is produced by two sets of parallel coils. This system of coils is known as the deflection system and responsible for either horizontal or vertical movement of the beam. The external power frequency magnetic fields may create additional deflection of the electron beam which results in image distortion, jittering or flickering. Jitter is defined as a disturbing motion of the total image or parts thereof. Flicker is a perceptible, temporal modulation of the luminance. Since most of the reported cases

are related to the EMI on VDUs, laboratory measurement on susceptibility of the VDUs has been conducted. The outcomes are discussed in the following section.

3.3.2 Laboratory Measurement on Susceptibility of VDUs

If the VDU is exposed to a high strength magnetic field, the electron beam emerging from the cathode will be deflected by the external field as well as the deflection circuitry. In order to investigate the susceptibility of different VDUs in commercial, a magnetic field immunity test rig has been built. The test rig is conformed to the IEC 1000-4-8, it consists of a field-generating induction coil, a pair of loop holding fixtures made by wood, a variable transformer and a step down transformer. The induction coil is designed such that it can generate magnetic field in three orthogonal orientations to the equipment under test (parallel to the screen oriented vertically, horizontal field parallel to the screen, and normal to the screen). During the test, the equipment under test is placed in the center of the induction coil. In each trial, the current is increased slowly until a noticeable jitter is seen, giving the upward threshold. Then the current is increased further until the jitter becomes intolerable to work with the screen, and the field strength at this point is called the intolerable threshold. Finally the current is slowly decreased until jitter disappears, giving the downward threshold. It should be noted that the test is subjective. For consistency, all the jitter evaluations were carried out by the same operator. Here are the summaries of the results:

Figure 3.1 The induction coil

A total of 36 samples of 9 different models of VDUs from 5 different manufacturers were tested. Table 3.5 shows basic information for each model. Tests were conducted with both text (70Hz) and 640x480x256 colour (75Hz) modes. The averaged values for each model are illustrated in Fig. 3.2. It is observed that the sample-to-sample variation for the same model is small, and less than 10% in most cases. Moreover, the susceptibility difference of models is slight. Among the models, Models D and H are outstanding (where the upper threshold is concerned) when the field is normal to the screen. It is not at all surprising that Models D and H are particularly good because they are the latest models collected for testing. Model I is the only sample with a 17-inch screen. Whilst it compares favorably with other models when the field is normal to the screen, it is particularly susceptible for the other two orientations. The larger the screen size is, the higher the susceptibility is.

Model	Screen size	Year of manufacture	No. of samples
A	14	1996	5
B	14	1994	8
C	14	1993	3
D	15	1997	7
E	14	1992	3
F	14	1995	3
G	14	1995	3
H	15	1998	3
I	17	1997	1

Table 3.5 Information on VDUs under Test

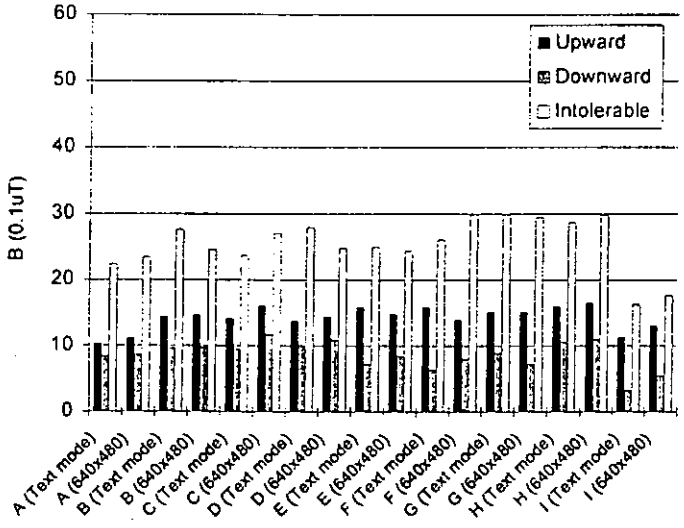

(a) vertical field parallel with the screen

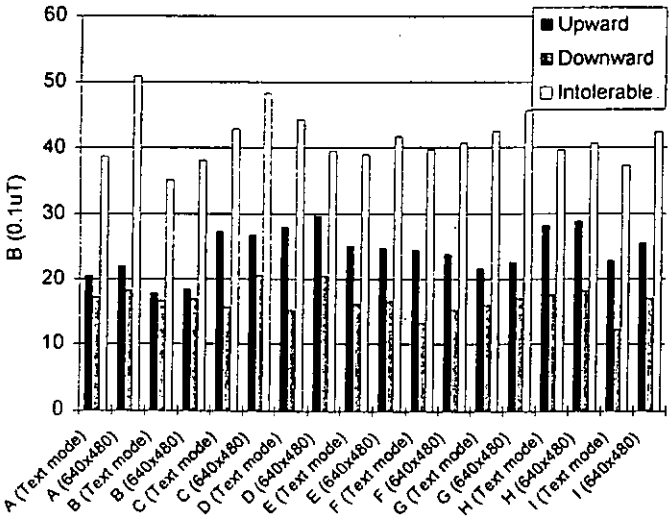

(b) normal to the screen

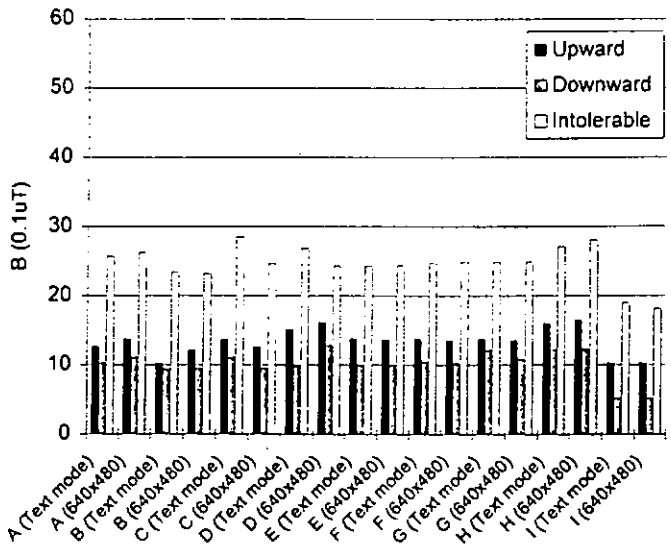

(C) Horizontal field parallel with the screen

Figure 3.2 Susceptibility Level against VDU Samples

The susceptibility level of the VDU is the lowest (i.e. the most susceptible) when the when the field is parallel to the screen and oriented vertically, followed closely by horizontal field parallel to the screen, and becomes higher when the field is normal to the screen.

In most severe cases (vertical field and horizontal field parallel with the screen), all models have an upward threshold above 10mG. Under typical settings, most of the VDUs have an upward threshold above 12.56mG, average on 15mG the immunity level stated in IEC 1000-4-8. In fact, the VDUs nowadays usually have a shielding enclosure made by magnetic materials. For further increase the immunity, an active compensation method can be applied. Two pairs of Helmholtz's coils are attached to the top, bottom and two sides of the monitor such that in most parts they followed the perimeter of the side they are attached to. By properly adjusting the magnitude and the phase angle of currents in each pair it is possible to produce a compensating field which will cancel or significantly reduce the effect of the interfering field on the VDU.

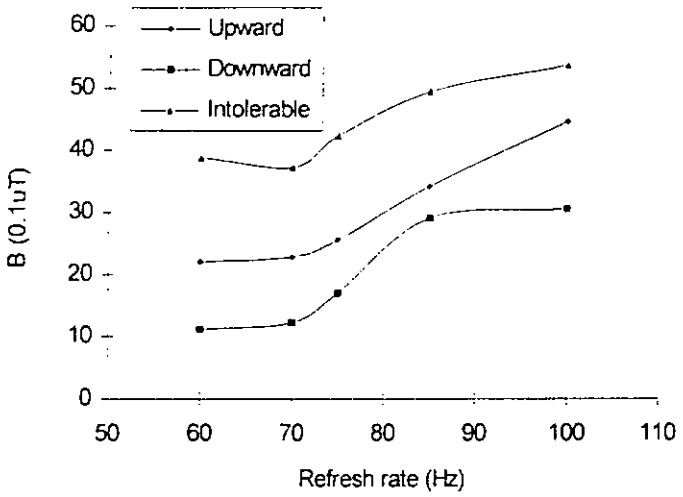

Figure 3.3 Susceptibility Levels against the refresh Rate (field normal to the screen)

The refresh rate of the VDUs also has a large influence on the susceptibility of the VDUs to the ELF magnetic field. Five refresh rates of the VDUs have been examined: 60Hz, 70Hz, 75Hz, 85Hz, 100Hz. The result is shown in figure 3.3. The susceptibility level of the VDU is the lowest (i.e. the most susceptible) highest when the refresh rate is 60Hz. In fact, the jitter frequency is equal to the difference between the frequencies of the refresh rate and the external magnetic field (50Hz). Therefore, the screen move at a frequency 10Hz when the refresh rate is 60Hz. Since this frequency is below the flicker perception point of human eyes, and hence very noticeable. The susceptibility level is substantially higher at a refresh rate of 85Hz, because the refresh rate is far above the power frequency. Moreover, at refresh rate 85Hz or higher, the jitter frequency is at a higher frequency, rendering it as blurring of characters rather than jitter.

3.4 Other Potential Susceptible Equipment

Medical equipment such as cardiac pacemaker is another susceptible device to electromagnetic interference [32,33]. When the pacemaker patient come closer to a

source emitting magnetic field, induced currents have to be expected in the pacemaker system. The pacemaker may not be able to distinguish such induced signals from the cardiac sensing signals (in the mV-range), especially for the power frequency (50 Hz) magnetic field have pulse rates close to the natural heart beat system (50 - 150 pulses per minutes). The pacemaker will revert to asynchronous mode and cannot switch back to the demand mode.

The probability that a malfunction will occur in the presence of an external magnetic field is strongly dependent on the pacemaker model, the value of the programmed sensing voltage, and the area of the pacemaker loop which is determined during implantation. Assuming sensitivities of 0.5 to 2mV for 50/60 Hz and worst case (600 cm^2 for the area of the pace maker electrode, homogeneous field perpendicular to this area), interference magnetic flux densities of 150mG to 600mG may be calculated [23]. Increased sophistication of pacemakers has made the question of possible electromagnetic interference more difficult.

Hearing aid rumble, magnetic recording medium like recorded tape, magnetic disc or magnetic card can also be encountered when immersing in the high magnetic field levels.

To create a safe, comfortable and functional environment for occupants and equipment, the mitigation of the ELF magnetic field is a must. The next chapter is a brief description of ELF magnetic field shielding.

Chapter 4 Magnetic Shielding Theory

Several mitigation techniques have been introduced in chapter one. They include changing of phase configuration, reducing the spacing of the conductors and increase the separation between the sources and the affected areas. Generally, the rewiring of the conductors is not easy to implement for existing installation. These methods mitigate the magnetic field through reducing the source magnetic field generated, the degrees of mitigation has a certain limit. The magnetic environment may be still unsatisfactory after the mitigation work has been applied.

Shielding has been identified as one of the another mitigation measures. Unlike rewiring, it mitigates the magnetic field through altering the spatial distribution of the magnetic field. Different degrees of mitigation can be achieved with different designs. The designer can determine the desired degrees of mitigation with applying different shield designs. Moreover, it is applicable in existing installations.

In all cases, shielding usually refers to a metallic enclosure that either partially or completely divides the region into shielding region and source region. The purpose of shielding is to prevent the devices in the shielding region from radiating electromagnetic noise outside the boundaries, or to prevent electromagnetic emission external to the shielding region from causing interference. Therefore, a shield is a barrier to the transmission of the magnetic field and can control the propagation of the field from one region to the other. The shielding mechanism is discussed in the following section.

4.1 High Frequency Shielding Mechanism

For a high frequency electromagnetic field, if the field vectors E and H at each point in space lie in a plane and exhibit no phase and amplitude variation, it is called a uniform plane wave. In this case, electric fields and magnetic fields are coupled or interrelated each other. Moreover, both fields are in time phase, although they are in directional quadrature.

When uniform plane waves which is emitted from a point source enters a shield, attenuation will occur. This process is known as electromagnetic shielding. The shield results are from three mechanisms as shown in figure 4.1: [34]

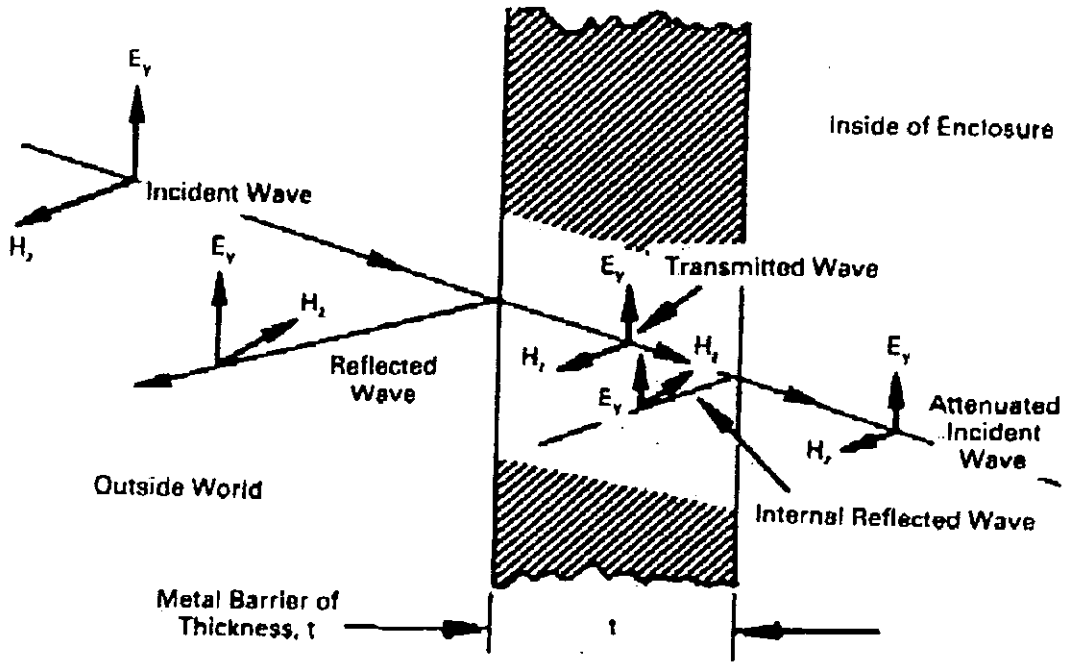

Figure 4.1 Interaction of a Shield with an Electromagnetic Field

1. Reflection Loss (R_{dB})

   Incident energy is reflected by the surface of the shield because of the impedance discontinuity of the air-metal boundary. This mechanism does not require a particular material thickness, but simply an impedance discontinuity.

2. Absorption Loss (A_{dB})

   Energy that does cross the shield surface (i.e., not reflected) is attenuated in passing through the shield.

3. Multiple reflection correction term (B_{dB})

   The energy that reaches the opposite face of the shield encounters another air-metal boundary and thus some of it is reflected back into the shield.

The degree of attenuation of a shield can be represented by its shielding factor. Here, it is defined as the ratio of magnitude by which the shield reduces the field strength as the result of its being in place.

Shielding factor is measured in decibels (dB) and is calculated as:

Shielding factor (in dB) $= 20 \log_{10}(H_o/H_1)$

Where H_o *- magnetic field strength without the shield*

H_1 *- magnetic field strength with the shield*

Thus, the shielding factor is

$$SF_{dB} = R_{dB} + A_{dB} + B_{dB} \qquad (4.1)$$

The correction term is significant only if A_{dB} is small than 15 dB, otherwise, it can be neglected.

In the case of a point source (a current loop) with an infinite shield, the absorption loss, A_{dB} and the reflection loss of a shield R_{dB} are calculated using the following equation [35,36]:

$$A_{dB} = 131.4t\sqrt{f\sigma_r\mu_r} \qquad (4.2)$$

$$R_{dB} = 14.57 + 10\log(fR^2\frac{\sigma_r}{\mu_r}) \qquad (4.3)$$

$$B_{dB} = 20\log(1 - e^{-2t\sqrt{\pi f\mu\sigma}}e^{-j2t\sqrt{\pi f\mu\sigma}}) \qquad (4.4)$$

where t- thickness of the material in m

f- frequency of the magnetic field

μ_r-relative permeability of the shielding material to free space

σ_r- relative conductivity of the shielding material to copper

R- source to shield distance in m

With these equations, the effectiveness of a shield against a plane wave from a poin source can be calculated. Table 4.1 shows that the absorption loss and the reflectio loss of 1mm thick aluminum and steel plate located at 1m distance from magneti field source with different frequencies.

	Aluminum (σ_r =0.61,μ_r=1)		Steel (σ_r =0.17 /μ_r=300)	
	A(dB)	*R(dB)*	*A(dB)*	*R(dB)*
50 Hz	1.08852	29.413	6.63689	-0.90702
5k Hz	7.258459	49.413	66.3689	19.09298
5M Hz	229.5326	79.413	2098.769	49.09298

Table 4.1 The absorption loss and the reflection loss of a 1mm shield with differer frequencies

It can be observed that a better shielding performance is achieved for higher frequency EMFs. The frequency term in both equations will dominate and shielding against the high frequency EMFs is easier to achieve. As shown in table 4.1, the absorption loss for a steel plane has a large variation for various frequencies. For 5MHz, the absorption loss near 2050 dB, while it remains only 6 dB at 50Hz. It is due to the skin depth δ of the shield materials is negligible compare to the shield thickness at high frequency. Therefore, a large attenuation can be easily achieved by the absorption loss. Table 4.2 shows the skin depth δ (in mm) of some common shielding materials under different frequency. Skin depth is given by

$$\delta = \sqrt{\frac{1}{2\pi f \mu_0 \mu_r \sigma}} \qquad (4.5)$$

Material	*Aluminum*	*Copper*	*Mumetal*	*Iron*
50 Hz	11.75	9.33	0.38	1.05
5k Hz	1.75	0.93	0.038	0.105
5M Hz	0.037	0.029	0.001	0.003

Table 4.2 Skin depth δ (in mm) of some common shielding materials

Although the shielding of high frequency EMFs is easily achievable, it is not the same case for the ELF field. It is because the skin depth increases as the frequency decreases, as indicated in equation (4.5). In real practice, the thickness of the shield is in the range of a few millimeters. It is comparable to the skin depth at the ELF for shield materials. Therefore the absorption loss becomes less. For high conductivity materials, the reflection loss is the dominant factor at low frequency. Therefore, the decrease in the skin depth ratio will not have a great influence. Hence high

conductivity materials have a comparable shielding performance with the magnetic material in ELF.

However, these equations are difficult to apply on real situation. It is only valid for uniform plane wave emitted from a point source to the shielding plate which is infinity long and wide. In real practice, there are different kinds of sources likes line source, long and parallel conductors. Moreover, the shields must be finite in reality. Furthermore, the electromagnetic fields in low frequency do not perform as uniform plane wave.

For the power frequency (50Hz) electromagnetic field, the near field region is about 955 km. Since the shielding always installed in the near field region of the ELF electromagnetic field, the ELF electromagnetic field can be seen as a quasi-static field in the near-field region. Hence, the electric field and magnetic field can be considered independently each other. In this case, the ELF magnetic fields do not perform likes a uniform plane wave, its amplitude decrease away from the source.

4.2 Low-frequency Shielding Mechanism

Electromagnetic shielding in low frequency can be seen as two independent events: magnetic field shielding and electric field shielding. One strategy for shielding ELF magnetic fields is to make use of the properties of materials as a means for altering the spatial distribution of the magnetic field.

There are two basic mechanisms for ELF magnetic field shielding : "Flux shunting" and "Eddy current cancellation" shielding mechanism. The first one is achieved by diverging the magnetic flux through a ferromagnetic (high permeability) material,

while the later one has a cancellation effect though an opposing induced flux within the conductive shield as shown in figure 4.2.

In the past, magnetic material has been the first choice for the high frequency shielding due to its small skin depth, hence a larger attenuation through the absorption loss. High conductive materials are seldom considered.

In ELF field magnetic shielding, both permeability (ferromagnetic) materials and conductivity materials can be effectively used. Different materials exhibit different degrees of shielding effectiveness, depending on their electrical and magnetic properties and have different costs associated with their purchase and installation. Tables 4.3 shows that the electrical properties of some shielding materials.

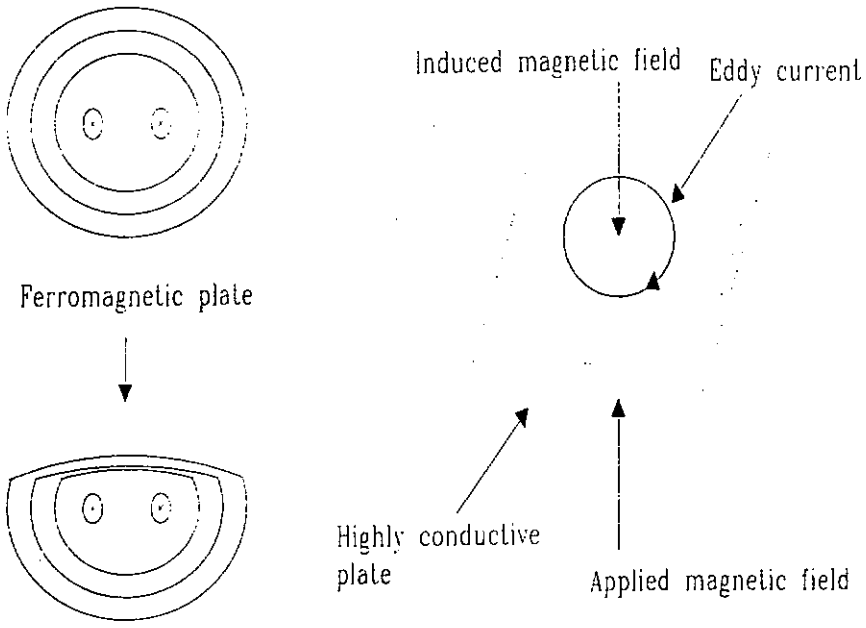

Fig. 4.2 Flux shunting mechanism and eddy current cancellation mechanism

Material	Relative Conductivity (to copper) σ_r	Relative Permeability (to free space)μ_r	$\sigma_r\mu_r$	σ_r/μ
Silver	1.05	1	1.05	1.05
Copper	1	1	1	1
Gold	0.7	1	0.7	0.7
Aluminium	0.61	1	0.61	0.61
Stainless Steel	0.02	500	10	0.00
Mumetal	0.03	20000	600	1.5 ›
Supermalloy	0.03	100000	3000	3 x1

Table 4.3 Electrical and magnetic properties of some shielding materials

4.2.1 Permeability Material

When a material with magnetic permeability is expose to the magnetic field, the boundary conditions of the magnetic field and magnetic flux density at the surface of the material are given by [37,38]:

i. Ampere's circuital law requires that the tangential component of magnetic field H must be continuos across the interface.
ii. Gauss's law of magnetism requires that the normal component of magnetic flux density B must be continuous across the interface.

Since $B = \mu H$ within the material and $B = \mu_0 H$ in the air, the field and flux density must abruptly change direction in crossing the interface in order to simultaneously satisfy both conditions. At the interface, the field and flux in the air side are nearly perpendicular to the surface as they enter the material, while the field and flux density are nearly tangential to the surface on the material size.

In the resulting overall structure, the magnetic flux from the field is drawn into the metal at an almost perpendicular angle of incidence and tends to concentrate in the low reluctance ferromagnetic path nearly tangential to the surface. The flux is directed along the shield inside the metal instead of passing through the shielding layer. This mechanism is effective even for DC fields. The degree of shielding is determined by the material permeability, shield dimension and the thickness of the shield. Mumetal, stainless steel, galvanized irons are examples of permeability materials used in shielding.

4.2.2 Conductive Material

While the high conductivity materials experiences a time-varying magnetic flux density $\boldsymbol{B}$, an electrical field $\boldsymbol{E}$ is induced within the material, as described by Faraday's Law, $\nabla x\boldsymbol{E} = -(\partial \boldsymbol{B} / \partial t)$ [37,38]. The induced electric field drives an induced current density within the material. This induced current density serves as a source for an induced magnetic flux that opposes the change in the imposed magnetic flux. This induced magnetic flux is of a polarity or direction as to counteract the original incident magnetic field. Therefore the net magnetic field in the vicinity is reduced. However, this mechanism is effective only in ac fields, where the imposed field is time-varying. Aluminum and copper are two common high conductivity materials used in shielding.

For conducting material with a unity relative permeability, the skin depth δ is always large in comparison with the shield thickness t. As shown in the table 4.2, the skin depths in copper and aluminum at 50 Hz are 9.3mm and 11.7mm, respectively. Even with a 100 times increase in frequency to 5kHz, both materials have skin depths are

of the order of 1mm. When the shield is thin ($\delta >> t$), the induced currents flow uniformly over the shield thickness. The resultant shielding may not as effective as the shielding that occurs when the skin depth is smaller than the shield thickness. Nevertheless, very significant shielding can still be accomplished, when current loops that circulate around the large scale dimensions of the shield result in an induced flux density that is comparable in magnitude to the imposed flux density.

4.3 Shielding Equation

For all shields, the degree of attenuation of a shield can be represented by its shielding effectiveness. It is determined by the material properties (permeability, conductivity), shield dimensions and the thickness of the shield. Here the definition of shielding effectiveness is defined as a ratio of the magnetic flux intensity $\boldsymbol{B}_o$ with the shield present to $\boldsymbol{B}_i$ with the field absent at the observer point, i.e. $SE = \boldsymbol{B}_o / \boldsymbol{B}_i$. (*In this thesis, the shielding effectiveness is using this definition*) For example, a shielding effectiveness 0.2 means that the resultant field at the observer point after shielding is 20% of the original field. (A unity shielding effectiveness means no shielding while a zero shielding effectiveness means perfect shielding.) Clearly, the smaller the SE values, the smaller the resultant field and better shielding performance.

For shields, like cylindrical and spherical shields, closed form expressions of the shielding effectiveness have been derived [38]. The goal of these studies is to calculate the penetration of fields through a homogeneous shield characterized by arbitrary scalar electrical constants.

Kaden [13] gives the expression for shielding effectiveness for cylindrical shields for a dipole source as follow:

$$SE = \frac{1}{\cosh(kt) + \frac{1}{2}(K + \frac{1}{K})\sinh(kt)} \qquad (4.6)$$

using the definitions $k = \frac{1+j}{\delta}$, $K = \frac{kr_s}{\mu_r}$,

where r_s is the shield radius, t is the shield thickness and δ is the skin depth..

The term kt in the hyperbolic function can be expressed as $\frac{t(1+j)}{\delta}$. It is related to the skin depth ratio.

On the other hand, $K = \frac{kr_s}{\mu_r} = \frac{r_s(i+j)}{\mu_r \delta}$, which is the ratio of the shield radius to the relative permeability and the skin depth of the shield material.

For permeability material (ferromagnetic), the μ_r, is always larger than unity. With a large μ_r, K is much smaller than one. Generally, the thickness of a shield is in the range of several millimeters, as the same order as the skin depth (the skin depth of GI is 1.1mm at 50 Hz). Therefore, the term kt for permeability material is nearly unity.

When $K<<1$, and $kt \approx 1$, analytical formula (4.6) can be simplified to the formula (4.6) [Appendix 2]

$$SE = \frac{1}{1 + \frac{1}{2}\frac{\mu_r t}{r_s}} \qquad (4.7)$$

For highly conductive material, K is always greater than one due to the μ_r is equal to unity. At power frequency, the skin depth is much larger than ferromagnetic material. For example, aluminum has a skin depth of 11.9 mm at 50 Hz.

When $K >> 1$, and the skin depth ratio $kt << 1$, analytical formula (4.6) can simplifiec as [Appendix 2]:

$$SE = \frac{1}{1 + \frac{1}{2} j\omega\mu_r \sigma t r_s} \qquad (4.8)$$

For the validation of these two approximate equations, the SE calculated by the tw equations have been compared to the one calculated from the original equation (4.6 and the commercial software OERSTED, which is based on the boundary elemer method (BEM). Three elements have been tested. They include a high conductivit material (aluminum, σ_r=0.61), a high permeability material (mumetal, (μ_r =1500(and a low permeability material (galvanized iron, μ_r =400). For all three cas shown in table 4.1, shield thickness and shield radius keep constant (t = 1.5mr r_S=0.1m).

	Aluminum	Galvanized Iron	Mumetal
SE (equation 4.1)	0.66	0.225	0.0089
SE (approximate)	0.672	0.25	0.0088
Numerical software	0.67	0.227	0.0088

Table 4.4 Comparisons of the approximate equations to the BEM solution

From table 4.4, it can be observed that the errors for the high conductivity and high permeability are small from the original equation (4.6). They are less than 2%. A relative-large discrepancy is observed for low permeability material. The error is nearly 10%.

4.3.1 Impact of material

As discussed in the previous chapter, shielding material can divide into two main groups according to their shielding mechanism: permeable material and conductive material. Permeability materials (e.g., Mumetal, iron, stainless steel) are characterized by its high relative permeability μ_r. The relative permeability is within the range of several hundreds (e.g. iron) to tens of thousand (e.g. Mumetal, Supermalloy). According to the formula (4.7), high permeability can enhance the shielding performance. However, in commercial, low permeability material is using instead of the high permeability material such as GI for economic consideration.

When a material owns high conductivity (e.g. aluminum, copper), according to formula (4.8), a better shielding performance is expected. A higher conductivity in the material let the current flow more easily. Then the induced magnetic flux can oppose the external magnetic flux will be more efficiently. In general, the shielding performance of this kind material is comparable to a low-μ_r material for the same size.

4.3.2 Impact of shield size

For a closed shield structure, the shield size is a critical factor of the shielding effectiveness. It should be noted that the trends of shielding effectiveness are different for the permeability materials and conductivity materials. According to the approximate equations, the shielding performance is deteriorated with increasing the

size for the permeability material. The conductive material shows an opposite trend, the shielding performance increases with the shield size.

CHAPTER 5 RECTANGULAR SHIELD

Heavy current carrying cables and busbars construct the main electrical distribution system in office buildings. These distribution power lines are used to transmit power from transformer or switchboards to different load centers in the building. Since they carry heavy current, they are one of the major sources of ELF magnetic fields.

Where a large number of cables have to be installed, or where the cable sizes are large, it is often preferred to use metallic cable trunking. Commercial trunking is rectangular or square in cross section (fig. 5.1) and is mainly made from galvanized iron (GI). The main purpose for trunking is to provide mechanical protection for the enclosed cables. Due to its metallic nature, it demonstrates some sort of magnetic shielding. In this chapter, the shielding characteristics will be discussed theoretically, numerically and experimentally.

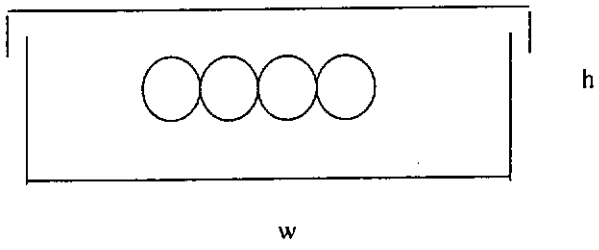

Figure 5.1 Rectangular trunking

Although the shield structure is similar to the cylindrical and the spherical shield, there is no analytic formula to evaluate the shielding effectiveness of rectangular shields (trunking). There has been little research into the shielding effect of trunking. In practice, the shielding performance of trunking used can only be estimated

approximately. Therefore, it is necessary to predict the shielding effect for different shield designs.

The study was divided into two parts. In the first part, the semi-empirical formulas of the *SE* of rectangular shield in the commercial range were derived by the theoretical analysis and numerical calculation. In the second part, the shielding characteristics and non-linearity effect on the commercial GI trunking were addressed. They were investigated by the numerical analysis and laboratory experiments.

5.1 Shielding Equation for Square Shield

One of the aspects of the shielding design process is the shield geometry. A closed shield is defined by its shield geometry, which completely divides the space into "source" and "shielded" region. Infinite planar shield, cylindrical shields, square and rectangular shields are examples of a closed shield.

From the above section, closed form expressions of shielding effectiveness have been obtained for cylindrical shield for materials having different shielding mechanisms. Both square shield and cylindrical shield are closed shield, and have geometry symmetric respect to the center. Due to the similarity of geometrical structures, their shielding performance and characteristics should be similar also.

Although there is no analytical formula of shielding effectiveness of a square shield, a square shield can be approximated by an equivalent cylindrical shield. One of the methods is to use the equivalent radius by equating the perimeter of the square shield to the circumference of the equivalent cylindrical shield. The equivalent radius can be expressed as,

$$r_{eq} = \frac{2L}{\pi} \qquad (5.1)$$

where L is the side length of the square shield.

The shielding effectiveness of a square shield can be obtained by substituting the equivalent radius R_{eq} into (4.7) or (4.8) according to the material properties of the shield. Validation with numerical method was carried out for the square shield. The numerical calculation was carried by the boundary element method (BEM) software. Three common shield materials, aluminum (Al, σ=3.57x10^7$(\Omega m)^{-1}$), galvanized iron (μ_r = 400) and mumetal (μ_r =15000) were considered. The shield has side length in the range from 0.1 to 0.5m, and thickness 1mm, which is within the commercial range.

The *SE* of the GI and mumetal were calculated through the closed-form expression (4.7), while Al was calculated through (4.8) by substituting the corresponding shield radius. Figure 5.2 shows the results of simulated value simulated by the BEM software and the values calculated by formulas (4.7) and (4.8). Since the value of shielding effectiveness of the Mumetal is small, the shielding effectiveness in the figure is shown in logarithm scale.

It is observed that there is a good agreement between values calculated from the formulas (4.7) and (4.8) and the simulated values. All three cases have differences less than 5%. It implies that the square shield could be approximated by cylindrical shield with equivalent radius. Moreover, the analytical formulas (4.7) and (4.8) can be used to estimate the shielding effectiveness of square shield made of permeability material or conductivity material respectively by substituting the equivalent radius.

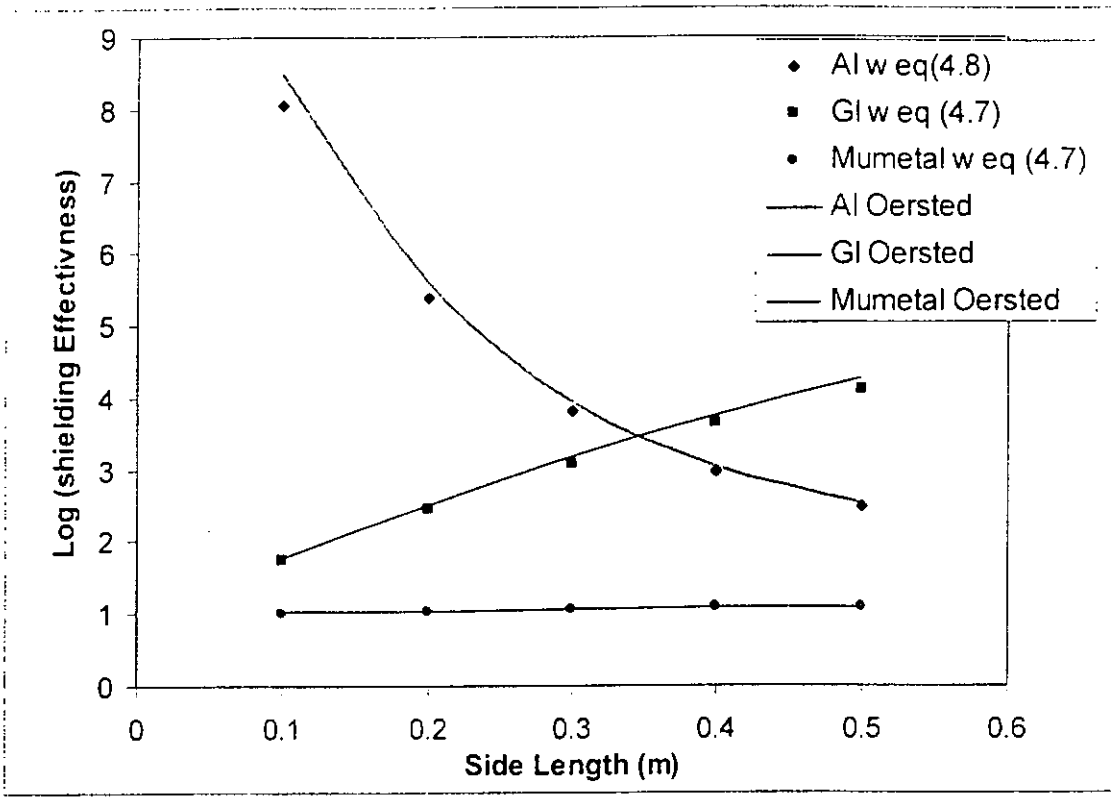

Fig 5.2 Comparisons of BEM solution with the approximate equation

5.2 Shielding Equation for Rectangular Shield

Both square and rectangular shields have a closed shielding structure. Due to their similarity in geometry, they should have similar shielding properties. In this section, it proposes a method to find out the closed form equation of the shielding effectiveness for a rectangular shield in the commercial range. From the above section, analytical shielding equations for square shields have been derived from the approximated cylindrical shield. These equations can be further improved to estimate the shielding effectiveness of a rectangular shield by multiplying some specific coefficients associated with their size, thickness and material properties.

These specific coefficients were obtained from numerical simulations and validated by experiments. By multiplying the coefficients to the analytical equation of the square shield, the shielding effectiveness of the corresponding rectangular shields

can be calculated. The using of the numerical software was complicated. Engineers may need several months to learn the software. Moreover, it is very time-consuming. A simple case may needs a few days for calculations. With these formulas, the shielding effectiveness of the commercial trunking can be estimated with certain accuracy through simple calculation procedure. The design process is simplified. Times, human resources, and material resources are saved for using these formulas instead of numerical simulations.

The difference on the geometry of rectangular shield to the square shield is that the height (h) and width (w) are not equal, i.e. $w > h$ for a rectangular shield. The discrepancy on the shielding performance depends on their geometry difference if they have the same thickness and material properties. Therefore, a rectangular shield with height h can be approximate to a square shield with the same height by applying a size coefficient to the approximate equation of the square shield obtained in above section. A size coefficient (S_h) is defined as the SE variation ratio due to different geometry between a square shield and rectangular shield which was obtained numerically by dividing the shielding effectiveness of the square shield to the shielding effectiveness of the rectangular shield with different width-height ratio. Therefore, the estimation of the SE of rectangular shield ($SE_{(w,h)}$) having a different width to height ratio can be calculated by multiplying the corresponding size coefficient S_h to the approximate equation of a square shield with the same height.

Moreover, the shielding effectiveness of the rectangular shield is also a function of its thickness and its relative permeability. Since the permeability is not even at different position within the trunking, the concept of equivalent relative permeability is considered here. To reflect the influence of those effects, a thickness coefficient

and equivalent relative permeability coefficient are added in the formula. The general shielding equation of the rectangular shield is written as (5.2):

$SE_{(w,h)} = SE_{square} \times S_h \times$ *thickness coefficient x equivalent relative permeability coefficient* (5.2)

5.2.1 Conductive Material

In practical, the currents applied are from several hundreds to around two thousand amperes (for a 1500kVA under fully load, the secondary current may reaches 2280A). Since cables carry currents below 100A are unlikely to create significant external fields, only the cables capable of carrying current over 100A are considered. For this current range, the cable areas are in the range from 35mm^2 to 630 mm^2. The corresponding sizes of the trunking are in the range of 100mm-300mm wide, 100mm-300mm high. The thickness in generally is between 1mm to 2mm due to weight constraints. Numerical simulation has been conducted for an aluminum rectangular shield model with different width-height ratio from 1 (square) to 3. The model height is set as 0.1m, 0.15m, 0.2m, 0.25m and 0.3m with different thickness 1mm, 1.5mm and 2mm, 2.5mm and 3mm. These dimensions are the common trunking size in commercial.

In figure 5.3, the shielding effectiveness against the width-height ratio for 100mm height rectangular shield is shown. And the corresponding size coefficient is shown in figure 5.4. Numerical formula of the size coefficient can be obtained by linear fitting. From the above figures, the shielding effectiveness is a function of the shield thickness. The effect of thickness on the size coefficient has been represented by the thickness coefficient as shown in figure 5.5. (For other shield height other than

100mm, the data curve are shown in appendix 1). Then, numerical formula has also been obtained for the thickness coefficient by linear fitting. In the case for conductive material, the relative permeability has no influence on the shielding performance, therefore the equivalent relative permeability coefficient is equal to unity.

The shielding effectiveness for an aluminum rectangular trunking of width w and height h can be estimated by the equation (5.3). The SE of the rectangular shield is obtained by multiplying the size coefficient and the thickness coefficient to the approximate shielding equation of square shield with the same height.

$$SE_{(w,h)} = SE_{square} \times S_h \times thickness\ coefficient \qquad (5.3)$$

Where $$SE_{square} = \frac{1}{1 + \frac{1}{2} j\omega\sigma\mu_0 t(\frac{2h}{\pi})} \qquad (5.4)$$

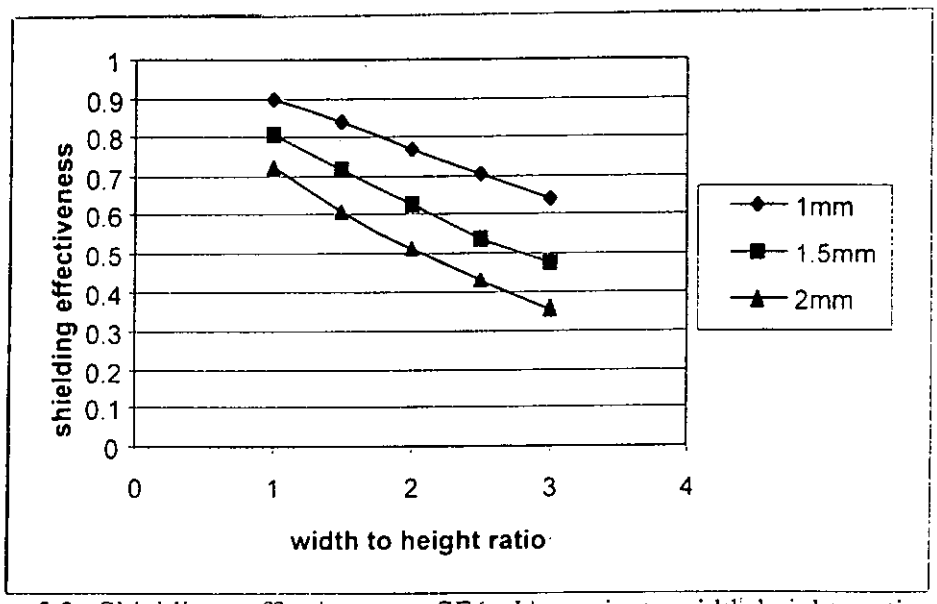

Figure 5.3 Shielding effectiveness $SE(w,h)$ against width-height ratio for an aluminum rectangular shield of height 100mm with different thickness

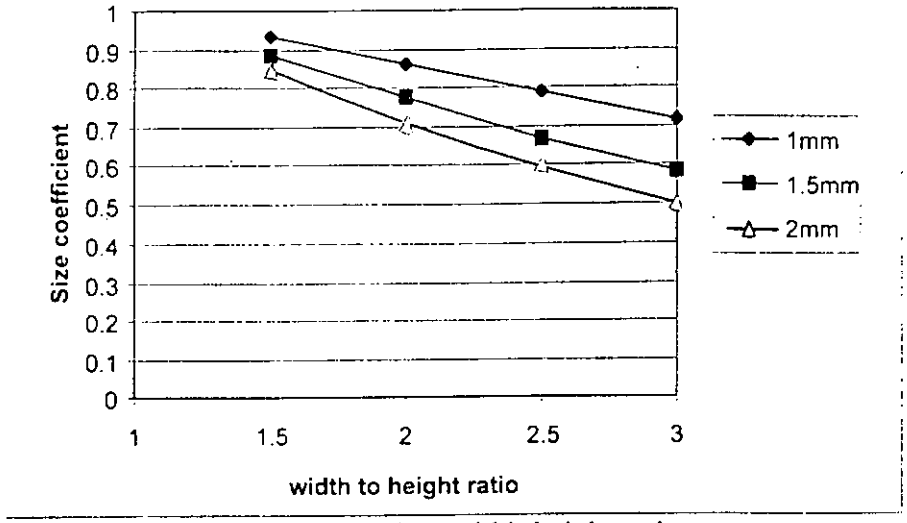

Figure 5.4 Size coefficient against width-height ratio

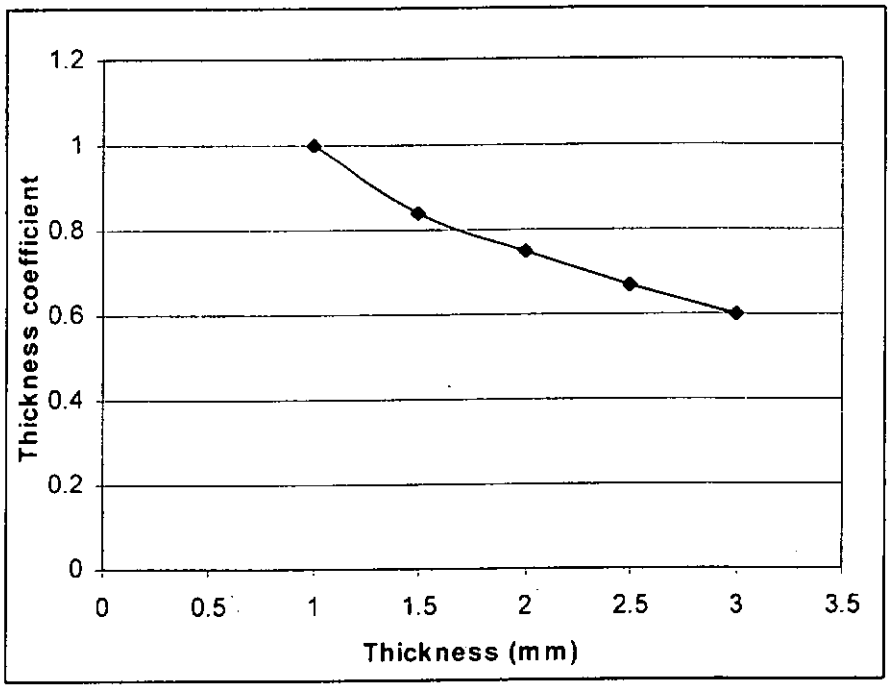

Figure 5.5 Thickness Coefficient

The size coefficient (S_h) and thickness coefficient of the aluminum rectangular trunking with different height are present in the following table 5.1. (For the square shield, w/h=1, the size coefficient is equal to 1)

These formulas can be used for calculating the shielding effectiveness of the aluminum trunking with the height range from 0.1m to 0.3m, width from 0.1m to 0.9m and thickness range from 1mm to 3mm. For the shield parameters slightly larger than these ranges, these formulas still can be employed, but a larger allowance should be added.

If the height of the shield is not specify in the approximate equations, the shielding effectiveness can be obtained through taking an average over the values obtained from the two shielding equations which have the closed height to the shield. For example, the shielding effectiveness of aluminum trunking with height 225mm can be obtained by taking the average of the shielding effectiveness from a 200mm and 250mm height trunking.

For h=100mm, $SE_{h=100mm}$ = ($S_{h=100mm}$ x $SE_{square,h}$ x Thickness Coefficient) Where $S_{h=100mm}$ ={1.1487-0.1447 (w / h)} (5.5) Thickness Coefficient = (1.189-0.212 t) (5.6)
For h=150mm, $SE_{h=150mm}$ = ($S_{h=150mm}$ x $SE_{square,h}$ x Thickness Coefficient) Where $S_{h=150mm}$ ={1.2054-0.2144 (w / h)} (5.7) Thickness Coefficient = (1.1929-0.2222t) (5.8)
For h=200mm, $SE_{h=200mm}$ = ($S_{h=200mm}$ x $SE_{square,h}$ x Thickness Coefficient) Where $S_{h=200mm}$ ={1.2397-0.2611 (w / h)} (5.9) Thickness Coefficient = (1.1993-0.2289 t) (5.10)
For h=250mm, $SE_{h=250mm}$ = ($S_{h=250mm}$ x $SE_{square,h}$ x Thickness Coefficient) Where $S_{h=250mm}$ ={1.266-0.2966 (w / h)} (5.11) Thickness Coefficient = (1.2336-0.264 t) (5.12)
For h=300mm, $SE_{h=300mm}$ = ($S_{h=300mm}$ x $SE_{square,h}$ x Thickness Coefficient) Where $S_{h=300mm}$ ={1.3391-0.3598 (w / h)} (5.13) Thickness Coefficient = (1.1868-0.213 t) (5.14) *(t is the shield thickness in mm)*

Table 5.1 Numerical formulas of size coefficient and thickness coefficient

5.2.2 Permeability material

For GI trunking, the empirical formulas are obtained in the same manner as for the aluminum trunking. The dimensions of the models are the same as given above. Except the shield thickness, width to height ratio, and shield size, there is one more variable in the case of permeability material, it is the equivalent relative permeability of the GI trunking. Due to its non-linear property, the equivalent relative permeability of permeability material (ferromagnetic) will change due to variation of flux density within trunking. For example, current magnitude, distribution of the current among conductors, cable arrangement and spacing will affect the flux density inside the trunking. And this will leads to a non-linear variation in the equivalent relative permeability of the material. The non-linear effect will be discussed later. By the past experience, the range of the equivalent relative permeability is within 200 to 1000. Therefore, the simulations have conducted for GI trunking model with different width-height ratio from 1 (square) to 3. The model height is set as 0.1m, 0.15m, 0.2m, 0.25m and 0.3m with different thickness 1mm, 1.5mm and 2mm and have equivalent relative permeability from 200 to 1000.

Figure 5.6 shows the *SE* against different width-height ratio for height 100mm, thickness 1.5mm rectangular shield. And the corresponding size coefficient is shown in fig.5.7. As above, numerical formula of the size coefficient can be obtained by linear fitting. As this time, the size coefficient is a function of the equivalent relative permeability and it is independent of the shield thickness. The effects of the equivalent relative permeability on the size coefficient could be represented by the equivalent relative permeability coefficient term as shown in figure 5.8. Then,

numerical formula has been obtained for the equivalent relative permeability coefficient by polynomial fitting.

The shielding effectiveness for GI rectangular trunking of width w and height h can be calculated by the equation (5.15). The SE of the rectangular shield is obtained by multiplying the size coefficient and the permeability coefficient to the approximate shielding equation of square shield with the same height.

$$SE_{(w,h)} = SE_{square} \; x \; S_h \; x \; permeability\ coefficient \qquad (5.15)$$

Where $SE_{square} = \dfrac{1}{1 + \dfrac{\mu_r t}{2(\dfrac{2h}{\pi})}}$

$$= \frac{1}{1 + \dfrac{\pi \mu_r t}{4h}} \qquad (5.16)$$

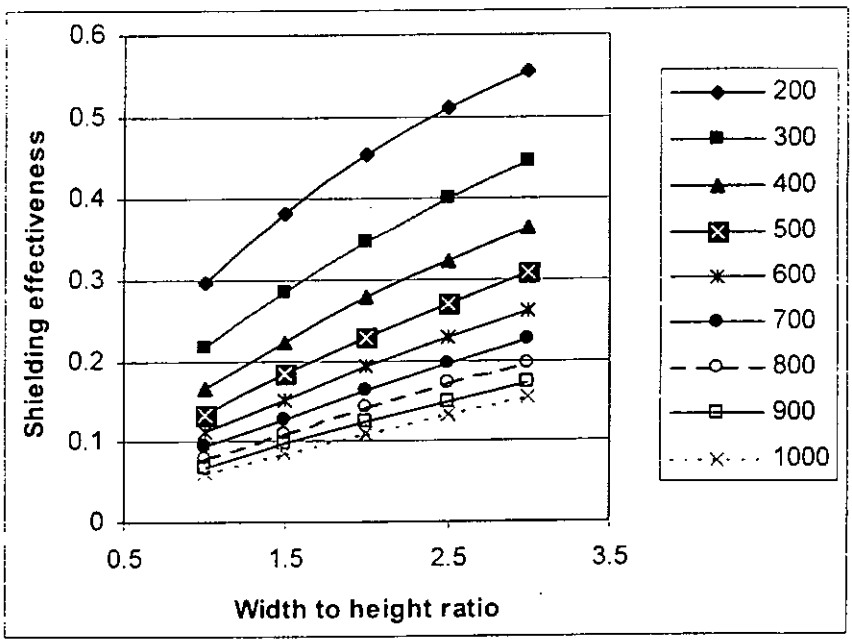

Fig 5.6 Shielding Effectiveness $SE(w,h)$ against width-height ratio for GI rectangular shields of height 100mm with different equivalent μ_r

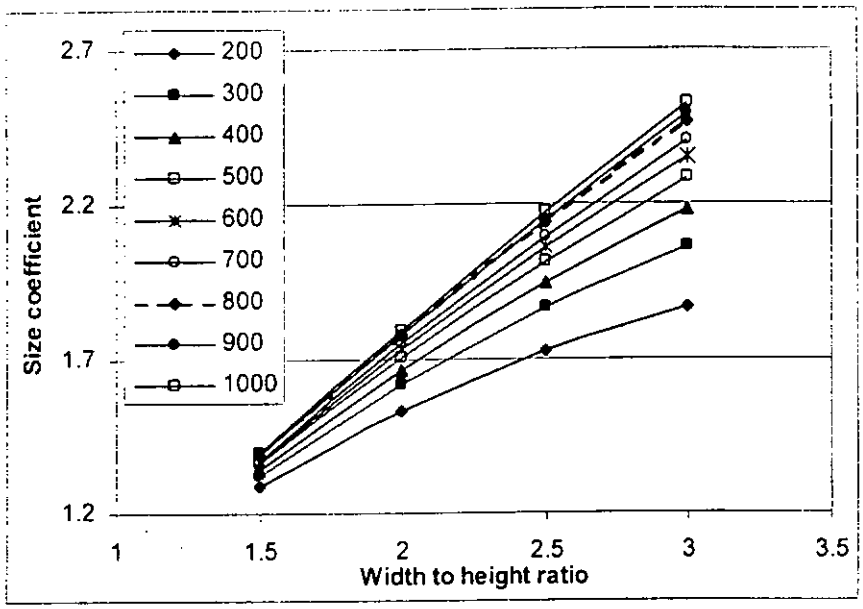

Fig.5.7 Size coefficient against width-height ratio

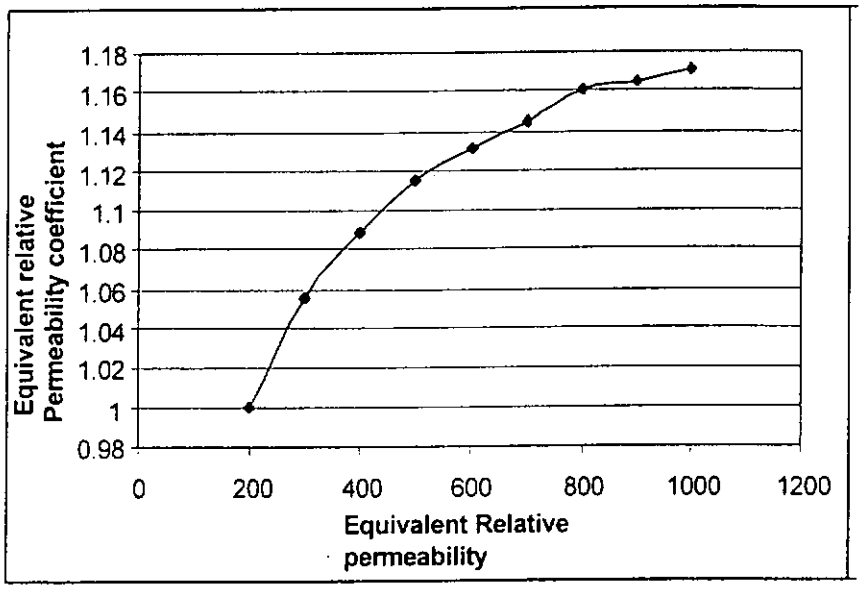

Fig.5.8 Equivalent relative permeability coefficient

The size coefficient (S_h) and equivalent relative permeability coefficient of the GI trunking with different heights are present in the following table 5.2. (Again, for the square shield, w/h=1, the size coefficient is equal to 1)

For h=100mm.

$SE_{h=100mm}$ = ($S_{h=100mm}$ x $SE_{square,h}$ x Permeability Coefficient)

Where $S_{h=100mm}$ = {0.6131+0.4336 (w / h)} (5.17)

Permeability Coefficient = $\{0.9107+0.0005\ \mu_r - 3 \times 10^{-7} (\mu_r)^2\}$ (5.18)

For h=150mm,

$SE_{h=150mm}$ = ($S_{h=150mm}$ x $SE_{square,h}$ x Permeability Coefficient)

Where $S_{h=150mm}$ = {0.7812+0.2731 (w / h)} (5.19)

Permeability Coefficient = $\{0.9018+ 0.0006\ \mu_r - 3 \times 10^{-7} (\mu_r)^2\}$ (5.20)

For h=200m,

$SE_{h=200mm}$ = ($S_{h=200mm}$ x $SE_{square,h}$ x Permeability Coefficient)

Where $S_{h=200mm}$ = {0.8932+0.1623 (w / h)} (5.21)

Permeability Coefficient = $\{0.8938+0.00069\mu_r - 3 \times 10^{-7} (\mu_r)^2\}$ (5.22)

For h=250m,

$SE_{h=250mm}$ = ($S_{h=250mm}$ x $SE_{square,h}$ x Permeability Coefficient)

Where $S_{h=250mm}$ = {0.9241+0.1158 (w / h)} (5.23)

Permeability Coefficient = $\{0.853+0.001\ \mu_r - 6 \times 10^{-7} (\mu_r)^2\}$ (5.24)

For h=300m,

$SE_{h=300mm}$ = ($S_{h=300mm}$ x $SE_{square,h}$ x Permeability Coefficient)

Where $S_{h=300mm}$ = $\{0.7202+0.3451(w / h) - 0.0646(w/h)^2\}$ (5.25)

Permeability Coefficient = $\{0.8811+0.0007\ \mu_r - 4 \times 10^{-7} (\mu_r)^2\}$ (5.26)

Table 5.2 Numerical formulas of size coefficient and thickness coefficient

These formulas can be used for calculating the shielding effectiveness of the aluminum trunking with the height range from 0.1m to 0.3m, width from 0.1m to 0.9m and thickness range from 1mm to 3mm. For the shield parameters slightly larger than these ranges, these equations still can be employed, but a larger allowance should be added.

The results from the approximate equations were compared to the experiment value. The setup of the experiment is described in section 5.4.

CASE 1

A single-phase current source (300A) with no spacing was enclosed in a 200mm x100m x 1.5mmGI trunking having an equivalent relative permeability 410. The SE measured is 0.272.

The shielding effectiveness can be calculated as the following procedure:

The height of the rectangular shield is 100mm.

By formula (5.16), $SE_{square} = \dfrac{1}{1+\dfrac{\pi 410(0.0015)}{4(0.1)}} = 0.171$

The width to height ratio is 2. Therefore, the size coefficient can be calculated by formula (5.17),

$S_{h=100mm} = \{0.6131+0.4336\ (2)\} = 1.4802$

The permeability coefficient can be calculated by formula (5.18),

Permeability Coefficient = $\{0.9107+0.0005\ (410) - 3 \times 10^{-7}\ (410)^2\} = 1.06527$

The shielding effectiveness can be calculated as 0.171x1.06527 x1.4802=0.269. The difference is about 2% in this case.

CASE 2

A three-phase four-wire circuit with current 600A arranged in flat touching configuration was enclosed in a 300mm x 100mm x1.5mm GI trunking having a relative permeability 450. The SE measured is equal to 0.329.

By formula (5.16), $SE_{square} = \dfrac{1}{1+\dfrac{\pi 450(0.0015)}{4(0.1)}} = 0.158$

In this case, the width to height ratio is 3. Therefore, the size coefficient can be calculated by formula (5.17),

$S_{h=100mm} == \{0.6131+0.4336\,(3)\} = 1.91$

The permeability coefficient can be calculated by formula (5.18),

Permeability Coefficient = $\{0.9107+0.0005\,(450) - 3 \times 10^{-7}\,(450)^2\} = 1.074$

The shielding effectiveness can be calculated as 0.171x1.074 x1.91=0.35. The difference is about 8%.

CASE 3

A single-phase current source (200A) with no spacing was enclosed in a 300mm x100m x 1.2mm Al trunking. The SE measured is 0.515.

By the formula (5.4),

$$SE_{square} = \frac{1}{1 + \frac{1}{2} j\omega\sigma\mu_0 d(\frac{2(0.1)}{\pi})} = 0.872$$

The width to height ratio is 3. Therefore, the size coefficient can be calculated by formula (5.5),

$S_{h=100mm}$ ={1.1487-0.1447 (3)}=0.714

The thickness coefficient can be calculated by formula (5.6),

Thickness Coefficient = (1.189-0.212 t)= 0.934

The shielding effectiveness can be calculated as 0.872x0.714 x0.934= 0.5815. The difference in this case is larger, about 13.5%.

From the three cases, the discrepancies were from 2% to 15%. Therefore, the calculated shielding effectiveness values should add 10-20 % allowance. These formulas can be used to estimate the shielding effectiveness of the commercial trunking if the shielding parameters are known. The effects of the non-linearity on the shielding properties are investigated experimentally in the next sections.

5.3 Source Parameters

The trunking shield parameters that affect the shielding performance can be divided into shield parameters and source parameters. Shield parameters refer to the parameters of the trunking shield that will affect the shielding mechanism which cause an variation in shielding ability directly, e.g., shield size, thickness, and material. All these parameters have significant effects on the *SE* for any trunking

shields. On the other hand, the source parameters of a trunking include magnitude and frequency of the applied current, distribution of the current among conductors, cable arrangement and spacing. All these parameters will affect the shielding performance through vary the magnetic flux density within the trunking. These parameters will only have significant effect on the *SE* if the trunking material is non-linear. Since the permeability material has a non-linear property, its equivalent relative permeability will vary with different source parameters. As a result, trunking with same physical properties may have different shielding effect if the source parameters cause a significant change in the equivalent relative permeability of the trunking.

5.4 Experimental Study on Source Parameters

In order to investigate the effects of the source parameters and the shielding characteristics of non-linear material trunking, a laboratory experiment on the commercial GI trunking was conducted. The application of these shielding properties on the shield design will be discussed in chapter seven. It will also discuss how it can compatible in practice with illustrated examples.

5.4.1 Experiment Procedure

The experiment setup is shown in figure 5.9. In the shielding experiment, three pieces of GI trunking with each length 2400mm were connected in serial by screwing GI plate (60x80mm). Four single core cables (XLPE 400mm^2, diameter 3.4cm) with length 7m were placed inside the trunking with a flat-touching configuration. At one end, the cables were connected to the current-injection part while the other end is

shorted. The current injection part consists of three 220/3.5V step down transformers, three auto-transformer and an harmonic generator for controlling current waveform. It can generate both three-phase or single phase current. For reducing the leakage field generated by the injection part, the three step-down transformers were enclosed in a large GI box. The background field level was below 2mG.

Magnetic fields along the lateral path in the middle trunking were recorded. FieldStar 4000 gaussmeter was employed to measure the 50Hz magnetic field data. It has an accuracy of 1% and resolution 0.04mG. Inside the gaussmeter, there are three independent coils simultaneously detect the magnetic field in three orthogonal directions. The gaussmeter were adjusted such that the detection coil is at the same location as the measurement point. Similarly, the height of measurement point is selected at the same height to the middle of the sensor coil inside the gaussmeter.

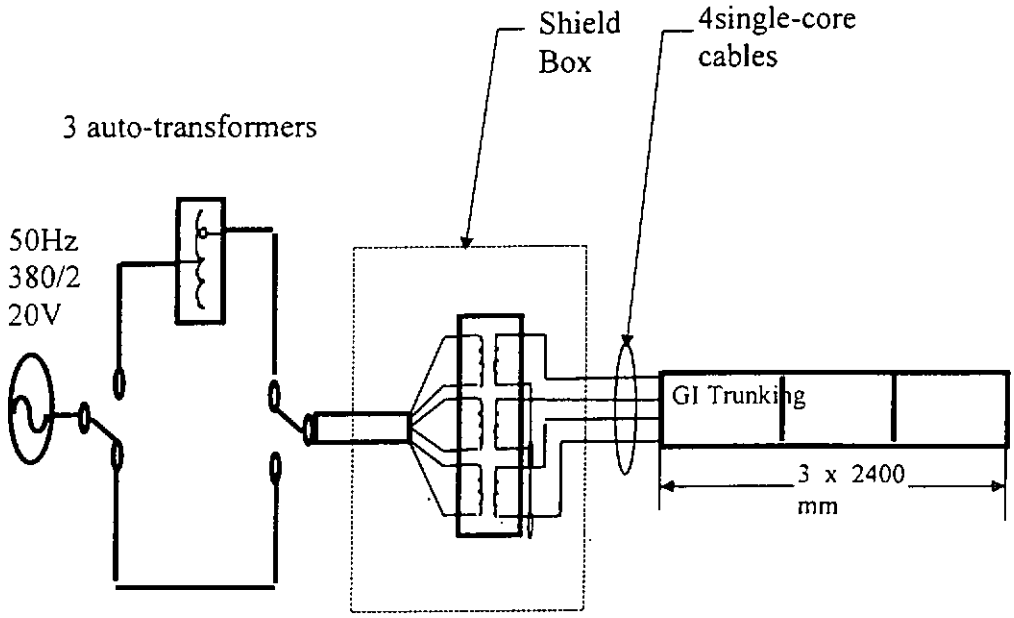

Three 7kVA 220/3.5V Step-down transformers

Figure 5.9 Setup of experiment

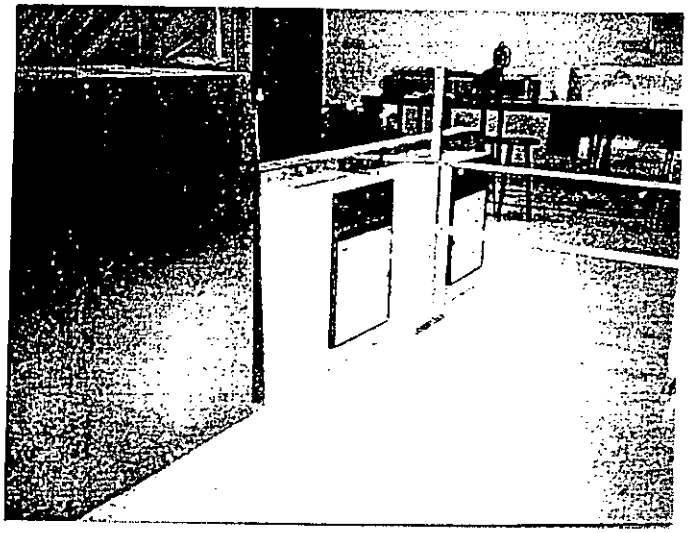

Fig.5.10 The setup of the test rig

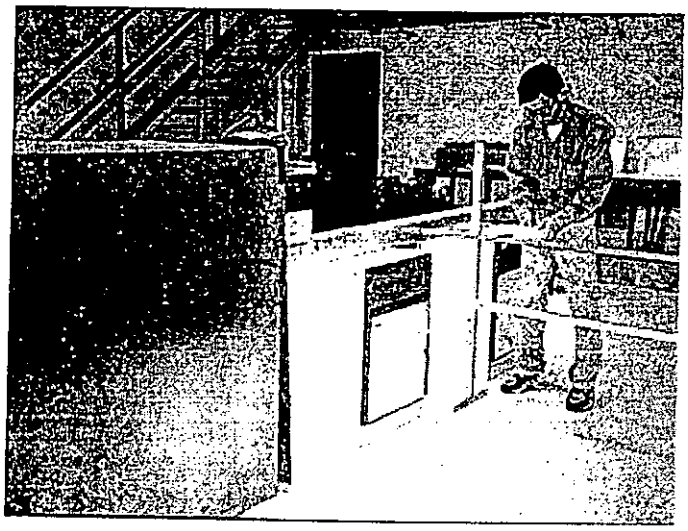

Fig. 5.11 Measurement of magnetic field

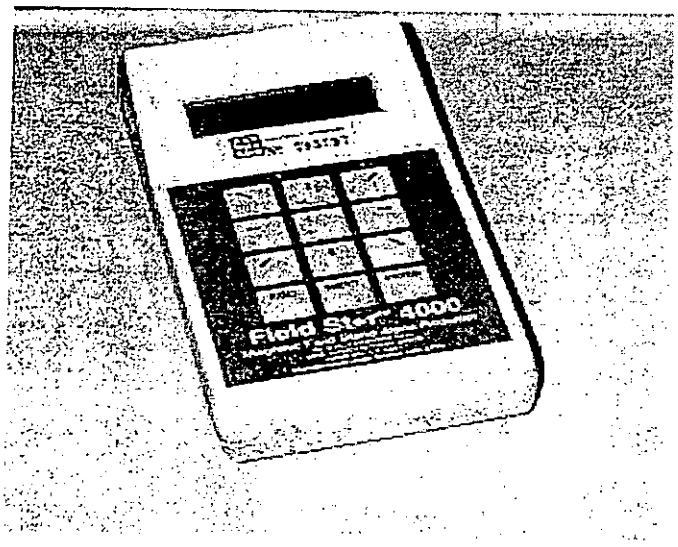

Fig. 5.12 Gaussmeter-FieldStar 4000

5.4.2 Comparisons with Numerical Calculation

Magnetic fields along the lateral path at the middle trunking were measured when the cable carried different currents (single phase and three-phase current in the range of 200A to 900A). The distance variation of magnetic field measured and the simulation values were plotted for three-phase 600A in a 400x100x1.5 trunking in the (figure 5.13). The simulation values were calculated by BEM software. This software only considered a constant value for the relative permeability within all area in the GI trunking. Since the permeability is not even at different position within trunking, the equivalent relative permeability is considered. By trying different values of equivalent relative permeability, the experiment data and the simulated values shows a good agreement when the equivalent relative permeability is set as 480. The percentage error is less than 2%. This implies that the BEM software can calculate the magnetic field for ferromagnetic shield if the equivalent relative permeability is known. In the following, the equivalent relative permeability was determined by this method.

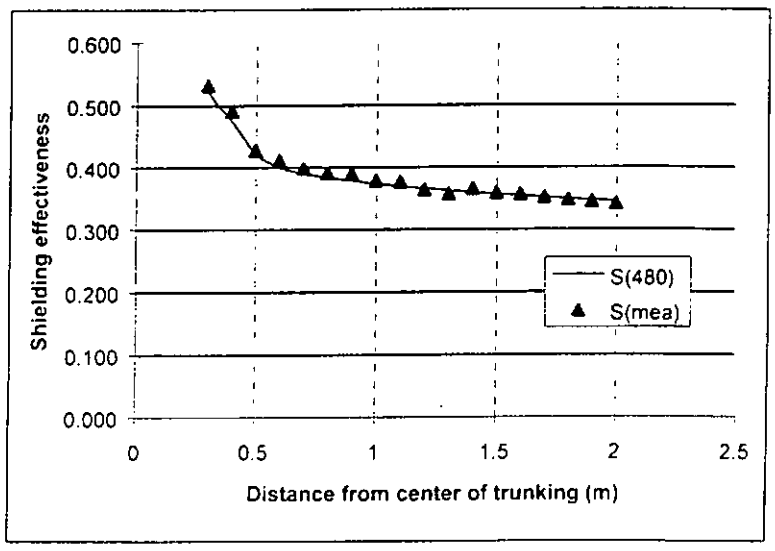

Figure 5.13 Simulation values and measured values of the shielding effectiveness against distance

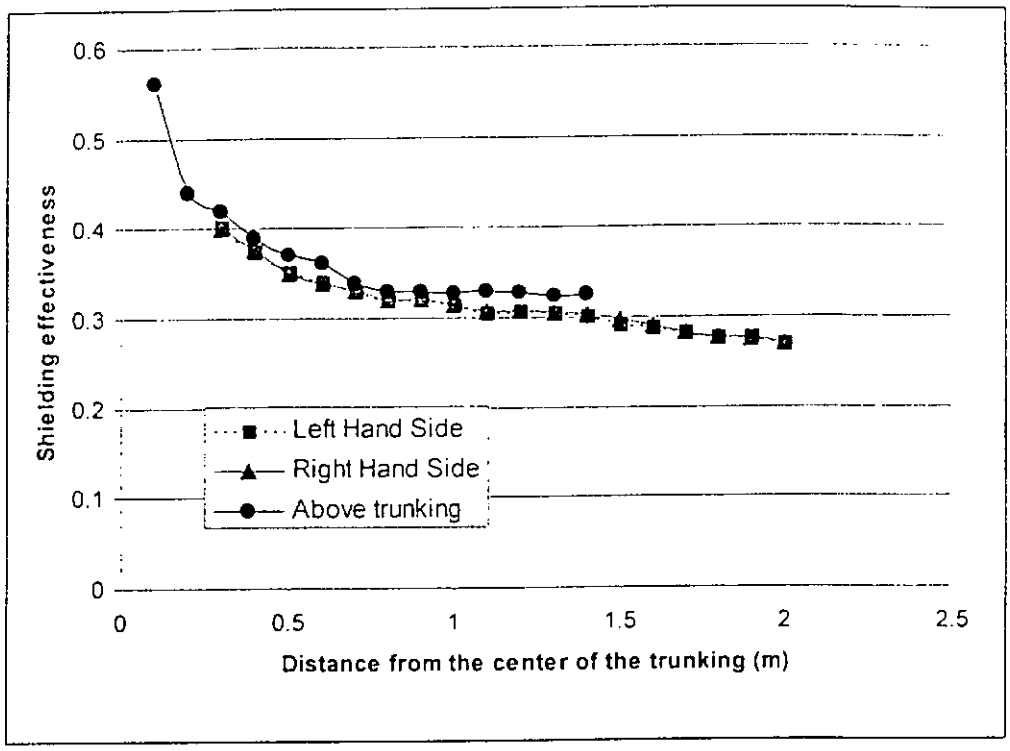

Figure 5.14 Shielding effectiveness measured above trunking and beside trunking

Measurements of the magnetic fields have been taken above and beside the middle trunking. The calculated shielding effectiveness are shown in figure 5.14. The measurement distance above the trunking was from 0.1m to 1.5m while the measurement distance beside the trunking was from 0.3m to 2m. Both left hand side and right hand side of the trunking have been measured. The data show similarity and the difference is within 1%. From figure 5.14, the shielding effectiveness taken above the trunking and beside the trunking are closed. The largest percentage difference is only 5%. For the same trunking, the shielding effectiveness are the same wherever the measurement taken place.

5.4.3 Impact of Source Current

Fig.5.15 shows the variation of the shielding effectiveness of a 300mm x 100mm x 1.5mm trunking for a three-phase current from 200-900 amperes. The measurement data at a distance of 1m were taken for comparison. From the figure, the shielding performance improves as the current increase. By trying different values of equivalent relative permeability in OERSTED to seek for a match between measured values and calculated values, an equivalent I-μ curve can be obtained in figure 5.16. The shielding effectiveness varies against the current magnitude because the equivalent relative permeability within the trunking is varied with different current magnitude applied. In figure 5.16, the applied current is linearly proportional to the equivalent relative permeability. Hence the equivalent relative permeability of the trunking will increase with larger current. Therefore, the shielding performance is better (smaller *SE*) with increasing current magnitude.

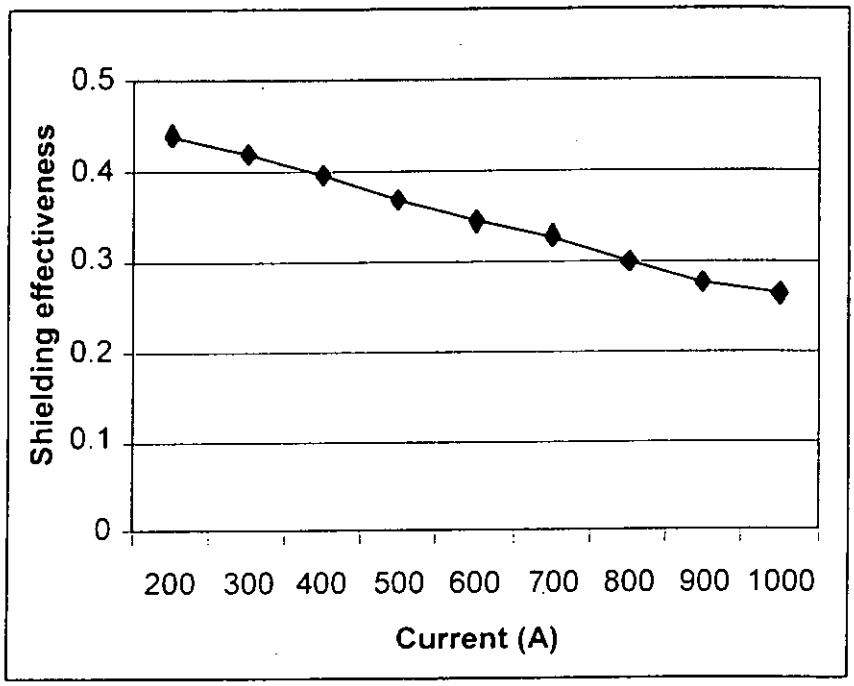

Fig.5.15 Shielding effectiveness against current

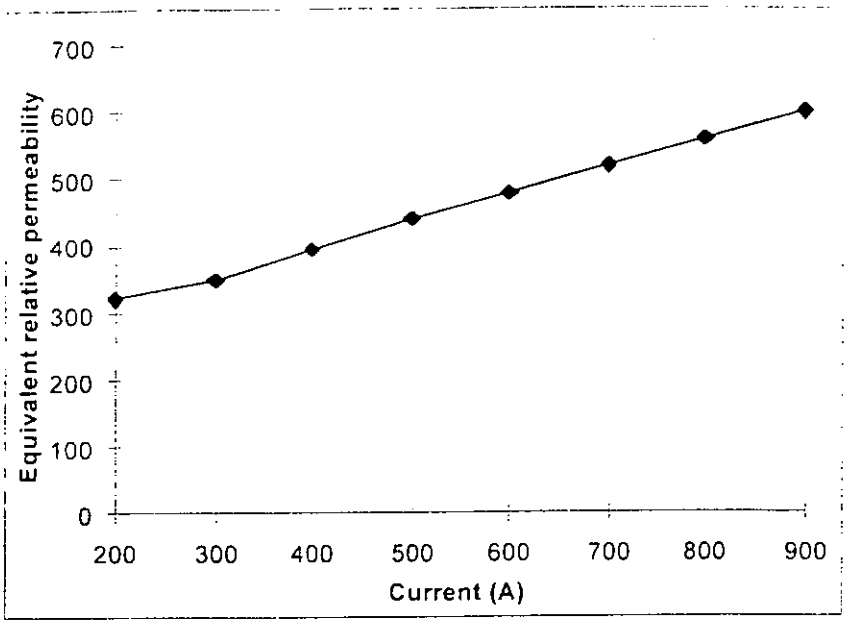

Fig.5.16 The *I*-equivalent μ_r curve

5.4.4 Impact of Source Configuration

In a linear trunking, the variation in source configuration is insignificant to the shielding performance. However, for a non-linear trunking, the source configuration, conductors spacing are important parameters to the shielding effect. At the same current magnitude, the magnetic field generated by the single-phase circuit and three-phase circuit are different. It is similar to two three-phase circuits with different phase or different configuration. The change in the equivalent relative permeability within the trunking is not known. Therefore, it is difficult to account the shield by increase the equivalent μ_r for different configuration.

Two different arrangement of a single phase circuits were investigated in the experiment. Within the GI trunking with width 300mm and current 190A, the two conductors were arranging as no spacing and with a spacing one-cable diameter

apart. The figure 5.17 shows the shielding effectiveness against the different source configuration.

It can be observed that the conductors with one diameter spacing have a lower shielding effectiveness (30%) than the one without spacing. Again, it is due to the non-linearity of the GI. As the magnetic field generated by a single circuit is proportional to the spacing of the two conductors, the configuration that has a larger spacing must have a higher magnetic flux present to the shield. Hence the shielding performance is better (lower *SE*) with an increase in the equivalent relative permeability, as shown in the blue line in figure 5.17.

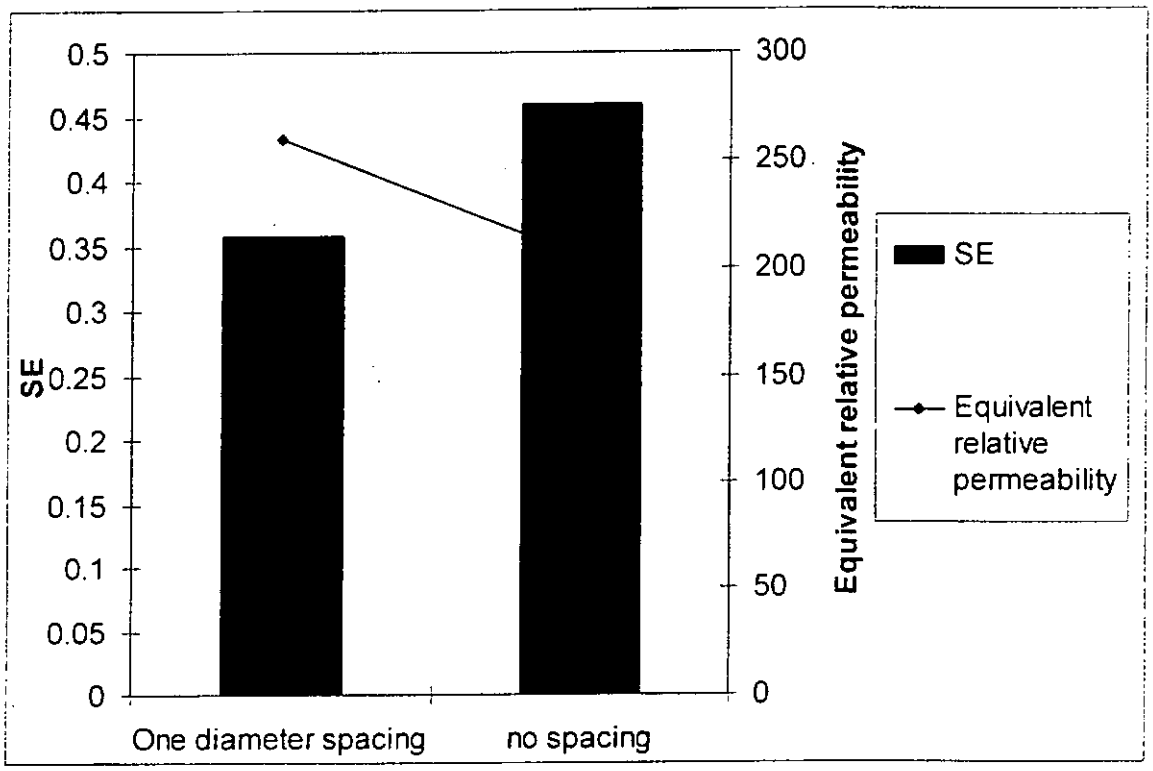

Fig. 5.17 Shielding effectiveness with different conductor spacing

The equivalent relative permeability for different source configurations were compared in table 5.3. The trunking is 300mm x 100mm x1.5mm and the applied current is 300A. It can been seen that the configuration with spacing have a higher equivalent relative permeability. It means that they have better shielding performance. Although the shielding ability is improved, the magnetic field outside the trunking would not be reduced. It is because these configurations will enhance the source magnetic field concurrently.

	1-phase flat-touching	1-phase one diameter spacing	3- phase flat-touching	3-phase one diameter spacing
Equivalent Relative Permeability	235	340	360	580

Table 5.3 Equivalent relative permeability for different source configuration

5.4.5 Impact of Size

In the above section, the affection of the shield size as a shield parameter has been discussed. A GI trunking will perform better when the size is smaller according to equation (4.7). Trunking with different width (200mm, 300mm, and 400mm) were tested in the experiment to investigate the effect of shield when it played as a source parameter. The shielding effectiveness of the trunking with a single-phase 190A source is shown in figure 5.18. And the blue line is obtained through the simulation for comparison. In the simulation, the GI is assumed to be a linear material. The equivalent relative permeability of the trunking with 300mm width which found by the method mention in 5.6.1 was used as a reference. And this value was used to simulate the trunking with width 200mm and 400mm.

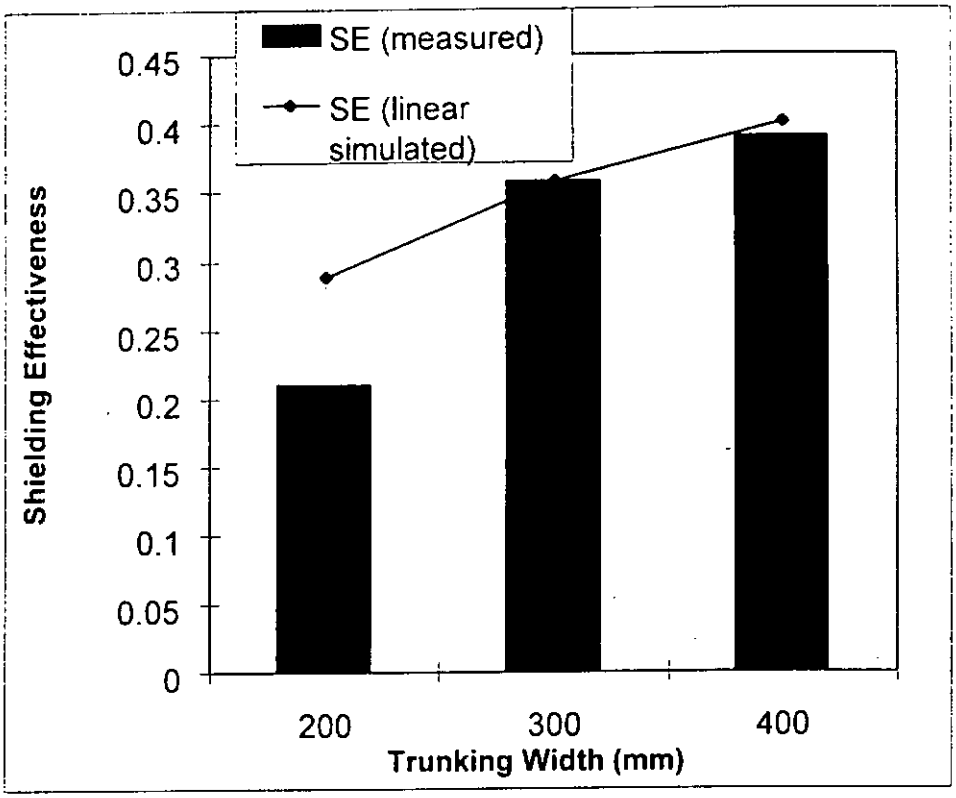

Fig. 5.18 Shielding effectiveness against trunking width

It can be observed that the simulated values are linear to the *SE*. However, at the 200mm width, the shielding effectiveness shows an abruptly decrease on the measured values. It may be due to the effect of shield size acts as a source parameter. A smaller size means that the distance from the source to the shield is shorter. Then the magnetic flux density impose to the non-linear GI may increase. Hence a higher μ_r may within the material and have a better shield performance. These additional shielding benefits will not appear in a linear material. For a smaller shield, a non-linear shield will not only provide benefit from the shielding characteristic, it also benefits through an increase in equivalent μ_r.

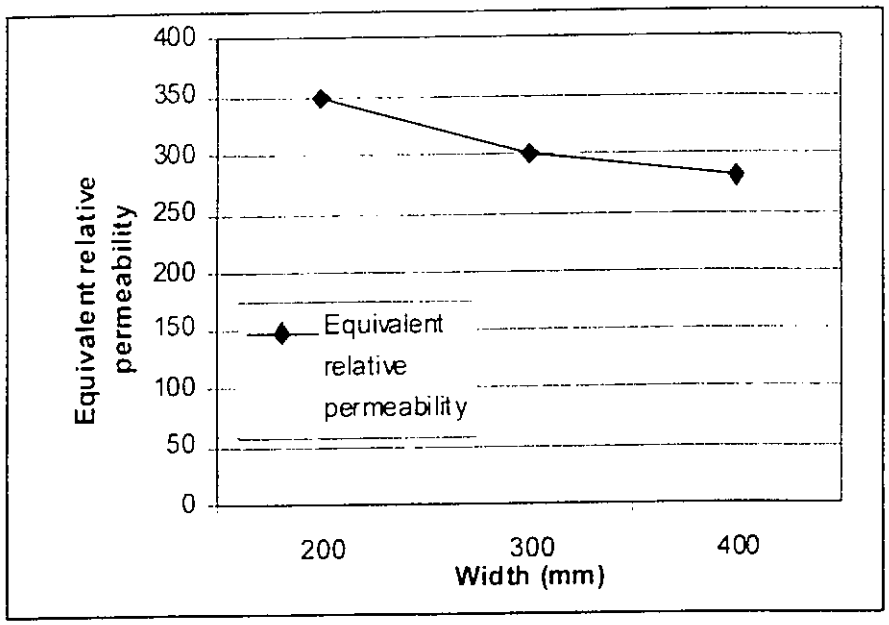

Fig.5.19 Equivalent relative permeability of trunking width

Figure 5.19 shows that the equivalent relative permeability has a further increase with width 200mm. If the shield is closer to the source, the equivalent μ_r will increases more rapidly. As a result, the shielding effect results from the increase of relative permeability will be much stronger.

5.4.6 Impact of Thickness

The thickness of the trunking also has a significant influence on the shielding performance. In the experiment, GI trunking with thickness 1.5mm and 2mm were tested. Both were with the width 300mm and height 100mm. As shown in figure 5.20 the thicker shield has a lower shielding effectiveness, a better performance. A thicker ferromagnetic field can provide more low-reluctance paths for the magnetic field diverted into it. Therefore, a better shielding performance is observed. The equivalent relative permeability of the trunking with 1.5mm thickness was found by the method discussed in 5.6.1. And this value was used to simulate the 2mm trunking. Both values show a good agreement to the measure values, it implies that

the thickness has no significant influence on the variation of the permeability. It is reasonable because the trunking thickness should has no contribution the permeability change, therefore, the addition shielding effect by the variation of magnetic flux density can be ignored. The decrease in SE is due to the its shielding mechanism only.

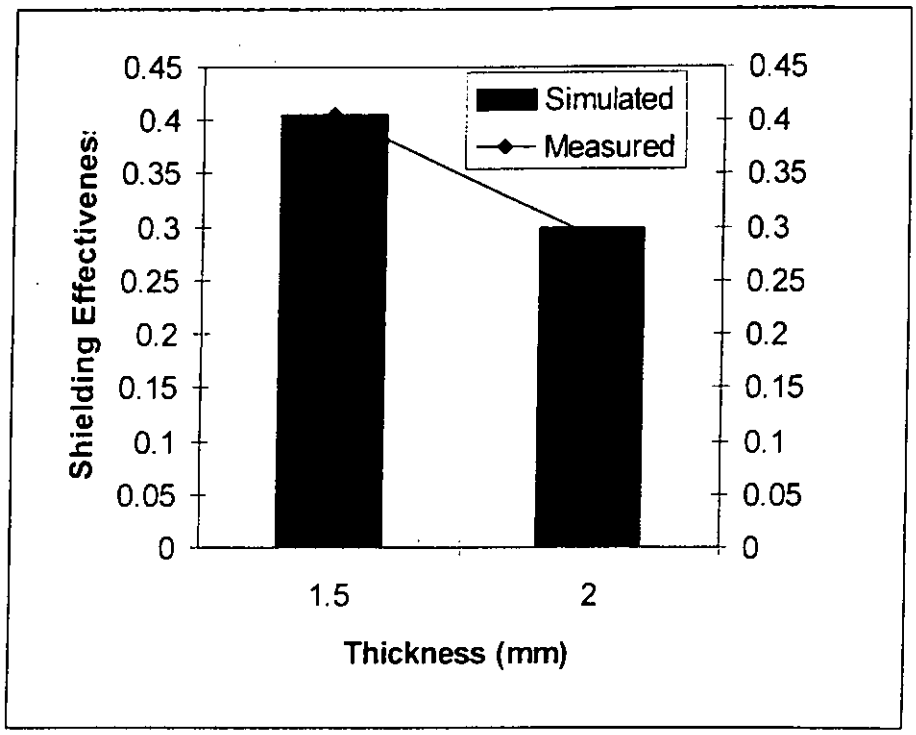

Figure 5.20 Shielding effectiveness against thickness

5.5 Practical Issue

5.5.1 Material Saturation

In the above cases, the equivalent relative permeability is increasing with the flux density within the trunking, hence a better shielding performance is obtained. However, this increasing trend eventually ceases due to saturation and then change at higher field levels. The saturation of ferromagnetic materials by high-level magnetic field results in the reduction of its equivalent relative permeability. In this region, a further increase of the magnetic flux density leads to decreases in the shielding performance.

The magnetization curve of the GI was found by a torodial core experiment. After the magnetization curve had been established, the equivalent μ_r-H curve could be plotted, as shown in figure 5.21. It can be observed that the equivalent μ_r increases with the H-value until it saturated at μ_r nearly 1200. According to the curve in figure 5.16, it is estimated that the three phase current need to reach 2300 A for material saturation to occur in the 300m x 100mm GI trunking. Generally, the distribution cables usually carry the currents up to a few hundred amperes. The saturation of a cable trunking seldom occurs. However, for a busbar trunking, the current carried by the busbars may be over one thousand amperes. Saturation of materials may occur. In the above experiment, the data were all within the region before saturation was reached.

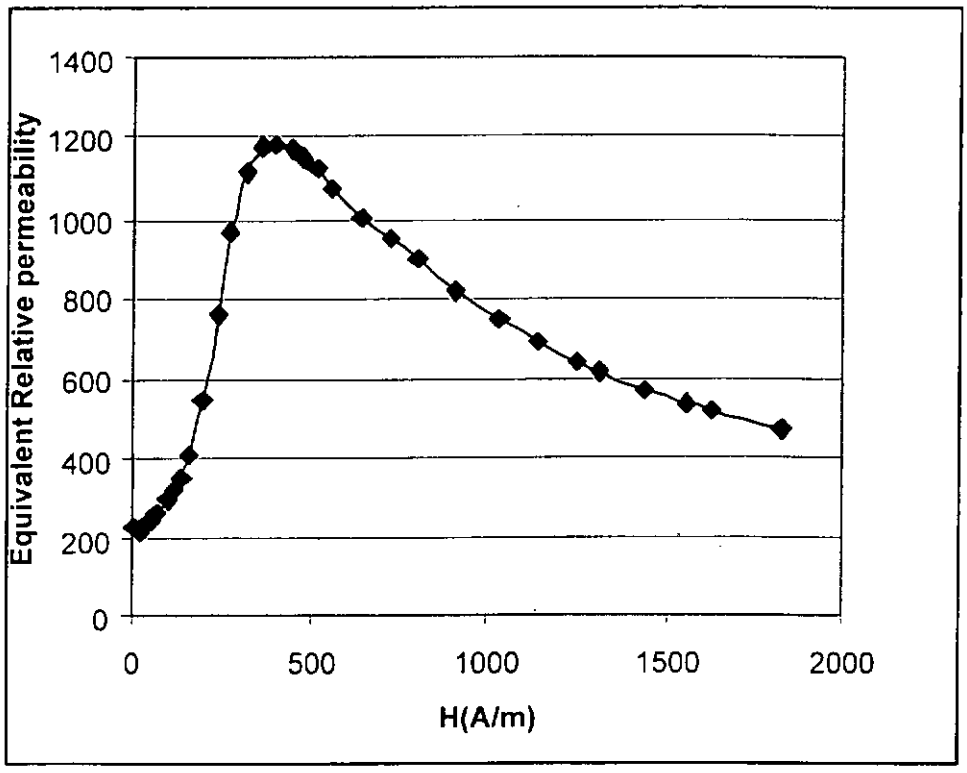

Figure 5.21 The equivalent μ_r-H curve of GI

5.5.2 Influence on Joint Seam

In practical, the trunking is finite in length. To enclose the long cables or busbars, the trunking is connected piece by piece. Undoubtedly, there will be leakage field flow through the joint seams. Because the trunking forms part of the earth-continuity conductor arrangement in the installation, it is necessary to ensure that all sections are bonded together. An experiment was conducted to investigate the influence on the shielding performance of the joint seams and the other bonding method.

The set up is the same as that described above. There were three examples for the joint, as shown in figure 5.22:

i. no connection (the seam is about 2-3mm thick)
ii. connected by screwing on GI plate(60mmx80mm)
iii. connected by screwing on copper washer

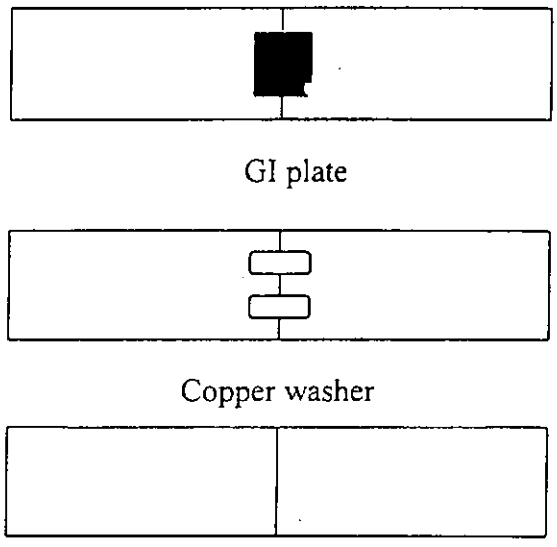

Fig. 5.22 Different connection method

Magnetic fields along the lateral path were recorded at the seam position. The measurement data at a distance of 1m were taken for comparison. Table 5.4 shows the ratio of the measured field of different seam connection methods compare to the reference field measured at the middle of the trunking.

	NO connection	GI plate	Copper Washer
$B/B_{reference}$	1.049	1.018	1.043

Table 5.4 The shielding effect of different seam connection

The effects of flux leakage for the three cases were small. The worst case w. occurring when there was no connection between trunking. However, the differen was only within 5%. It may be due to the shielding gap was narrow (2mm). With (plates connection, there was only a sight difference between the seam and the midd of trunking. It provides a low-reluctance path for the magnetic field in the joint sea The joint seam has a minor effect on the shielding performance.

CHAPTER 6 PLANAR SHIELD

6.1 Introduction

When shielding against large sources, for example a substation or an affected room inside a building, metallic sheets have to be used. In practice, several sheets are combined to divide the shielded region from the sources. Different from trunking, planar shields exhibit an open shield topology. It means that it cannot completely divided the whole space into the source and shielded region. The magnetic fields can pass the shield by leakage, edge, and seam, as well as penetrate it. Therefore, it is hard to get exact, closed form expressions for the shielding.

In previous theoretical analysis, much work on planar shielding has been focused on the closed shield topology. The assumption is that the shielding material is both homogeneous and infinite in planar dimensions, such that neither leakage through seam or edge is significant. However, this is not the case of the practical, real world shield.

This section presents the shielding properties of a finite width planar shield found in real practice. The shielding properties are discussed and verified by laboratory experiments and numerical calculation. The parameters associated with its design include the source orientation, source to shield distance, leakage around the edges and the seam, and material. These findings can help to design cost-effective shields in buildings, and achieve better shielding performance.

6.2 Usable Region

The main difference between an infinite planar shield and a finite width planar shield is that the latter one will has leakage around its edges. It is obvious that the shielding

ability will decrease from the center to its edges. There will be only a less or no shielding effect behind the shield when the location is near the edges. Therefore, the location for an object needed to be shield is vital. Since the distribution of the shielding effectiveness is not even across the shield, it is necessary to identify the usable region. Here, the usable region is defined as a region with 20% tolerance of SE respects to that in the center of the shield. It can be ensured that the shielding effectiveness will not be higher than 20% to the center within this region.

In order to know the limits on the application with the edge leakage, numerical calculation was used to find out the usable region respect to the center of the shield. GI (μ_r=400) planar shields with three different widths (w) 1.2m, 2.4m, 3.6m with the source to shield distance (d) 0.25m, 0.5m, 0.75m were calculated by the BEM software. The data at 0.2m above the shield was taken for comparison.

From the data, it is observed that the 20% tolerance region is independent to the width of the shield, but strongly dependent on the source to shield distance. The ratio of the source-shield distance to the 20% tolerance region is about 0.416 as shown in equation (6.1). That is, if the source to shield distance (d) is 0.25m, then the 20% tolerance region will be 0.6m, i.e., 0.3m within the center of the shield. It can also be observed that from figure 6.2, a larger width is unable to delay the increase rate of the *SE* along the width from center to the edges. However, a treble increase in the source-shield distance, from 0.25m to 0.75m has reduced the increasing rate effectively. The equation is valid for planar shield with width in several meters. For a wider shield or other height level above the shield, the usable region can be found in a similar way.

For the design of a planar shield, it is advisable to install the shield as far as possible from the source. It can effectively increase the usable region. The objects need to be shield should within in the usable region, to enjoy the optimum effect from the shield.

$$R_{usable} = Source\ to\ shield\ distance\ /\ 0.416 \qquad (6.1)$$

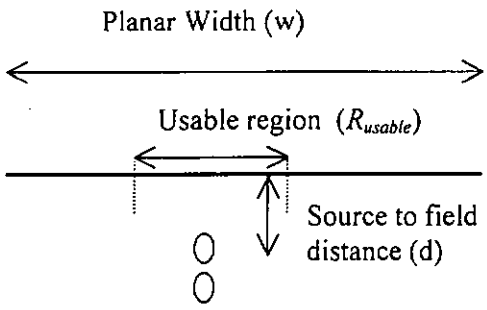

Fig 6.1 Geometry of the usable region

It should be noted that the above discussion deals with the increasing rate of *SE* due to edge leakage only. It aims to show how to increase the usable region. However, it is not related to the actual field level. Although the increasing shield width is not effective for increasing the usable region, a wider shields always enjoys a higher performance, lower value in *SE* than a narrow one. A wider shield can lower the portion of the leakage field from the edge. Comparison of *SE* with different planar width is shown in figure 6.3.

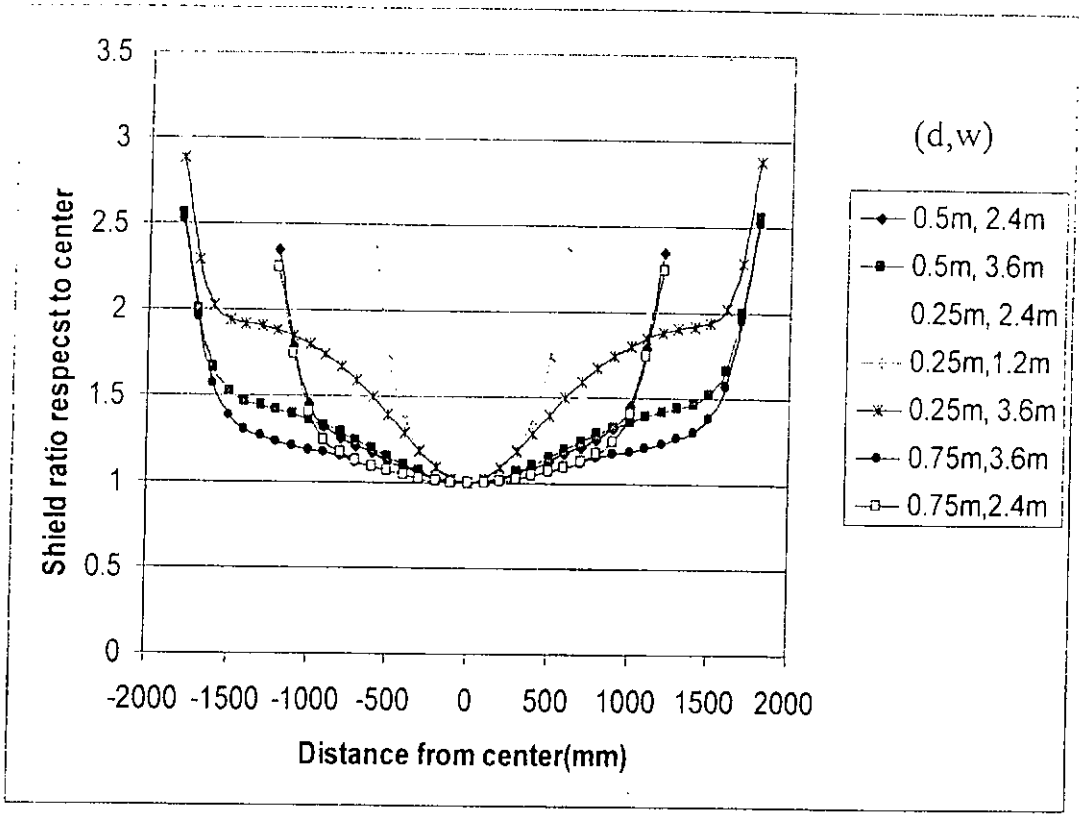

Fig. 6.2 The shift in *SE* in reference to center with different source-shield distances (d) and planar widths (w) at 0.2m above the shield

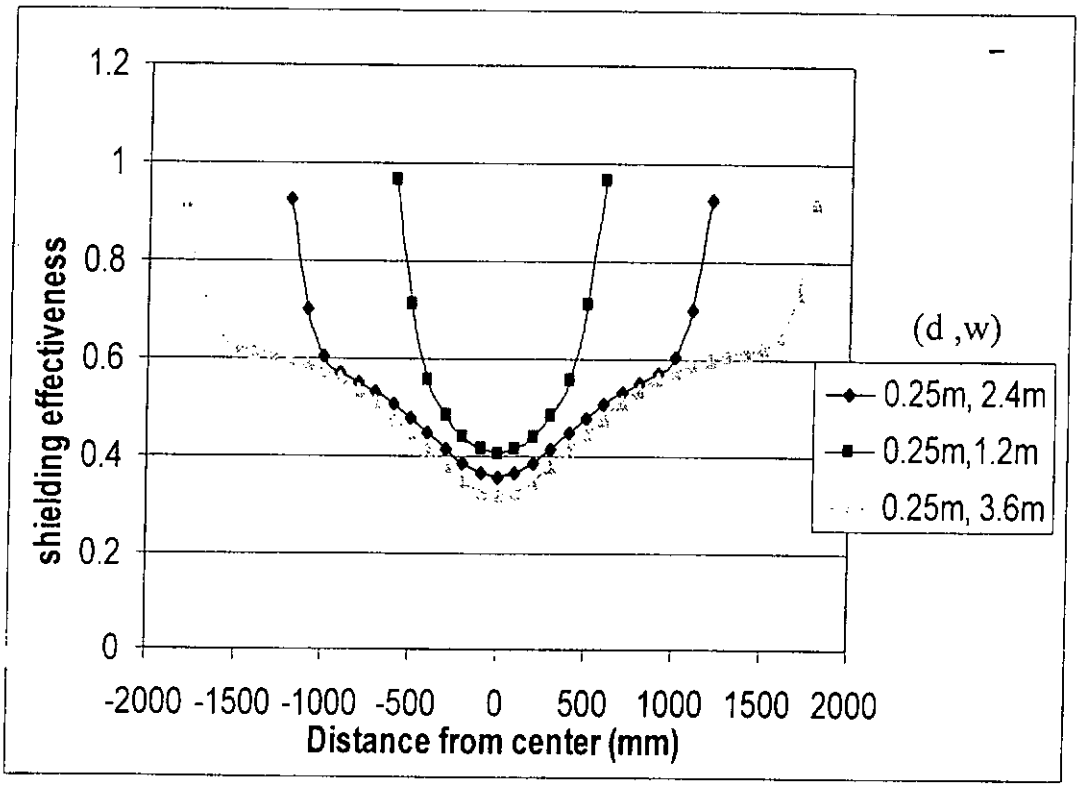

Fig. 6.3 Calculated *SE* with different planar widths

In practice, the desk level is about 1m over the floor. Since the VDU's are generally located at this level, therefore, the distribution of the shielding effectiveness at this level was also under investigation.

The results are similar to the above as shown in figure 6.4. The 20% tolerance region is independent to the width of shield, but dependent on the source to shield distance. At this time, the dependencies are not so obvious, the ratio of the source-shield to the 20% tolerance region is 0.35. For practice, these data can be used as a reference for shield design of planar shielding in office.

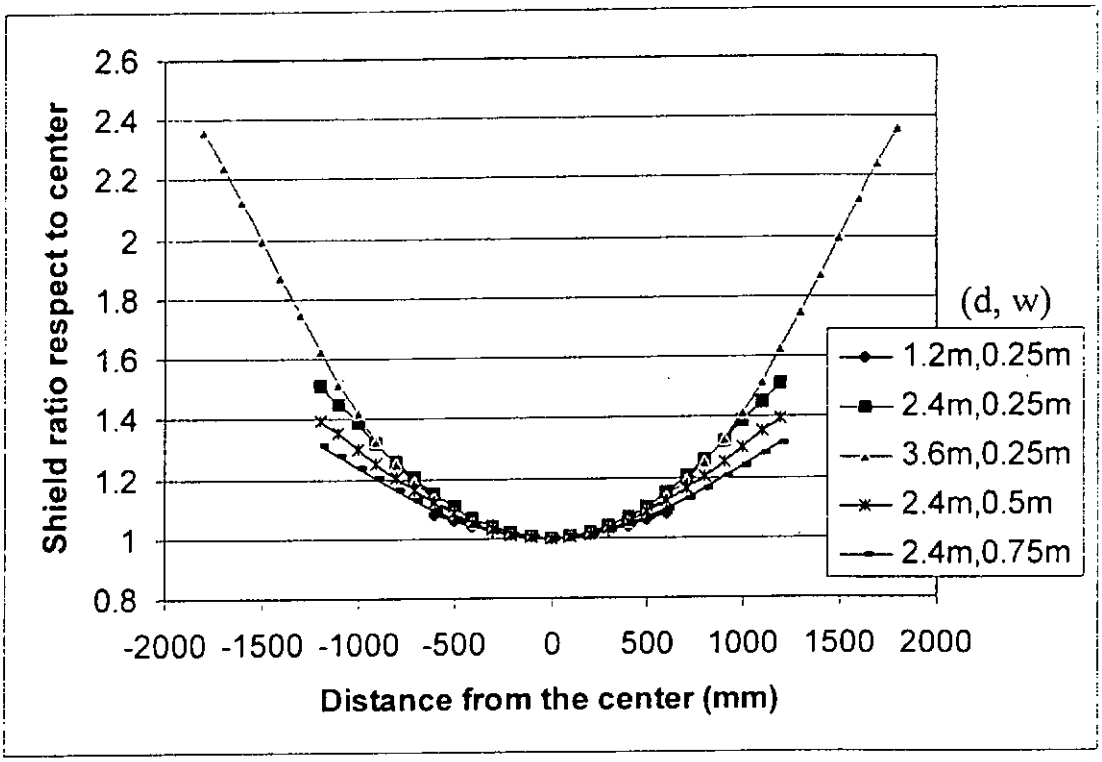

Fig. 6.4 The shift in *SE* in reference to center with different source-shield distances (d)and planar widths (w) at 1m above the shield

6.3 Experiment Procedure

To further investigate the characteristics of the planar shield in real practice, a planar shield experiment has been conducted. The measurement arrangement is shown in figure 6.5. Aluminum and galvanized iron sheets were tested. The tested metallic sheet with dimension 1.2m x 2.4m was placed on a wooden table over a single-phase busbar system. The source was a single-phase circuit with copper busbars. These two busbars with 0.14m spacing were located 0.25m below the shield. The current injected was 300 amperes and the frequency is 50 Hz.

At one end, the busbars were connected to the current-injection part while the other end was shorted. The current injection equipment consists of three 220/3.5V step down transformers, three auto-transformer and a harmonic generator for controlling the applied current. It can generate both three-phase or single- phase currents. To reduce the leakage field generated by the injection part, the three steps down transformers were enclosed in a large metal box as in the trunking experiment. The background field level was below 2mG.

This setup can generate magnetic field that tangential and normal to the shield when placing the busbars vertically or horizontally respectively (figure 6.6 and 6.7). The magnetic flux density at points of interest over the metallic sheet was measured and then the shielding effectiveness was calculated.

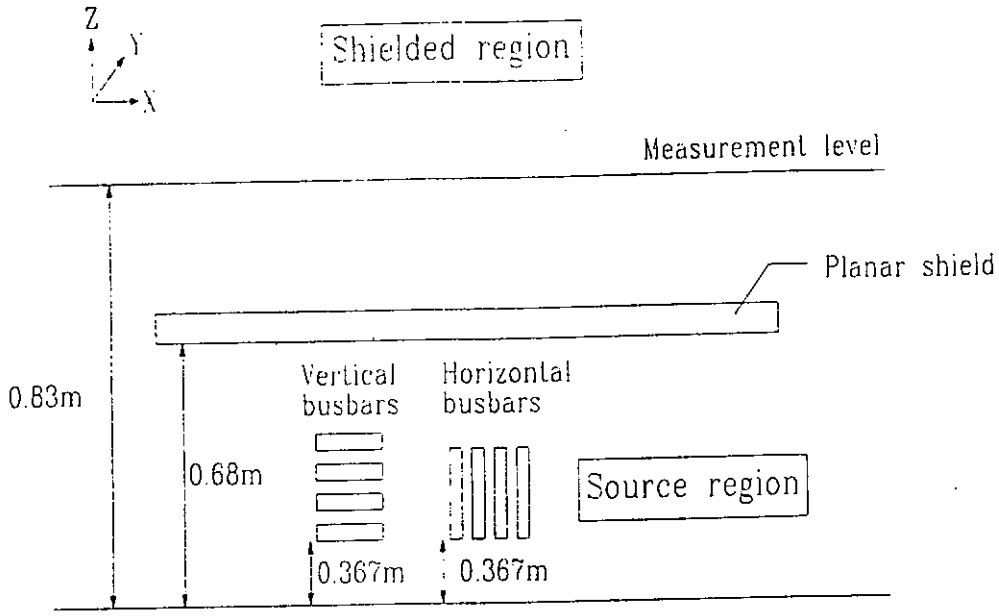

Figure 6.5 Setup of experiment

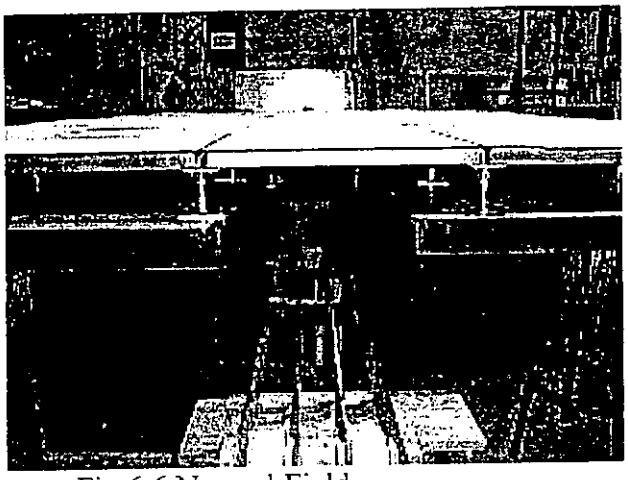

Fig 6.6 Normal Field

Fig. 6.7 Tangential field

6.4 Material Impact

Magnetic flux densities were measured along the Z-direction at the center of the sheet. A comparison was made with the results calculated by using the commercial software based on BEM. Figure 6.8 and 6.9 shows the measured and the simulated shielding effectiveness of the aluminum and the galvanized iron against the distance from the shield with different source orientations. The thickness for the aluminum

and galvanized iron sheets were 1.5mm. For the aluminum sheet (figure 6.9), there is a large variation in the pattern of shielding effectiveness with various source orientations. When the incident field is tangential to the shield, the shielding effectiveness is flat near the shield and then increases gradually. However, the shielding effectiveness drops rapidly at the beginning and then starts increasing slowly when the incident field is normal to the shield. A point to notice is that the shielding effectiveness is very sensitive to the source orientation. In table 6.1, the variation of shielding effectiveness against the orientation at 0.98m above the shield is compared. The shielding effectiveness of aluminum is much smaller for the normal source field than the tangential one. The shielding performance is doubly efficient when the source field is normal to the shield.

For the galvanized iron sheet (fig. 6.8), the trends of the shielding effectiveness for both source orientations are almost the same. Both curves have saturated at further away from the shield. The influence of the source orientation is much smaller. It has a smaller shielding effectiveness when the field is tangential than the normal. As shown in table 6.1, the difference is only 10%.

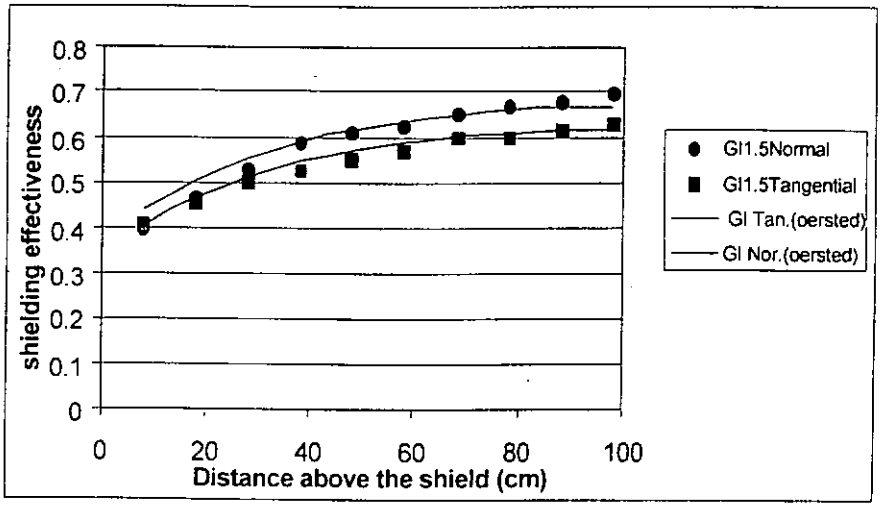

Fig.6.8 Measured and the simulated shielding effectiveness of the galvanized iron

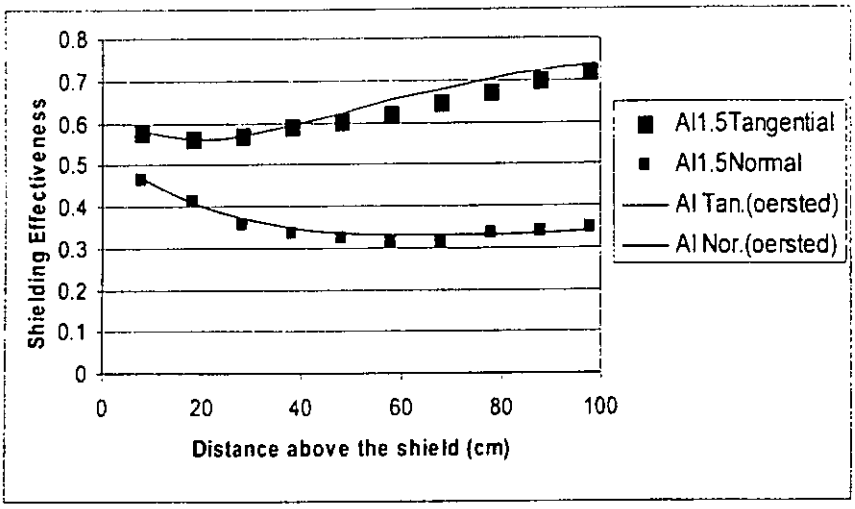

Fig.6.9 Measured and the simulated shielding effectiveness of the aluminum

	Normal Field	Tangential Field
Aluminum	0.39	0.71
Galvanized Iron	0.62	0.69

Table 6.1 *SE* of material with different source orientation at 1m from the shield

It is interesting to note that aluminum may have the most optimum or the worst shielding performance, depending on the source orientation. In fact, the variation of performance against different orientation is due to the shielding mechanism. Galvanized iron owns high permeability. It provides low frequency shielding by "flux shunting" mechanism. The magnetic flux from the source is compressed into the magnetic material and away from the region to be shield. This method is characterized by its boundary condition, the tangential component of the magnetic field is nearly zero. When the source magnetic field was mainly normal to the shield, with nearly zero tangential magnetic field (generated by scattering), the shield only has a weak effect on the field. However, In the case of the source magnetic field was mainly tangential to the shield with a nearly zero normal magnetic field, since the tangential field is not zero, the magnetic flux is diverted into the shield and the

phenomenon of magnetic shielding is observed. Since GI is a low permeability material, the dependence on the source orientation is not so obvious.

On the other hand, aluminum is a highly conductive material which provides shielding by a mechanism known as "eddy current cancellation", and its boundary condition is the normal component of the magnetic field is nearly zero. When the incident field orientation is tangential to the shield, there is only a small-scattered field in normal direction. Since this is already the boundary condition of the high conductivity shield, there is very little shielding effect. However, when the orientation of incident field is normal to the shield, eddy current will be generated, thereby an opposing field will create to reduced the incident field. Hence, shielding effect is observed.

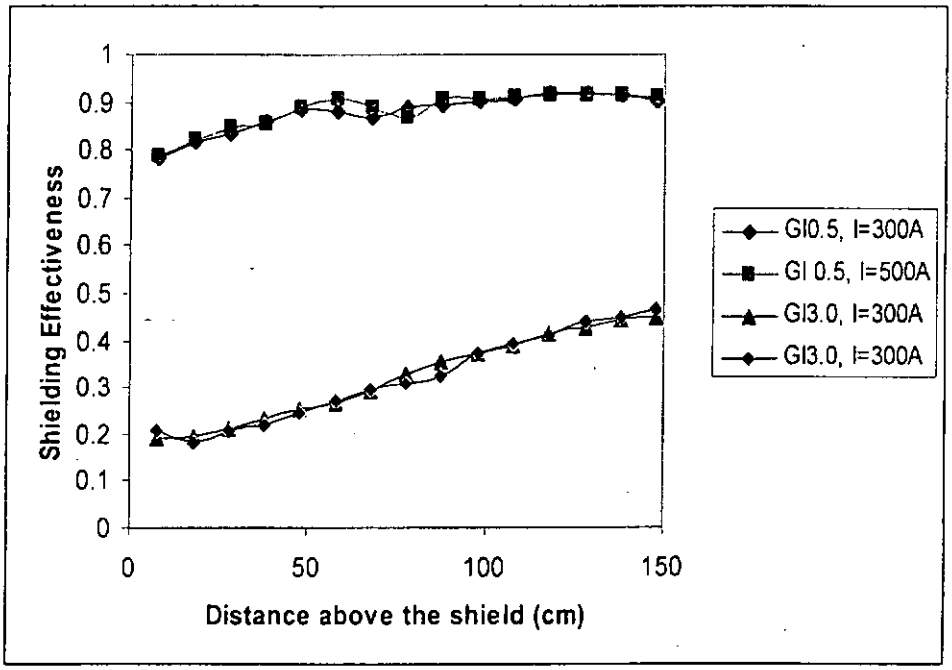

Fig.6.10 SE of GI 3.0mm and GI 0.5mm sheets with different source current applied

For the rectangular shield, the source current is an important factor to the shielding performance due to the non-linear property of the GI. However, as shown in figure 6.10, this impact is not significant in the case of planar shield. Two different

thickness 0.5mm and 3mm GI has been tested. The data shows a discrepancy less than 2% with 300A and 500A current applied. The effect of the source current can be ignored in the case of planar shield.

6.5 Distance Impact

Both distances from the source and measurement point to the shield affect the shielding performance greatly. In the above figure 6.8 and figure 6.9, it can be observed that the value of shielding effectiveness increases gradually as the measurement point moves away from the shield.

On the other hand, the impact of distance from the source to the shield is clearly seen in figure 6.11. Magnetic fields in the center of the shield were measured against a shield with a source distance of 0.5m, 0.6m and 0.8m from the shield. It is observed that the shielding effectiveness is slightly higher at larger distance. It is because the field at the measurement point is increasingly dominated by the flux leakage around the edges of the shield with the larger distance. The performance is better when the source is near the source. However, as mention above, the larger source to shield distance could increase the usable region.

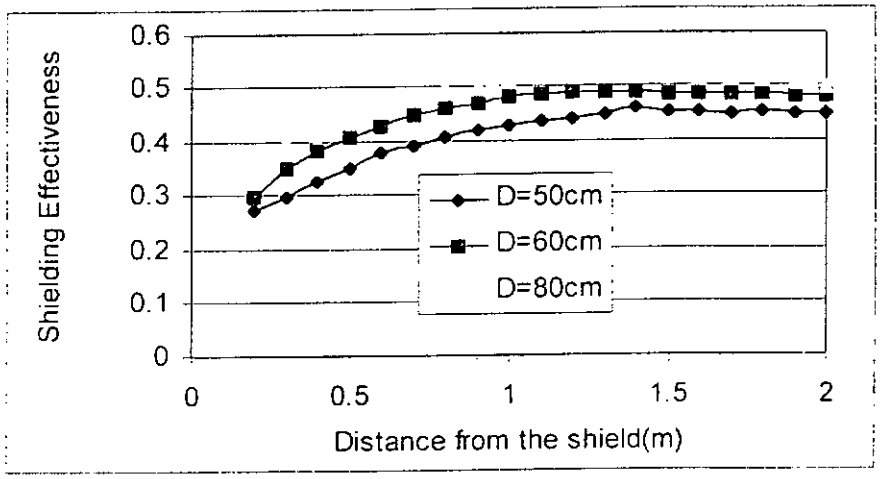

Fig.6.11 The shielding effectiveness with different distances between the source and the shield

6.6 Edge Effect

In section 6.1, the concept on the usable region is based on the compensation of the edges leakage. In the experiment, the edge effect was examined. Magnetic field measurements were conducted along the x-axis across the planar shield. The width of the shield was 1.2m. The edges were 0.6m from the center. Figure 6.12 shows that shielding effectiveness at the 0.6m from the center is much higher than at the center. It may be due to the domination of the leakage field at the edges of the finite-width planar shield. Since the planar shield does not completely separate the source and shielded regions, the magnetic field may leaks through seams or around the edges of the shield apart from the field penetration. Near the center, the magnetic field is mainly contributed by the penetration mechanism, with a very small portion of the leakage field. The portion of the leakage field becomes greater and greater from the center to the edges. Near the two edges, the shield has only a minor or no shielding effect. Besides the two edges, shielding effectiveness is even greater than 1. It implies that there exists an enhancement of magnetic fields. The shield may induce a negative effect to the vicinity of the shield. The location for an object need to be shielded is vital and should be carefully selected. Therefore, it is important to consider the concept of the usable area in the shield design.

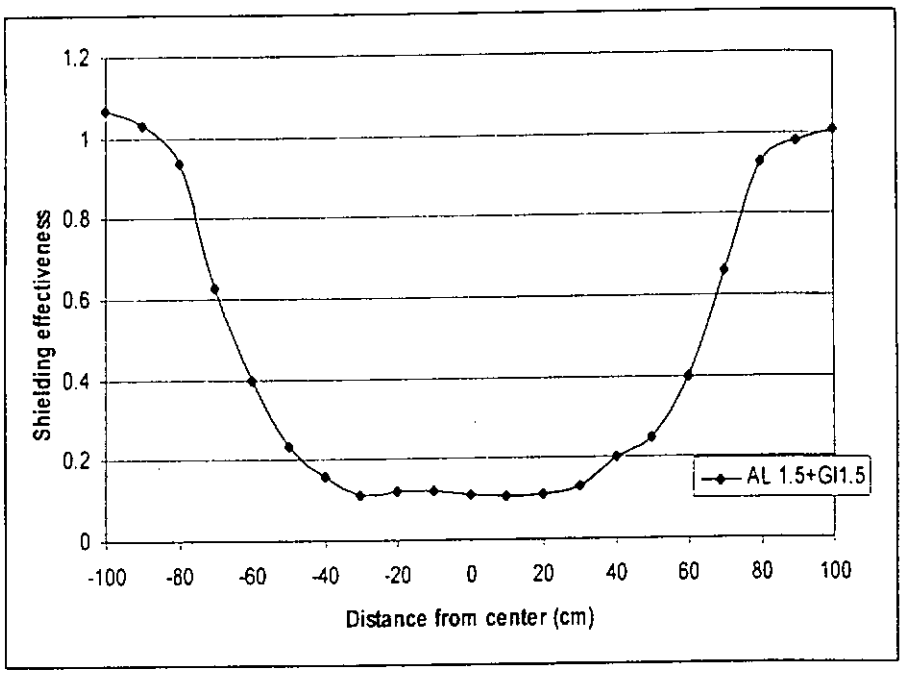

Fig.6.12 The shielding effectiveness along the height of the planar shield

6.7 Multi-layers Shield

A shield of the required thickness can be constructed from thin sheets of the same material. The thinner the material the easier it is to handle during the installation. It can also be constructed from layers of different materials with different physical properties such as a combination of materials with high permeability and high conductivity

As discussed in 6.4, the aluminum may have the optimum or worst performance depends on the orientation. In this section, the shielding performance of the double-layers shield combined with different material properties is examined. In the experiment, the combination shields of total thickness 3mm with different portions of aluminum and galvanized iron were tested. The results are shown in the figure 6.13 and 6.14 for the magnetic fields are tangential and normal to the field respectively. The magnetic flux densities were measured along the center of the plane.

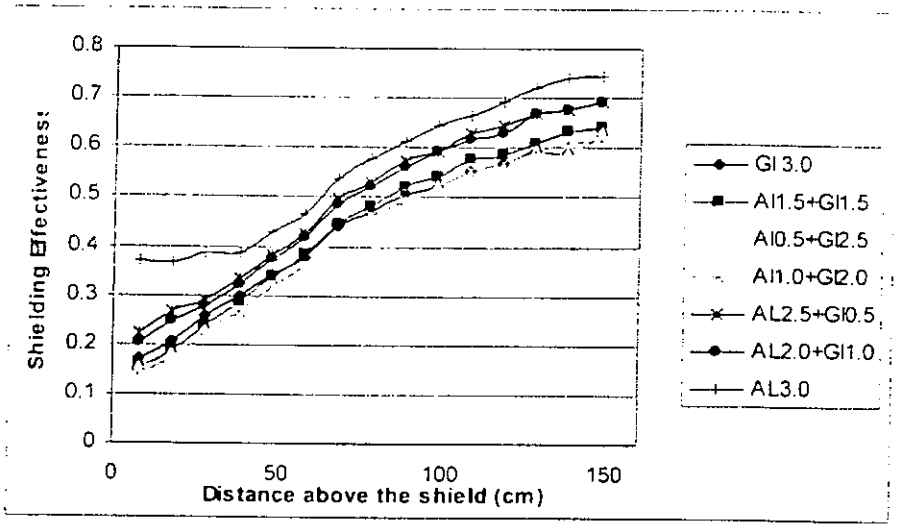

Figure 6.13 SE against different portion combination in a tangential source field

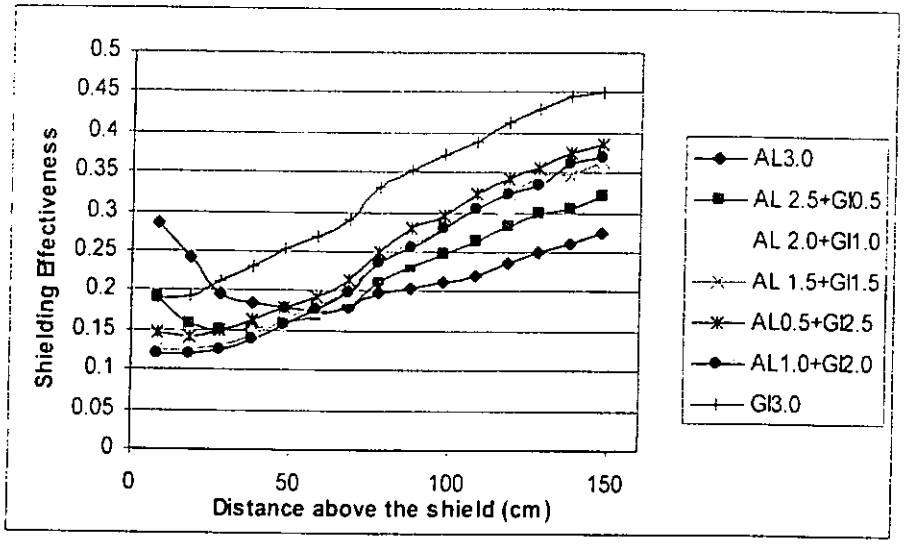

Figure 6.14 SE against different portion combination in a normal source field

For the field in normal direction (fig. 6.14), the shielding effectiveness near the shield is smaller as the portion of aluminum decrease. The combination of Al 1mm and the GI 2mm perform the best at this stage. However, this trend takes a reverse after the distance is about 0.6 m away from the shield. The thicker the aluminum, the smaller the shielding effectiveness (better shielding performance). The aluminum with thickness 3mm shield has the best performance the further away the shield.

For the tangential field (fig. 6.13), the shielding effectiveness is smaller as the portion of aluminum decreases. Moreover, this trend is maintained as the distance increase. The optimum is occurring when the portion of aluminum is 1.0mm. The worst case is occurred when aluminum with thickness 3mm although it has the best performance on the above case. It can be seen that the combination of Al 1mm and the GI 2mm has the best performance. Multi-layers shield composed of high conductivity and high permeability can provide enhanced shielding over shields composed of only a single layer.

When the source orientation is unknown, it is difficult to decide what kind of material should be use for shielding. Multi-layers shield composed of high conductivity and high permeability can provide enhanced shielding over shields composed of only a single layer and independent to the source orientation. Hence, no matter what orientations of the magnetic field, conductive material and permeability material can be used together as an effective planar shielding in a variety of applications incorporated in the design for magnetic shielding.

6.8 Joint Method

In practice, the metallic sheet has finite dimensions. For shielding a large area, several metallic sheets are connected piece by piece. Undoubtedly, there will be leakage field flow through the joint seam. The leakage from the seam will affect the shielding performance if it is significantly large. In this section, the influence of leakage from the seam has been examined. An experiment was conducted to investigate the shielding performance of the joint seams, and the other bonding method for compensation.

Fig.6.15 shows different tested condition on seam connection of the metallic sheets. There are three cases have been tested as shown in the figure.

Case 1. No connection

Case 2. Overlap 20cm and clamped by screw

Case 3. Overlap 20cm

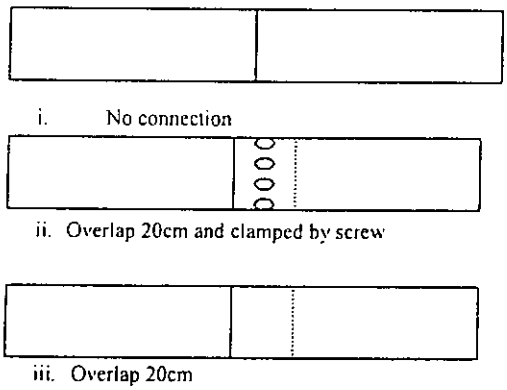

Fig.6.15 Connection of the shields

Both Al and GI sheets with thickness 2mm were used in the experiment. The tested sheets are connected as the above conditions. Magnetic flux densities were measured along the center of the seam and compare to the one along the center of the sheet. Measurement results are shown in Fig.6.16 to 6.19. It can be observed that there is commonly a larger difference between the values from the center of the sheet and the seam position with no connection. That implies that the leakage dominates the penetration at the seam position if no compensation work has been done. This leakage would reduce the total shielding performance of the planar shield. After the overlapping is applied, except for the aluminum in the normal incident field condition, the differences among the center of the sheet, the center of the seam with or without screw are small in all cases. Of course, the shielding effectiveness with

the screw is lower than the one without screw. The results reveal that the overlapping at the seam position can compensate the leakage at the seam to maintain a constant performance along the sheets.

For the aluminum in the normal incident field condition, the differences are rather large among the center of the sheet, the center of the seam with or without screw as shown in figure 6.17. In this case, the compensation by the overlapping is not enough for the leakage at the seam position. Other additional compensation methods, likes using aluminum tape may be considered.

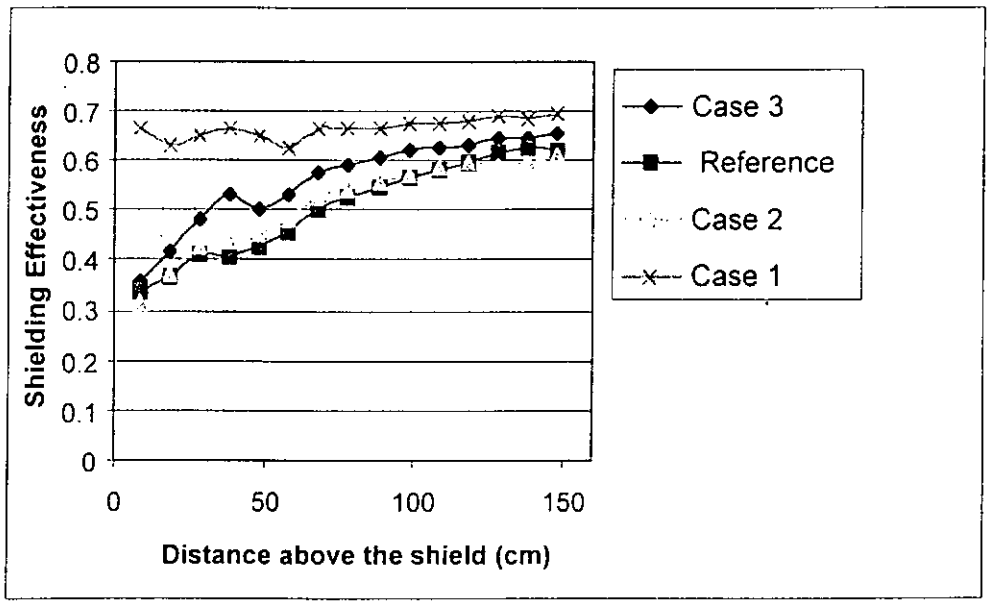

Fig.6.16 Shielding effectiveness of GI in normal field

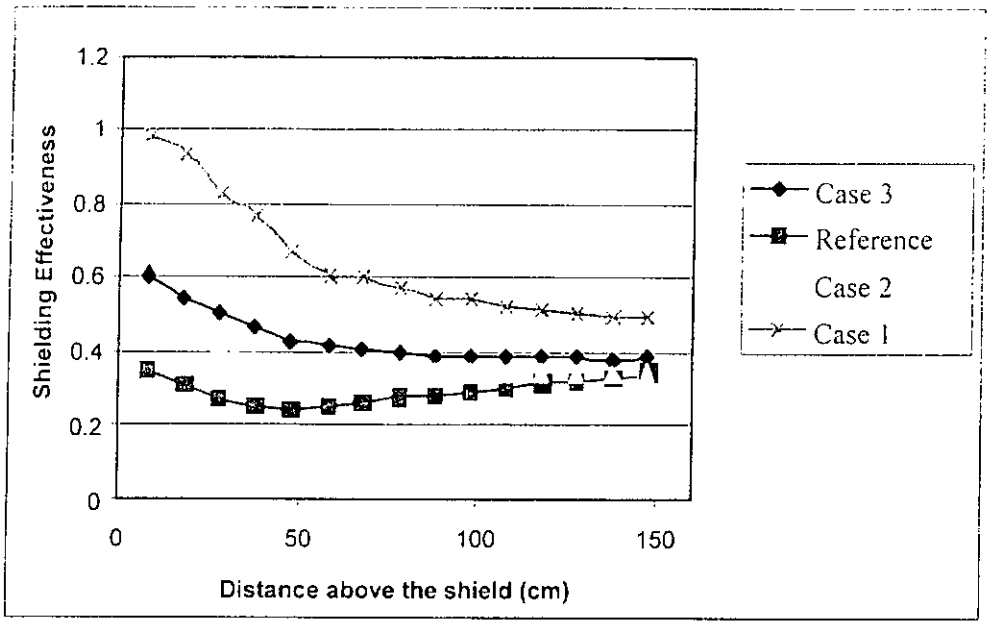

Fig.6.17 Shielding effectiveness of Al in normal field

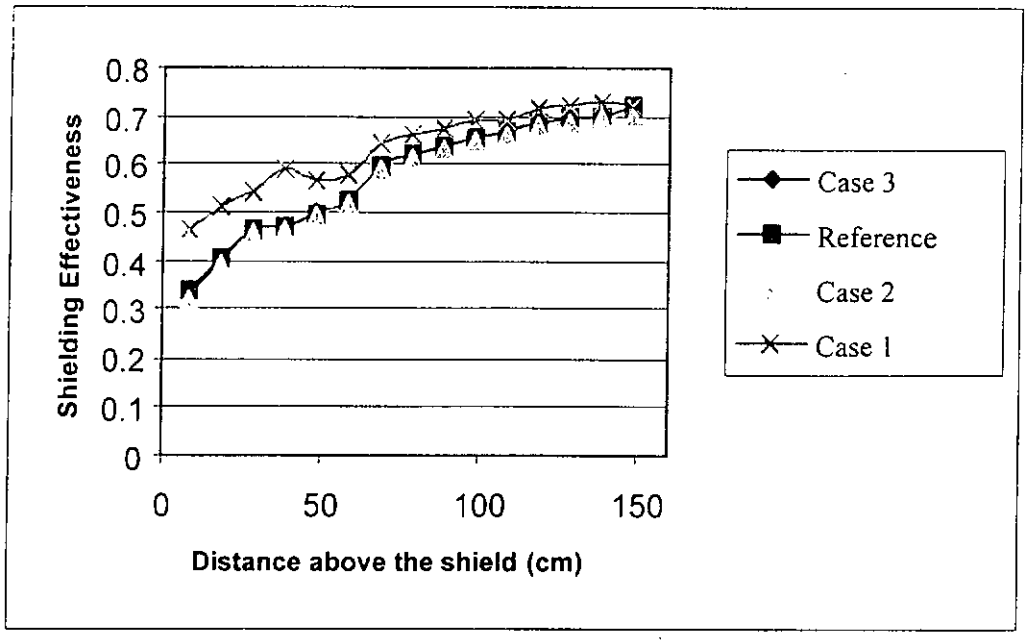

Fig.6.18 Shielding effectiveness of GI in tangential field

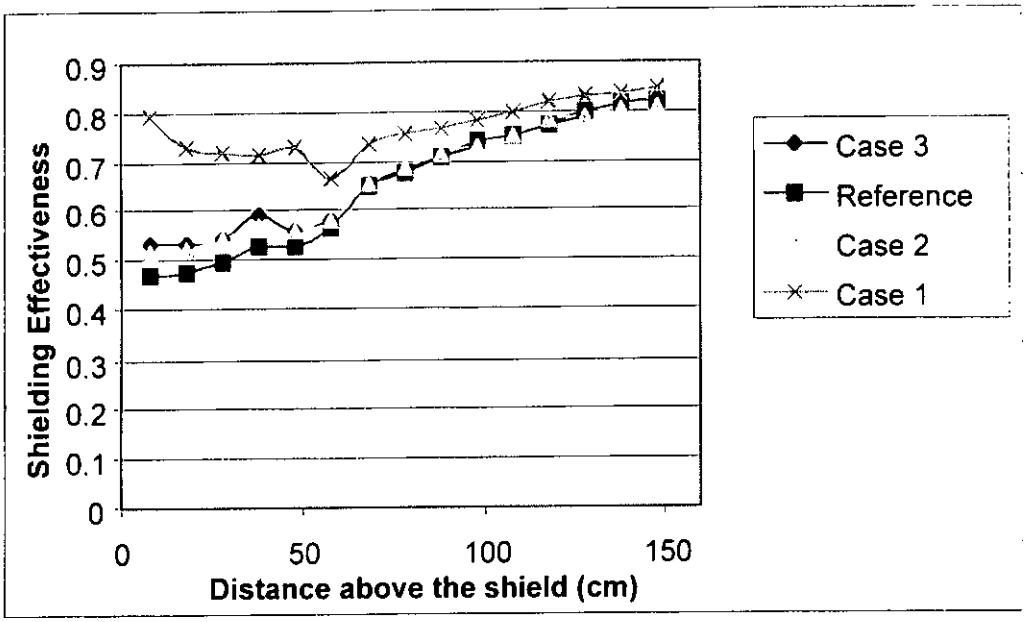

Fig.6.19 Shielding effectiveness of Al in tangential field

CHAPTER 7 CONSIDERATIONS ON THE SHIELD DESIGN

The shielding properties of the rectangular shield and the planar shield have been discussed in previous chapters. These findings are very useful to design a cost-effective shielding in real applications. Besides, there are some others factors must be considered. In this chapter, the application of these properties in shielding design will be discussed. Some guidelines on the design process will be given It will also discuss how it can be compatible with practice with illustrated examples.

7.1 Design Process

Figure 7.1 is the flowchart for the design process of magnetic shielding. Economic factor is always the first priority to consider for every case. In practice, there are some common ELF magnetic field mitigation techniques, which are more economic than magnetic shielding. Magnetic shielding should only be recommended if these less expensive options will not provide the desirable degree of field reduction. The second process is the selection of the use of the planar shield or rectangular shield. The selection is based on the sources of the magnetic field, the nature of the area to be shielded. Planar shield is usually used for shielding larger sources such as, transformer rooms or the affected room while rectangular metallic enclosure are frequently used to house cables or busbars in electrical installation systems.

For the design process of the trunking and planar shield, there are many parameters involved. For example, size, thickness and material, etc. All these parameters are significance to the shielding performance. To optimize the shielding ability of the magnetic shield, selection of these parameters must be carefully taken. In section 7.3 and 7.5, some guidelines have been given for the design of the trunking and the planar shield respectively.

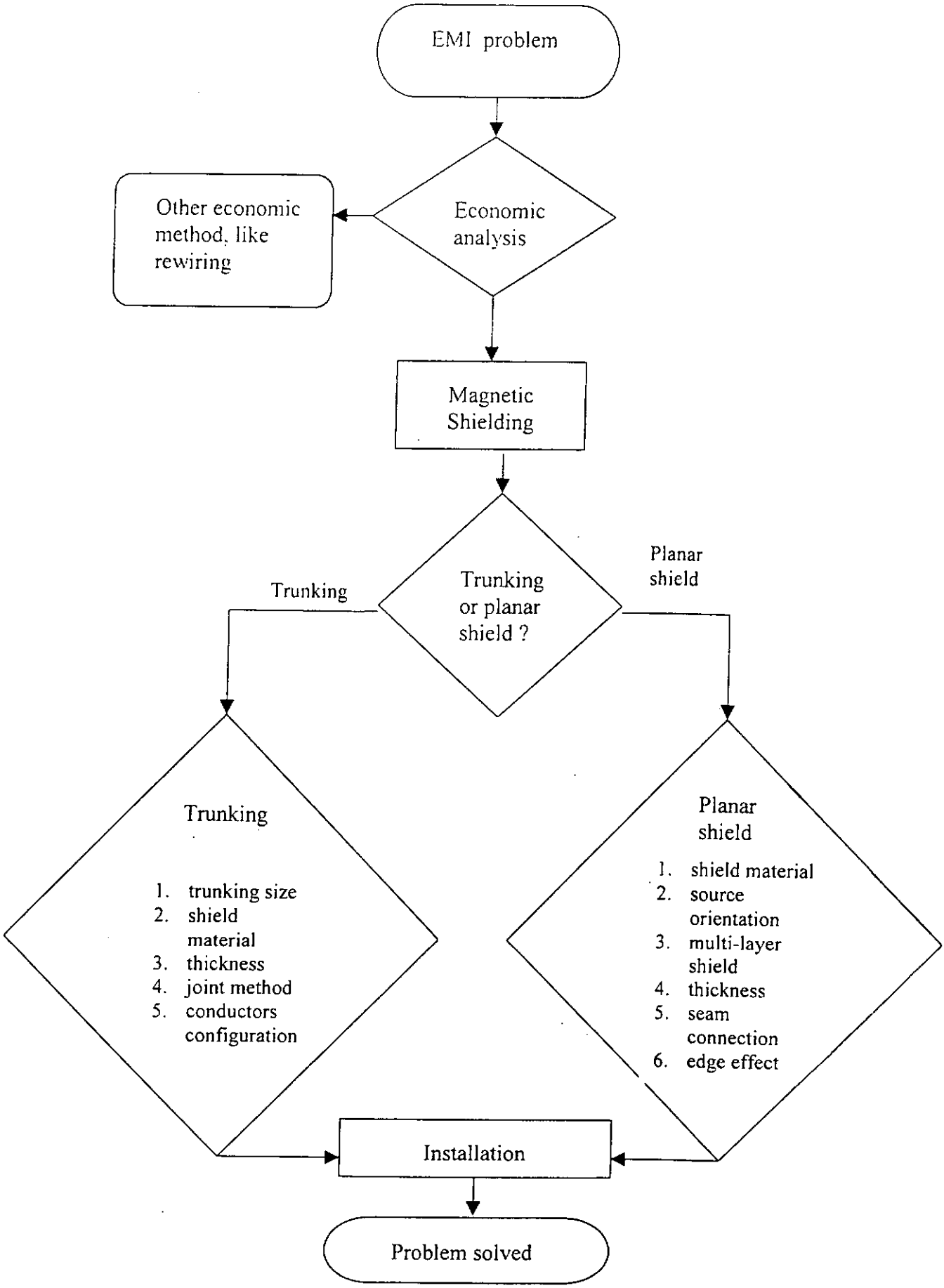

Figure 7.1 Flowchart of the design process

7.2 Economic Analysis

In applying various mitigation measures, a primary concern is to minimize the cost of such measures. The cost of applying mitigation techniques must be higher for existing installations than in the early stage of new installation. Therefore, careful consideration must be taken before employing any measures. Shielding is one of many available methods of mitigation of ELF magnetic fields and its application in preference to other techniques should be evaluated on a technical and economic basis. However, magnetic shielding is always more expensive than other measures. Except the directs costs of materials and installation, other intangible costs such as the cost of down time of power supply or cost of utilizing valuable office space for installation should be considered.

Different materials exhibit different degrees of shielding effectiveness and have different cost associated with their purchase and installation. Hence, a choice of one type of material in all shielding applications may not be economically justified.

The shielding of a large area like an affected room is a very expensive mitigation option. It should be recommended if all other measures, such as rewiring cannot provide the desired degree of field reduction. In such cases, the materials cost will play a more important role. For example, the costs of shielding a substation room using different material with dimensions 8m x 4m x 4m are compared on Table 7.1. Aluminum, galvanized iron and mumetal are the shielding material commonly used in many applications. The high-resolution video cameras and displays always have Mumetal shields to minimize distortion errors to ensure high quality recording and playback. Although it has a better performance than the others, the costs is prohibitive due to the basic cost of the metal sheets. Comparing to mumetal, the

costs of aluminum and galvanized iron are much more reasonable. Therefore, aluminum and galvanized iron are recommended to use for shielding against the large area unless they cannot provide the shielding performance that mumetal does.

Material	Mumetal	GI	Al
Thickness	1.6 mm	1.5 mm	1.5 mm
Dimension	8m x 4m x 4m	8m x 4m x 4m	8m x 4m x 4m
Cost	$ 2340000	$ 9111	$ 10444

Table 7.1. The costs of shielding a room with different materials

7.3 Considerations on the Design of Trunking

Where a large number of cables have to be installed, or where the cable sizes are large, it is often preferred to use cable trunking. In commercial, trunking is rectangular in cross-section and is mainly made from galvanized iron. There are many variations of the trunking system, which has a full range of fittings and accessories to enable it to meet the specification of any installations. Trunking is easy to erect. It can be screwed direct to walls and suspended across trusses. When the run is vertical, pin racks should support the cables. Because the trunking forms part of the earth-continuity conductor arrangement in the installation, it is necessary to ensure that all sections are bonded together.

In the past, the shielding effect of the trunking was seldom a consideration in electrical installation design. Therefore, the trunking is usually made of the low permeability galvanized iron for the sake of cost. For enclosing the cables or busbars which may cause a significant ELF magnetic field, the corresponding size of the trunking is in the range of 100mm-300mm wide, 100mm-200mm high. The thickness of the metallic trunking is generally limited to sizes up several millimeters. In general, the cables or busbars are installed parallel to the width of

the shield. Here are some factors needs to be considered in the design of trunking.

7.3.1 Trunking Size

The first parameter to be decided on the design is the trunking size. In commercial practice, the cable sizes for the distribution of large currents are shows in the tables 7.2. The cable capacity of a trunking is determined by a "Space factor method "as described below [39], and the space factor shall not exceed 45% of the net internal cross-sectional area of the trunking.

Space factor method:

i. For each cable it is intended to use, obtain the cross-sectional area of cable from table 7.2. [40]

ii. Add the cross-sectional areas of all cables and divide by 0.45 for a space factor 45%.

iii. Select a trunking whose cross-sectional area is equal or larger than the value obtained from (2) above.

Conductor area (mm^2)	Cross-section Cable area(mm^2)	Current Carrying Capacity (A)
35	95	156
50	133	189
70	177	240
95	227	290
120	283	336
150	346	375
185	434	426
240	551	500
300	683	573
400	881	683
500	1075	783
630	1320	900

Table 7.2 Overall cross-sectional areas and current-carrying capacity for single-core cables

In practice, the common size of the trunking is shown in the following tables 7.3.

Trunking size (mm) Width (w)x Height (h)	Trunking Thickness (mm)
100 x100	1.4
150 x 75	1.2
150 x 100	1.2
150 x 150	1.6
200 x 75	1.6
200 x 100	1.6
200 x 150	1.6
200 x 200	1.6
225 x 75	1.6
225 x 100	1.6
225 x 150	1.6
225 x 200	1.6
225 x 225	1.6
300 x 75	1.6
300 x 100	1.6
300 x 150	1.6
300 x 200	1.6
300 x 225	1.6
300 x 300	2.0

Table 7.3 Common size of trunking

In previous chapter, it was reveal that the shield size has various influences on the performance with high permeability material and high conductivity material. When the trunking is made of permeability materials, the shield size should be chosen as small as possible without violates the space factor method. The shielding performance will be better for a smaller size ferromagnetic trunking since it enjoys an additional shielding effect by increasing in relative permeability. On the other hand, the choosing of trunking made of conductive material should be utilizing the space allowed as much as possible. The shielding performance is increasing proportional to the shield size. Both measures can provide a better shielding performance.

7.3.2 Shield Material

The second parameter is the selection of material. Galvanized iron trunking is commonly used for enclosing cables and busbars in low-voltage installations because of cost. In fact, there is another substitute, aluminum. This high conductivity material shows comparable shielding ability to the GI. The materials cost of these two materials is nearly the same. Moreover, there are several advantages over the GI. First of all, it is lightweight. The installation work is easier to process. The second advantage is related to the shielding characteristic. Differ to galvanized iron, it owns higher shield ability with increasing shield size. A larger space inside the trunking can be served as allowance for expansion in conditions of higher temperature. Impedance of the conductors is larger when the shield size is small. A larger space leads to a reduction in the impedance of conductors. Hence, a less voltage drop is obtained. The most important is the prediction of the shielding performance is much easier and accurate than the GI trunking. It makes the design work more convenient.

7.3.3 Shield Thickness

After the selection of the shield size, the thickness of the shield should be considered. It is undoubted that increasing the shield thickness will always benefit the shielding ability of a shield. However, a choice of the thickest shield in all trunking applications will not be justified. A metallic sheet is difficult to form or machine if it is too thick. It will not only increase mechanical load onto building, it also increases the difficulty of installation. In practice, the trunking thickness is always less than 2mm. For trunking shield design, increasing shield thickness to achieve a better shielding performance is not recommend unless other variations of

shield parameters cannot satisfy the requirement. If it is inevitable, it is wise to use a lightweight material like's aluminum or consider the possibility of the double layer-shield.

7.3.4 Joint Method

When there is no connection between trunkings, the leakage from the joint is about 5% compare to the middle of the trunking. Although the difference is within 5 %, bonding between different section of trunking is a must. It is because the trunking form parts of the earth-continuity conductor arrangement in the installation, it is necessary to ensure that all sections, forming the current protective conductors of the system are bonded together. Other than copper washer or the GI plate, it can also connected by running a separate conductor in the trunking and bonding this wire to the trunking itself.

7.3.5 Conductors Configuration

As shown in the pervious chapter, the *SE* will be smaller as the conductor spacing increase or a configuration that will benefit a higher flux to the shield. However, it is not recommend having these configurations in practice even though it has a lower *SE*. For the necessary to provide a higher flux within the trunking, these configurations will need to generate a greater source magnetic field. Although the shielding ability is improved, the magnetic field outside the trunking would not be reduced, since the source magnetic field has an increase at the same time, too.

7.3.6 Guidelines on the Design Process of Trunking

- The trunking size is decided by the space factor method.

- For trunking made of permeability materials, the shield size should be chosen as small as possible without violates the space factor method. On the other hand, the choosing of trunking made of conductive material should be utilizing the space allowed as much as possible. Both measures can provide a better shielding performance.

- Aluminum is a new substitute to the common shield material galvanized iron. This high conductivity material shows comparable shielding ability to the GI and has several advantages over the GI.

- In practice, the trunking thickness is always less than 2mm due to weight constraint. Increasing shield thickness to achieve a better shielding performance is not recommend unless other variations of shield parameters cannot satisfy the requirement.

- As trunking form parts of the earth-continuity conductor arrangement in the electrical installation, bonding between different sections of trunking is a must. Other than copper washer or the GI plate, it can also connected by running a separate conductor in the trunking and bonding this wire to the trunking itself.

- Thermal dissipation, voltage drop and variation of impedance of the conductors are also needed to consider when using trunking

7.4 Illustration of Design Procedure

With knowledge on the different impact on the design parameter, parametric design of rectangular shield is feasible. The discussion in the following demonstrates how these shielding characteristics are applied in the design process.

In typical office building, vertical cable risers are installed in the electrical room on each floor for providing convenient tapping-off points. Suppose the current carried by a pair of vertical cables is 800A by a single-phase circuit with one diameter spacing. If the cables are not enclose in the trunking, the surrounding ELF magnetic field will be 147mG at about 1m, 36.86mG at 2m, 9.2mG at 4m and 2.3mG at 8m from the cables. Within the 4m from the electrical room, the area is immersing in ELF magnetic field nearly 10mG. ELF magnetic field interference to office equipment may occur in this area. Therefore, it is necessary to use a rectangular GI shield to enclose the cables for mitigating this unwanted field.

According to tables 7.2, the conductor area capable to carry 800A is 630mm^2. Since it is a single-phase circuit, the total cross section cable area is 2640mm^2. By dividing space factor 0.45, the values become 5870mm^2. According to the "space factor method", the cross-sectional area of the selected trunking must be larger than 5870mm^2. From table 7.3, all the trunking satisfy that condition. According the discussion in the pervious section, a smaller size GI trunking has a better shielding performance. The selection of the size should be as small as possible. However, the width of the cables configuration is over 150mm, therefore, the 200mm x 100mm (w x h) trunking is selected. The relative permeability is estimated as 550. After the selection of the shield size, the thickness of the shield should be considered. In

chapter 5, it reveals that the shield thickness will not vary the equivalent relative permeability. The equivalent relative permeability remains constant for different thickness shield. From the empirical formulas, the shielding effectiveness is 0.27 for 1mm, 0.188 for 1.5mm and 0.153 for 2mm thick trunking. Obviously, the shield thickness always benefits the shielding ability of a shield. However, a thicker shield implies a heavier mechanical load, it also increases the difficulty of installation and the material cost. Hence, a choice of the thickest shield in all trunking applications may not be justified. The magnetic fields for different thickness trunking applied are shown in table.7.4. In this case, trunking with thickness 1.5mm is enough for the mitigation. It mitigates the ELF magnetic field to 7mG at 2m, 1.7mG at 4m and 0.4mG at 8m.

The shielding performance can be further improved by increasing the equivalent relative permeability of the GI trunking, such as increasing the conductor spacing. However, it is not recommend for implementation. Although the shielding ability is improved, the actual field level of the ELF magnetic field outside the trunking would not be reduced, since the source magnetic field has increased simultaneously.

Thickness	1mm	1.5mm	2mm
Magnetic Field at 1m	39.7	27.6	22.4
Magnetic Field at 2m	10	7	5.63
Magnetic Field at 4m	2.4	1.7	1.4
Magnetic Field at 8m	0.6	0.43	0.35

Table 7.4 Magnetic field (mG) from trunking with different thickness

7.5 Considerations on the Design of Planar Shield

For the design of the planar shield, there are several parameters: shield material, source orientation, multi-layer shield, shield thickness, seam connection and the edge effect. Here are some discussions on the selection of these parameters.

7.5.1 Shield Material

Aluminium, galvanized iron and mumetal are common shielding materials. Due to the planar shielding always involves in large scale shielding design, expensive shield material likes mumetal is seldom used. It will only consider unless other materials cannot achieve the required mitigation. In practice, galvanized iron and aluminium are usually used for planar shielding. Low carbon steel is also preferred for new construction because of its relatively low material cost and shielding properties, particularly for ELF.

Shield materials may have different properties due to its shielding mechanism. For ELF magnetic shielding, galvanized iron and aluminium are characterized by different boundary conditions due to their different shielding mechanism. Galvanized iron (GI) is permeability material, which the magnetic field tends to zero at its boundary. When the incident magnetic fields from the source are mainly normal to the shield and the tangential magnetic field is nearly zero, the high permeability shield may has little effect on the field. However, if the incident magnetic fields from the source are mainly tangential to the shield, the shield will disturb the field due to its nature, and shielding effect is observed.

High conductivity material, like aluminum, has another shield mechanism termed "eddy current cancellation". This mechanism is characterized by the fact that the normal component of the magnetic field tends to zero on its boundary. When the magnetic fields from the source are tangential to the shield, the shield may have very little shielding effect in normal direction. On the other hand, a significant shielding will be occurred when the orientation of the magnetic field is mainly normal to shield. Thus the eddy current will be created opposite to the magnetic field, so that it will reduce the external magnetic field.

Due to the shielding mechanism, a suitable match between the source orientation and the shielding material is a key point to enable full utilization of the shield potential. High permeability material performs better if the magnetic field is mainly tangential to the shield, while the high conductivity material is more suitable for a normal field.

7.5.2 Source Orientation

In above section, it was indicated that the match between shield materials and source orientation is an important factor for the shielding performance. Therefore, it is necessary to know the source orientation before choosing the material. In previous chapters, power distribution cables and busbars are modeled as line sources since they are relatively long and run in parallel. If the shielding of a planar shield is against this type of source, the source orientation can be easily recognized. However, for a point source likes transformer or other equipment, a measurement of magnetic field may be needed to determine the dominant source orientation.

7.5.3 Multi-layer Shield

Sometimes, due to the complex geometry of the source, it is very hard to find out the source orientation. When the source orientation is an unknown, it is difficult to decide what kinds of material are suitable for shielding. In section 6.7, a multi-layers shield composed of conductivity and permeability can provide enhanced shielding over shields composed of only a single layer and independent to the source orientation. Moreover, the shielding performance is comparable to the expensive shielding materials likes mumetal. Hence, no matter what orientations of the magnetic field, conductive material and permeability material can be used together as an effective shielding material in a variety of applications, and is most economical when incorporated in the design for magnetic shielding.

7.5.4 Decision on Suitable Thickness

It is clear that the shielding performance can be improved by increasing the shield thickness. Although the increase in thickness can achieve better shielding performance, choosing a suitable thickness is crucial. For example, increasing a GI planar shield thickness means increasing its weight and difficulty in the installation work. A higher installation cost may result. When the shield thickness is to be thicker than 2mm in the planar shielding design, it is recommend constructing from several layers of thinner sheets of the same material. The thinner the material the easier it is to handle during the installation. It can also be constructed from layers of different materials with different material properties, such as a combination of

materials with high permeability and high conductivity, for enhancing the performance.

7.5.5 Consideration of Seam

In practice, all planar shields must have finite leaks where penetrations and seams occur in the boundary of the joint. The shielding effectiveness at the seam position is very dependent on how the metallic sheets are jointed. The best seam is one that is continuous both in terms of metal composition and continuity of the seam. For example, welded seam is the most reliable. However, it is expensive since the materials must have a certain thickness, and not applicable to all materials. Clamping or soldering are other possible methods of jointing.

As planar shielding is constructed from plates or sheets, it is important to account for the effect of discontinuity and joints on its effectiveness. The influence of leakage from the seam has been investigated in the section 6.2.5. It reveals that the overlapping one-sixth of the width and screws clamping at the seam position is enough for compensate the leakage at the seam to maintain a constant performance along the sheet for galvanized iron. For aluminum, this method is not enough to compensate the seam leakage. The difference between the shielding effectiveness at the seam and the center of the sheet is still large after overlapping. Therefore, other additional improvement is needed. For example, use an additional aluminum tape to lap the joints.

7.5.6 Consideration of Edge Effect

In the section 6.2.3, the edge effect of the planar shielding has been discussed in detail. It is verified that the best shielding effect is in the center of the shielding since the portion of the leakage field from the edges are the smallest. Away from the center, there is an increasing shift of the *SE* to the edges. The concept of the usable region can gives a clearer picture of the shielding distribution. In this region, the tolerance of shielding performance is less than 20 % refer to the center position. It is recommended to ensure the object needs to be shield must in that region. Otherwise, a large reduction of shielding effect may results. It also reveals that the tolerance region is strongly dependent on the source to shield distance. Larger sources to shield distance will results a larger tolerance region.

The shielding performance of the planar shields is also a function of the shield width due to the edge effect. A wider shield can lower the portion of the leakage field from the edge. If the shield is small in size, the edge leakage will be dominant at most of the shielded area. If the width of the shield is just enough to cover the source or the shielded object, significant leakage is around the boundary. To reduce this unwanted effect, the width of the planar shield should be designed as wide as possible. Moreover, the objects or areas need to shield should always within the usable region.

7.5.7 Guidelines on the Design Process of Planar Shielding

- A suitable match between the source orientation and the shielding material is a key point to enable full utilization of the shield potential. High permeability material performs better if the magnetic field is mainly tangential to the shield, while the high conductivity material is more suitable for a normal field.
- It is necessary to know the source orientation before choosing the shield material.

- Multi-layers shield composed of conductivity and permeability can provide enhanced shielding over shields composed of only a single layer and independent to the source orientation.

- As planar shielding is constructed from plates or sheets, it is important to account for the effect of discontinuity and joints on its effectiveness. It reveals that the overlapping one-sixth of the width and screws clamping at the seam position are effective compensation methods. Other measures include welded seam and aluminum tap.

- When the shield thickness is to be thicker than 2mm in the design, it is recommend constructing from several layers of thinner sheets of the same material. The thinner the material the easier it is to handle during the installation.

- The location for an object needed to be shield is vital. It is recommended to place the object within the usable region to ensure the tolerance of the shielding performance is less than 20% refers to the center position.

7.6 Raised Floor Panels

In modern offices, raised floors (figure 7.2) are commonly installed for servicing equipment. Likes metallic trunking, the original purpose is not related to the magnetic shielding. Busbars or cables can be installed below the raised floors so that the office environment is more management. Due to its metallic structure, it also demonstrates some sort of magnetic shielding. In practice, the raised floor is made from galvanised iron and concrete. The shielding performance of raised floors has also been investigated. The set-up is similar to the planar shield experiment in chapter 6, magnetic fields were measure from 0.1m to 0.6m along the z-axis at the centre of raised floor. The experiment results show that raised floor having similar shielding characteristic to galvanized iron, as shown in figure 7.3. It is also performs better for a tangential source field. However, the discrepancy for source orientation is smaller than 10%. The shielding effectiveness is varies from 0.6 to 0.8. Although the shielding performance is fair, it can enhance the shielding performance with using other metal sheets as shown in Fig.7.4.

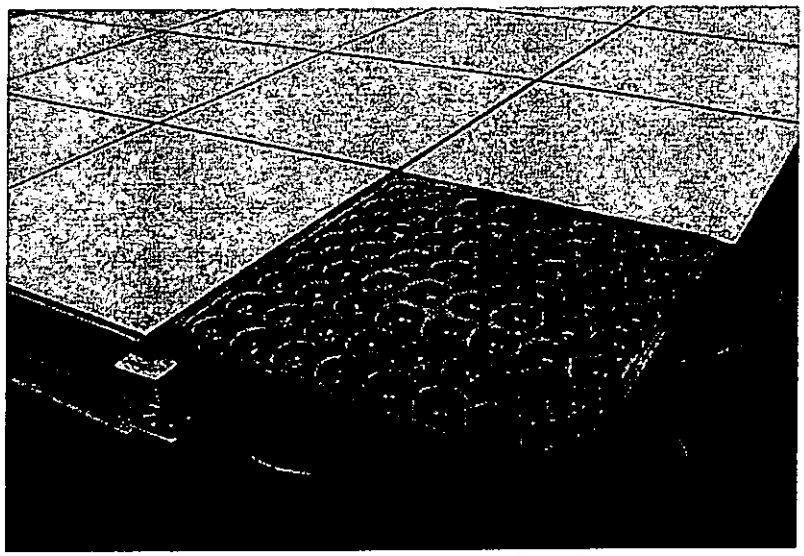

Figure 7.2 Raised Floor Panel

Two galvanized iron sheets with thickness 0.5mm and 1.5 mm were tested with the raised floor present and absent. It is observed that the additional raised floor makes the shielding effectiveness a further decrease. The raised floor panels can help to improve shielding performance significantly if it is installed together with other suitable metallic sheets in buildings. Therefore, the concept of the raised floors should be considered since no additional cost is needed.

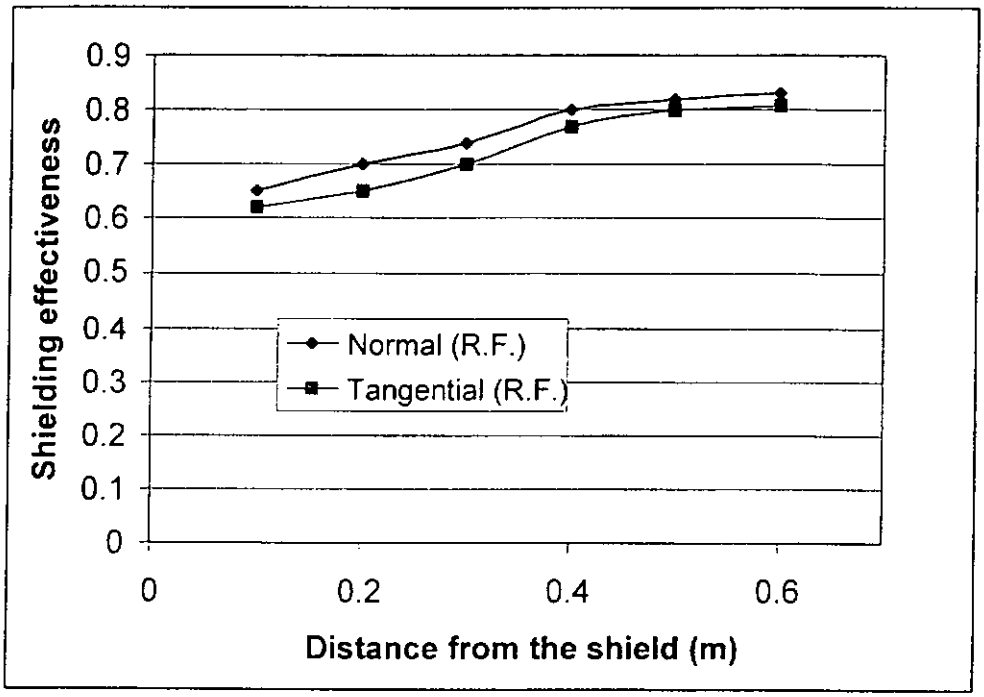

Fig.7.3 Shielding effectiveness of raised floor

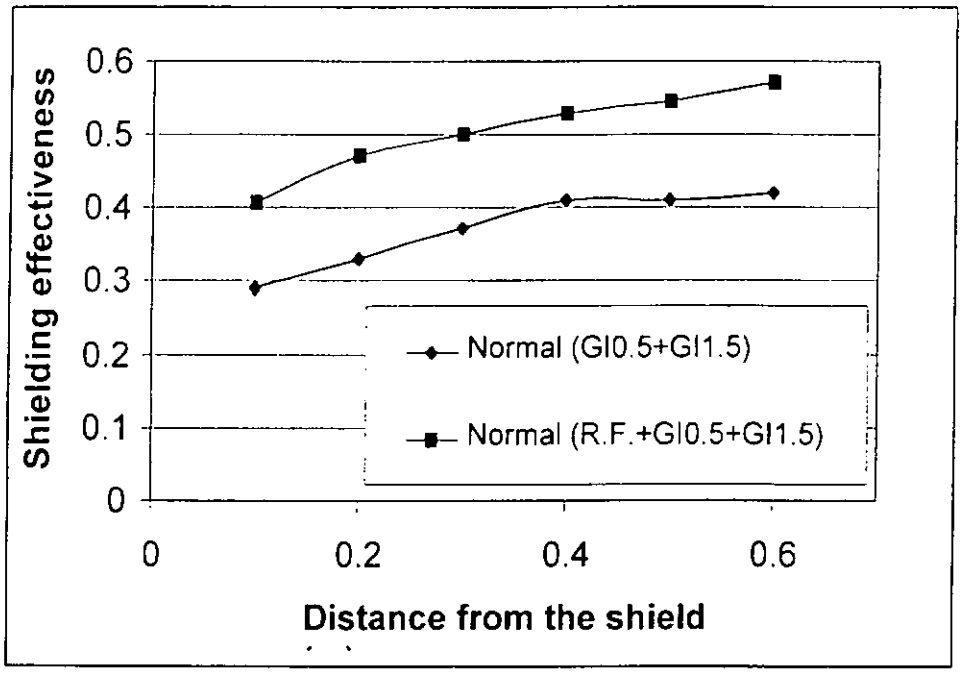

Figure 7.4 Comparison of shielding effectiveness with additional raised floor added

7.7 Planar Shield Design

With a clear picture about the shielding characteristics of the planar shield, the design of the planar shield should be easier. Moreover, the shielding design could be more efficient if it can take advantage of the known characteristic. In this section, it will discuss how to apply these properties to the shielding design. The improvement by utilizing the shield characteristics in the shield design is addressed by making comparison with typical design in practice.

In commercial practice, because of insufficient planar shielding information or data are available. GI or low-μ carbon steel was always chosen in most of the shielding application for the sake of cost. In fact, the shielding performance of planar shields can be further improved by suitable design. In the following section, it will illustrate how to increase the shield performance by utilizing the shielding characteristics discussed above with a simulated model.

As shown in Fig. 7.5, the source of the model is a pair of spaced line sources (spacing 20cm) carrying currents of equal magnitude and opposite direction. The area needs to be shield is 4m wide. In common practice, the width of the planar shield will be set as 4m, just cover the area needs to be shield. The shield thickness is 3mm and the shield is 1m from the source. The current carried by the conductors is 500A. The shielding effectiveness values were calculated at 0.5m above the shield at 0m, 1m, 2m and 3m from center.

In chapter 6, it reveals that a suitable match between the source orientation and the shielding material is a key point to enable full utilization of the shield potential. As shown in table 7.5, aluminum has a better performance than using the GI as shield material in the simulation case. It is because the source generates a field mainly normal to the shield. In this situation, conductive material will have a better performance. Therefore, the match between source orientation and the shield material is very important. The source orientation should be known before choosing the shield material.

In reality, the source orientation may be complex and hard to identify. In that case, the use of the multi-layer shield is suggested. As discussed above, multi-layers shield composed of high conductivity and high permeability can provide enhanced shielding over shields composed of only a single layer. The main advantage is that the shielding effectiveness will not suffer a great variation if the source orientation is changed. Single layers shield is too relied on the source orientation. Aluminum shield will has a double shielding ability when the field is normal to it. In the simulation case, the shielding efficient by using a multi-layer shield of the GI

(2mm) and Al (1mm), is the most optimum and steady, as shown in table 7.5.

Distance from center	0m	1m	2m	3m
GI, 3mm thick	0.071	0.1598	0.595	0.644
Al, 3mm thick	0.065	0.071	0.36	0.48
GI2mm+Al1mm	0.03	0.057	0.351	0.509

Table 7.5 Comparison of *SE* with different shield materials

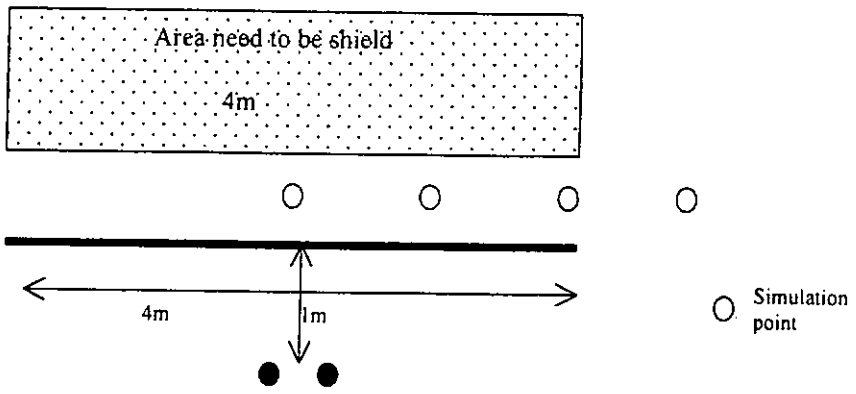

Fig. 7.5 Geometry of the simulated model

In the commercial design, it is usually that the size of the shield is just enough to cover the area need to be shield. From the table 7.5 it can be observed that the SE values increase rapidly from the center to the edges. At the two edges of the shielded area, the shielding effectiveness varies greatly from the center. It is due to the edge effect.

Simulation has also been conducted with doubling the width of the shield to 8m. The material properties (GI) and the shield thickness (3mm) are the same as pervious. From the comparison of the *SE* as shown in table 7.6, it can be observed that there is a great improvement of shielding performances for the location away the center. The increase in shield width can effectively reduce the leakage from edges. Therefore the design must be as wide as possible, not just enough to cover the area need to be shield.

Distance from center	0m	1m	2m	3m
Width : 4m	0.071	0.1598	0.595	0.644
Width : 8m	0.08	0.087	0.1	0.17

Table 7.6 Comparison of *SE* with different width planar shields (GI 3mm)

Here is a failure experience, which is caused by the lack of awareness of edge effect in the design stage. A company had a complaint the computer monitors still had jitter although a 4mm thick galvanized iron shield have been already installed to mitigate the ELF magnetic field generated on the lower floor. The area on the floor below, directly under the affected office area was occupied by nine 500kVA single-phase transformer and the LV switchroom. The substation was owned and operated by the local supply authority while the switchroom was under the full control of the tenant.

A GI planar shield of 4mm thickness has been installed in the ceiling of the transformer room. The magnetic field has significantly reduced in the area above the centre of shield. However, the area at the vicinity of the shield is still imposing in a high magnetic field. The magnetic field over 40 mG on the floor, and 20 mG on the desk level in the office area. In some areas, there exists an increase in magnetic

field after the shield is installed.

The shield area is only just large enough to cover the transformer room area. Therefore, the fields may leak through at the edges, as well as penetrate the shields to the office area. The shielding effect is significant reducing due to edge effect, moreover, there are some areas have an enhancement in the magnetic field. It is a standard case that the lack of awareness on the edge effect of the planar shield design. To avoid the edge effect, the concept of the usable region should be considered. It is recommended that the area to be shield should always within the usable area. Moreover, the selection of the width of the planar shield should be as wide as possible. A wider shield can lower the portion of the leakage field from the edge and increase the shielding performance.

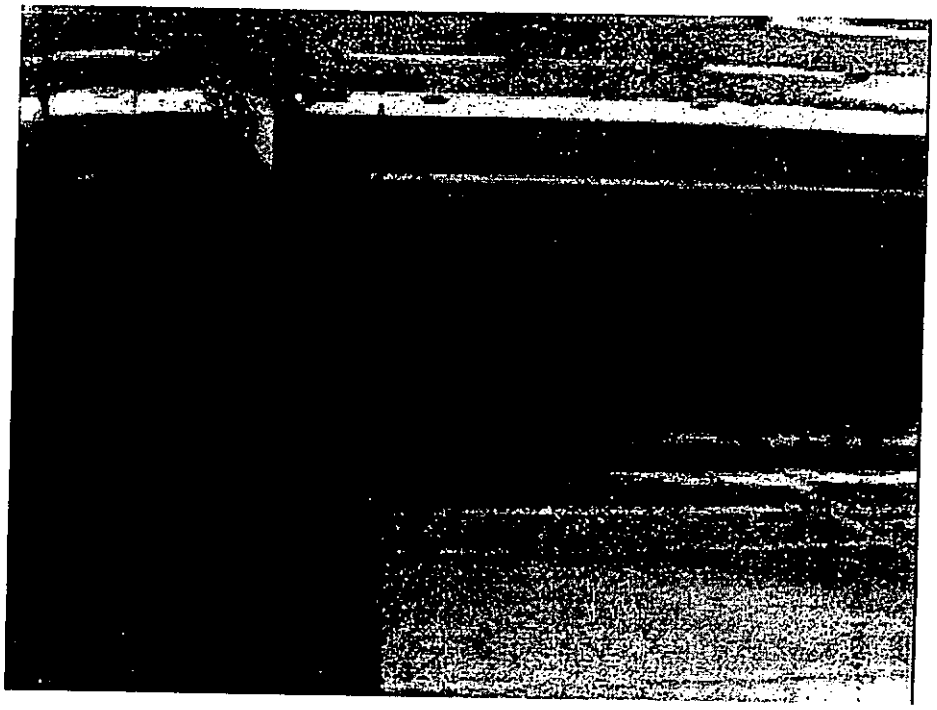

Fig.7.6 Planar shields in practice

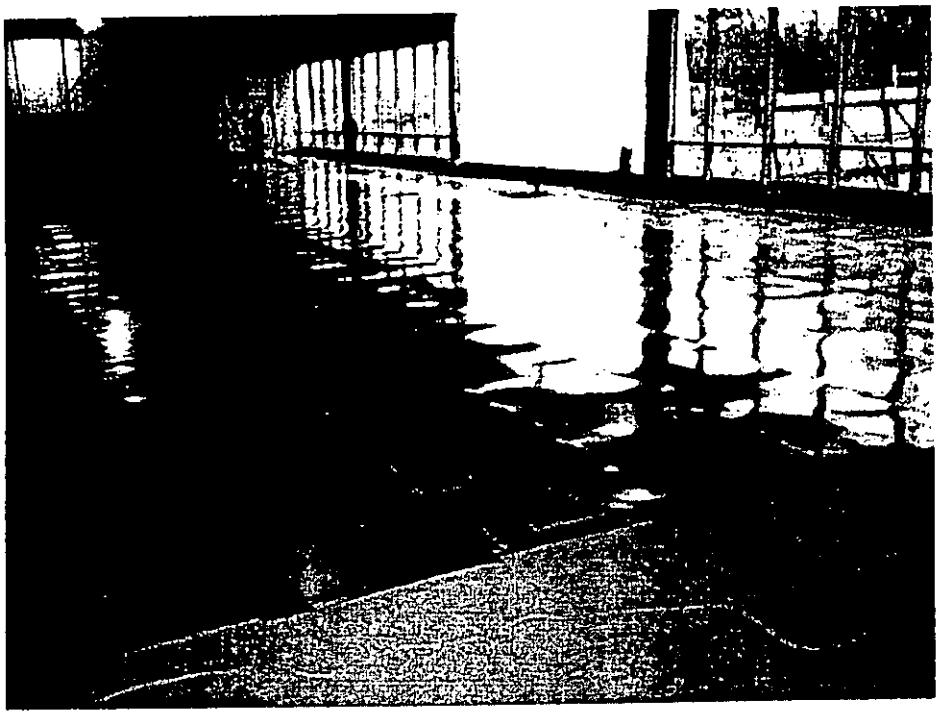

Figure 7.7 Planar shielding of an affected room

CHAPTER 8 CONCLUSIONS

The objective of this project is achieved by the investigation of the ELF magnetic field shielding in buildings. Semi-empirical formulas for evaluating the shielding effectiveness of the trunking have been derived. Moreover, the shielding characteristic and practical issues regarding design and installation have also been examined. For planar shield, the characteristics in real practice were examined in detail through numerical analysis and experiment measurement. All these findings can provide information on the shield design to achieve EMC inside building.

The magnetic environment in office building was investigated. Most of the office areas were exposed to the ELF magnetic field as lower as 1mG and few mG near the office appliances. However, in the areas near the distribution conductors installed in the false ceiling or under floor, the ELF field may reached several hundreds mG at the ground and fell to 40-50 mG at the desk level. It is enough to induce ELF EMI with the electronic equipment. The specific example is a VDU. Laboratory measurement shows that the most of the models will have visible jitter started at about 10mG.

ELF magnetic field mitigation by magnetic shielding has been introduced. Shielding material can be divided into two different types according to shielding mechanism. Permeability material is used to shield by "flux shunting" mechanism. In this case, the magnetic flux is diverted into the magnetic material and away from the region to be shield. Conductive material is used to shield by "induced current cancellation" mechanism. Induced currents are present in the conductive materials when exposed in a

time-varying magnetic field. This induced current density serves as a source for an induced magnetic flux that opposes the change in the imposed magnetic flux. This induced magnetic flux is of a polarity or direction to counteract the original incident magnetic field.

The rectangular shield has a closed shield structure. Its shielding characteristic is similar to other closed shield, for example, cylindrical shield and square shield. For a closed shield structure, the shield size is a critical factor on the shielding performance. The shielding performance of permeable materials deteriorates with increasing shield size in practical range, while conductive materials show an opposite trend. The shielding performance is better for larger shield size. Shield material is another important factors that influence the shielding performance. High- permeability material (μ_r>10000) has an outstanding shielding performance than others. A low-permeability (about several hundreds) trunking have a comparable shielding effectiveness to the conductive trunking. However, in commercial, low-permeability material is using instead of the high-permeability material such as GI for economic consideration.

The semi-empirical shielding formulas of metallic trunking have been derived numerically. These equations can be applied to estimating the shielding effectiveness of metallic trunking in practice. For the permeable material, the *SE* of the trunking shield is obtained by multiplying the size coefficient and the thickness coefficient to the approximate shielding formulas of square shield with the same height. While the *SE* of a conductive trunking shield is obtained by multiplying the size coefficient and the permeability coefficient to the approximate shielding equation of square shield with the

same height. With the verification of the experiment data, the differences are range from 5% to 13.5%. Therefore, the calculated shielding effectiveness values should add a 10-20 % allowance. Although the discrepancy is relatively large, it is considered as adequate in engineering and an effective approach to estimate the shielding effectiveness of commercial trunking. With these formulas, the shielding effectiveness of the commercial trunking can be estimated with certain accuracy through simple calculation procedures. The shielding design process is simplified. Times, human resources, and material resources are saved for using these formulas instead of numerical simulation.

Galvanized iron trunking is usually used in large buildings for enclosing distribution conductors. It is a ferromagnetic material and exhibits non-linear property. Its equivalent relative permeability varies with the flux density present inside the trunking. Consequently, the shielding performance will be affected. Source parameters are defined as those that affect the magnetic flux density within the trunking. The influences of source parameters on non-linearity are studied through laboratory experiment and numerical calculation. In the numerical evaluation, the GI trunking is modeled as a linear shield with a constant equivalent relative permeability.

The applied current in the source is identified as a source parameter. The shielding effectiveness has a linear decrease with increasing the applied current. The equivalent relative permeability is linear proportional to the current magnitude.

The source configuration and the conductors spacing are also identified as important parameters of the shielding effect. Different configurations with different spacing have

been examined in the measurement. At the same current magnitude, the configurations with larger spacing have a better shielding performance with a higher equivalent relative permeability. This feature is also observed for the different configurations. Although the shielding ability is improved, these configurations will enhance the source magnetic field instantaneously.

Shielding performance of a GI trunking is enhanced further with decreasing its size. As the shield is closer to the source, the equivalent relative permeability is increasing. The shielding performance has an abrupt increase if the shield size is much closer to the source.

Aluminum trunking can be seen as a substitute for commercial GI trunking. This high conductivity material shows comparable shielding ability to the GI in commercial range. In fact, there are several advantages over the GI. First of all, it is lightweight. The installation work is easier to process. Moreover, it owns higher shield ability with larger shield size. A larger space inside the trunking can be served as allowance for expansion in conditions of higher temperature. A larger space may also leads to a reduction in the impedance of conductors. Consequently, a reduced voltage drop is obtained. The most important is the prediction of the shielding performance is much easier. It makes the design work more convenient.

Practical issues such as the jointing methods are also investigated through laboratory measurements. In general, the transmission cables usually carry the current up to few hundred amperes. At this range, the relative permeability of the GI is still remains in the linear region. The saturation of the cable trunking seldom occurs. However, it should be

noted that for a busbar trunking, the current carried by the busbars may over one thousand amperes. Saturation of materials may occur.

Design considerations and guidelines of a rectangular shield are also addressed base on its shielding characteristics. Design engineers can select the most suitable trunking for shielding purposes.

The shielding properties of a finite width planar shield in practice have been studied. The shielding properties are discussed and verified by laboratory experiments and numerical calculation. The impact of source orientation, material, sources to shield distance, edge effect and the shielding performance of multi-layer shield has been demonstrated. It is found that a suitable match between the source orientation and material will benefit the shielding performance. The experiment result also reveals that a multi-layers shield composed of high conductivity and high permeability can provide enhanced shielding over shields composed of only a single layer, and independent of the source orientation. It is recommend to use the multi-layer shield if the source orientation is unknown or complex.

Practical issues such as the leakage at the seam position is also under studied. Different compensation methods have been tested. Generally, a small overlapping over the seam position could provide an enough compensation for the seam leakage.

Due to the edge effect (leakage from the edges), the planar shield will have limits on its application. Experiment result shows that there is no or enhancement of magnetic field

at the vicinity of the shield side in some cases. The concept of the usable area has been introduced. Within this region, the shielding effectiveness could be ensuring that not over 20% respects to the center of the shield. The shielding performance within this area is ensured. Besides, the design of the shield size should be as wide as possible. A wider shield can lower the portion of the leakage field efficiently from the edge and increase the shielding performance. Considerations of the planar shield design are also addressed.

All these findings can help to design cost-effective shields in buildings for mitigating the ELF magnetic field, and achieve better shielding performance. The compatibility electromagnetic environment in the buildings can be ensured. Hence, a safe, comfortable and functional environment for occupants and equipment in commercial buildings with large current carrying conductors can be obtained.

After reviewing the literature and doing the work reported in the thesis, the author found that several areas need to be further studied. They are listed below:

1. The shielding properties of other popular shielding materials should be investigated. It might be possible to build a data table of its size coefficient, permeability coefficient, etc, such that the estimation of the shielding effectiveness of each shielding material is easier. Moreover, the magnetization curves of the ferromagnetic should be further studied for avoiding material saturation.

2. The shielding ability of the shielding material in higher frequency range should be studied. To achieve EMC in buildings, shielding against high frequency EMF are also one of the main target.

3. The application of the planar shield characteristic needs to be further developed. It can be achieved by developing accurate and standard formulas or some design curves to the engineer and researcher.

REFERENCES

1. Wertheimer, N. and Leeper, E. " Electrical wiring configuration and childhood cancer". *American Journal of Epidemiology*, Vol.109, pp.273-284 (1979)

2. Kaune, W.T and Forsythe, W. "Current densities measured in human models exposed to 60 Hz electric field". *Bioelectromagnetic*, Vol. 6, pp.13-22 (1985)

3. Sander, R., Brinkman, J. and Kuhne, B. "Laboratory studies on animals and human being exposed to 50 Hz electric and magnetic field".*Proceedings of the International Conference on Large high-Voltage Electric System,* Paris, Francel-9 Septmeber, 1982, paper 36-01 (1982)

4. Sandström. M., Mild. K.H., Sandstrom. K.J.M. and Berglund. A. " External Power Frequency Magnetic Field – Induced Jitter on Computer Monitors". *Behavior & Information Technology* ,Vol.12, No.6, pp.359-363 (1993)

5. Baishiki, R.S. and Deno, D.W. "Interference from 60 Hz Electric and magnetic fields on personal computers". *IEEE Transaction on power Delivery, Vol.PWRD-2,* pp.558-563, April (1987)

6. Kwok, Y.F. "An Examination of magnetic interference on the performance of video display units due to electric current conductors in buildings". *Hong Kong Engineer*, June 1993, pp17 (1993)

7. Lee, T.M. "The effects and shielding of electromagnetic interference originate from currents in power cables". *Proceedings of power Engineering Conference*, Singapore, 27 Feb.-1 March,1995, pp.222 (1995)

8. McAuley, J.C. "Immunity of Visual Display units to 50Hzmagnetic Fields". *ERA Report 90-0390R*, ERA Technology.

9. Sandström. M., Mild. K.H., Stenberg.B. and Wall. S. " A Survey of Electric Field and magnetic Fields Among VDT Operators in Office". *IEEE Transactions on Electromagnetic Compatibility*, Vol.35, No.3, pp.394-397 (1993)

10. "Electromagnetic Interference in Buildings". *Building Services* , September 1991, pp.55-56 (1991)

11. Du, Yaping " ELF magnetic field mitigation in high rise buildings". *Proceedings of CIBSE/ASHRAEHKI/BSE Symposium on Electrical Services in Buildings*, 6 Nov. 1996, Hong Kong, pp5-1. (1996)

12. S.Levy, "Electromagnetic Shielding of an infinite conducting plane placed between circular coaxial cables", *Proceeding of IRE,* Vol.21, June 1936. pp.923-941 (1936)

13. Kaden. H, "Wrbestrome und Schirmung in der Nachrichtentechnik", Springer, Berlin, pp.78-91 (1959)

14. Du, Yaping and Burnett, J. " Magnetic Shielding Principles of Linear Cylindrical Shield at Power -Frequency," *Proceeding Of IEEE 1996 International Symposium o EMC*, Santa Clara, CA, USA. pp.488-492 (1992)

15. Moreno, P. and Olsen, R.G. "Some Observation about Shielding Extremely Low Frequency Magnetic Field by Finite Width Shields", *IEEE Transactions on Electromagnetic Compatibility*, Vol.38, no.3, pp.460-468 (1996)

16. Du, Yaping, Cheng, T.C. and Farag, A.S. "Principles of Power-Frequency Magnetic Field Shielding with Flat Sheets in a Source of Long Conductors", *IEEE Transactions on EMC*, Vol. 38, No.3, pp.450-458 (1996)

17. ACE User Manuel, ABB Corporate Research, Dept. KF.S-72178 Vaste, Sweden, 1993.

18. OERSTED User Manuel, Integrated Engineering Software,Canada,1995

19. "Codes Of Practice for minimum fire service installations and equipment and inspection and testing of installations and equipment ", March 1994, HKPU

20. Staelin, David H., Morgenthaler, Ann W. and Kong Jin Au, *Electromagnetic waves*, Prentice Hall, 555pp.(1994)

21. Clayton. R. Paul, Syed A. Nasar, *Introduction to Electromagnetic Fields.* , McGraw-Hill, 725pp (1987)

22. The Swedish Occupational Safety and Health Administration, Low frequency Electrical and Magnetic fields - The Precautionary Principles of National Authorities- Guidance for Decision Makers, Septmeber (1996)

23. "Interim Guildlines on Limits of Exposure to 50/60 Hz Electric and Magnetic Fields", International Non-ionizing Radiation Committeee of the International Radiation Protection Association, *Health Physics*, Vol.58, No.1, pp.113-122, January (1990).

24. "Threshold limits values for Chemical Substances and Physical Agents and Biological Exposure Indices". The American Conference of Governmental Industrial Hygienists, (1990-1991)

25. "Environment Health Criteria 69 Magnetic Field "United Nations Environment Programme/ World health Organization/ International Radiation Protection Association, Geneva, World Health organization. (1987)

26. "Recommendation for Non-ionizing radiation, GS11". The National Radiation protection Board Guidance on Standards (1988)

27. DIN/VDE 1989, Frankfurt, Germany :Verband Deutscher Elektrotechniker(1989)

28. ENV 50166-1: " Human Exposure to Electromagnetic fields-Low frequency (10Hz to 10 kHz)", European Committee for Electromechanical Standardization (CENELEC), pp.10 (1995)

29. Guide to Connection of Supply by Hong Kong Electric Co., December (1995)

30. BSEN 61000-4-8:1994, and IEC 1000-4-8:Testing and Measurement Techniques- Power Frequency Magnetic Field Immunity Test (1993)

31. BS EN 50082-1 :Generic Immunity Standard for Residential, Commercial and Light Industry (1992)

32. Moss, A.J. and Crtensen, E. "Evaluation of the effects of electric fields on implanted cardiac pacemakers". Palo alto, CA: Electric power Research Institute; ERPI-EA3917 (1985)

33. Bridges, J.E, and Frazier, M.J. "The effect of 60 Hz electric and magnetic fields on implanted cardiac pacemakers". Palo alto, CA: Electric Power Research Institute; ERPI-EA1174(1979)

34. Hemming, L.H. *Architectural Electromagnetic shielding Handbook: A Design and Specification Guide.* IEEE Press 218pp (1992)

35. White, Donald R.J. and Mardiguian, M. *Electromagnetic shielding.* EMF-EMI control, Inc. Gainesville, Virginia 475pp (1988)

36. "Magnetic Field Mitigation to reduce VDU Interference". Electricity Supply Association of Australia Limited. 63pp (1996)

37. Hoburg, J.F. "Principles of Quasistatic Magnetic Field Shielding with Cylindrical and Spherical Shields", *IEEE Transactions on Electromagnetic Compatibility,* Vol.37, No.4, Novermeber,1995

38. Hasselgren, L. and Luomi, J. " Geometrical Aspects of Magnetic Shielding at Extremely Low Frequency, " *IEEE Transactions of EMC*, Vol.37, pp.409-420 (1995)

39. Wong, J. *Low Voltage Electrical Installation Handbook.* HK and Kowloon Electrical Engineering and Appliances Trade Union 589pp (992)

40. BS 5467: Specification for 600/1000V and 1900/3300V armored electric cable having thermosetting insulation 40pp (1989)

Appendix 1

Size Coefficient and Thickness Coefficient of Trunking

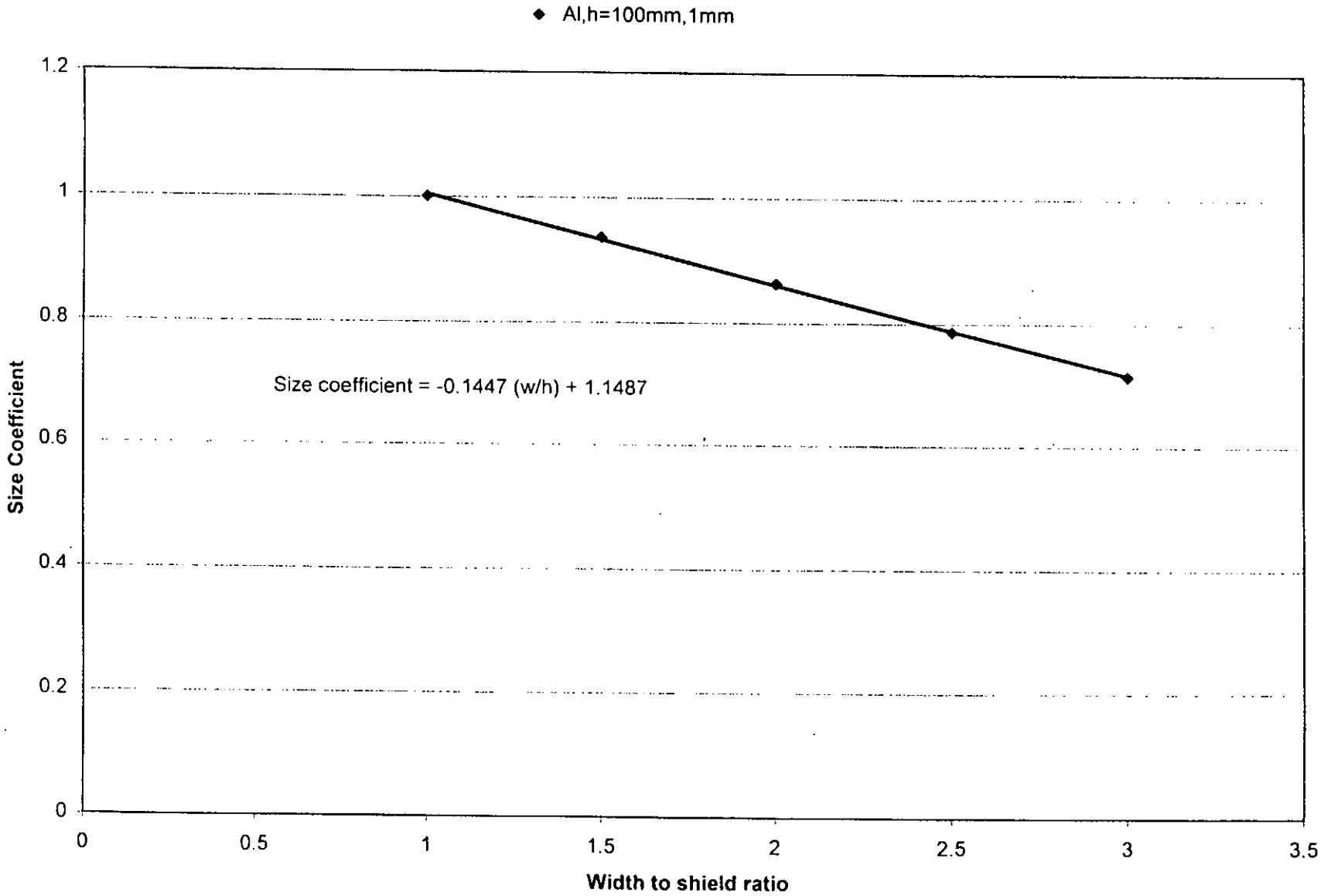
Al,h=100mm,1mm
1.2
1
0.8
0.6
0.4
0.2
0
Size Coefficient
Size coefficient = -0.1447 (w/h) + 1.1487
0
0.5
1
1.5
2
2.5
3
3.5
Width to shield ratio

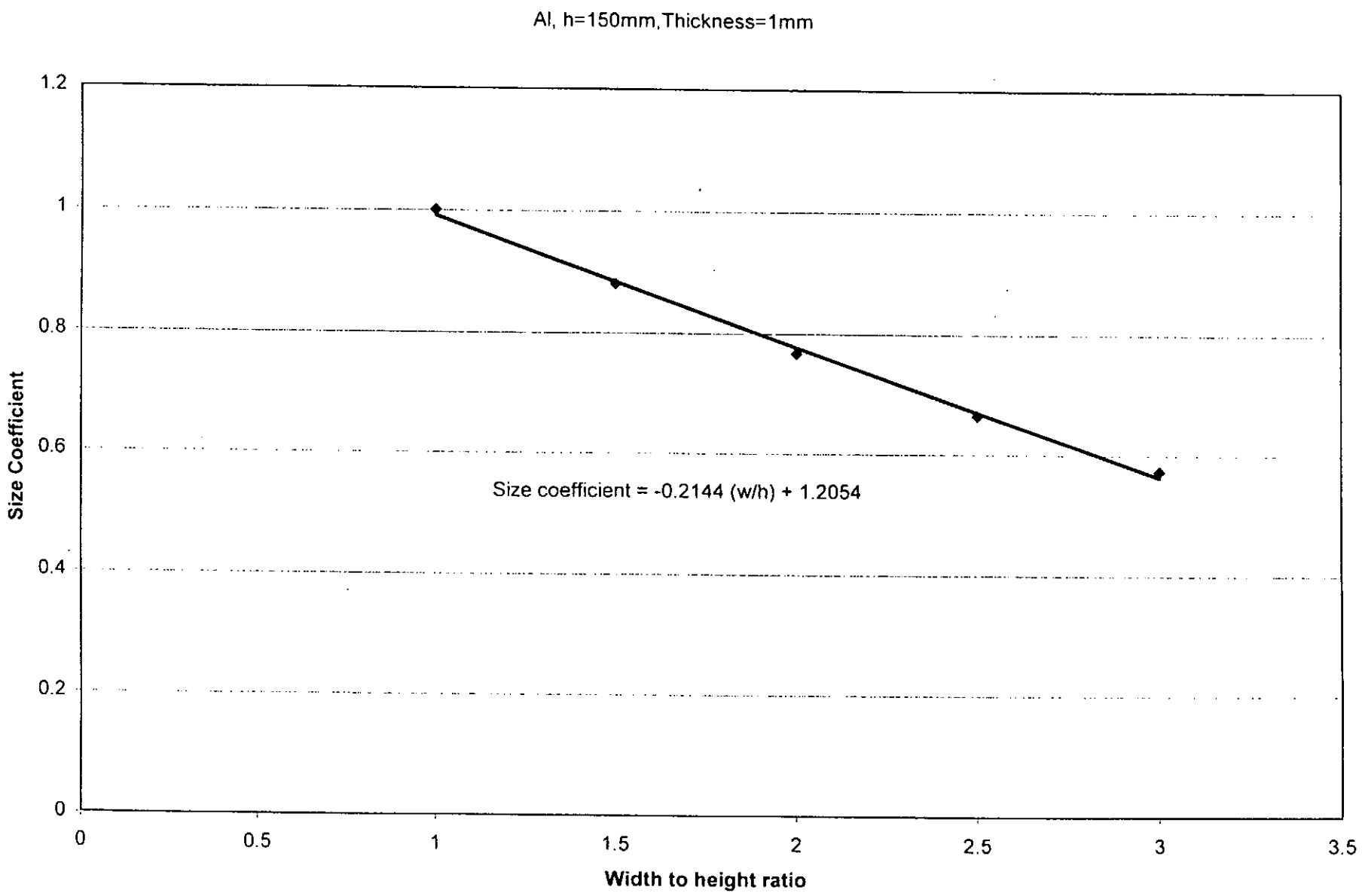
Al, h=150mm,Thickness=1mm
Size Coefficient
1.2
1
0.8
0.6
0.4
0.2
0
Size coefficient = -0.2144 (w/h) + 1.2054
0
0.5
1
1.5
2
2.5
3
3.5
Width to height ratio

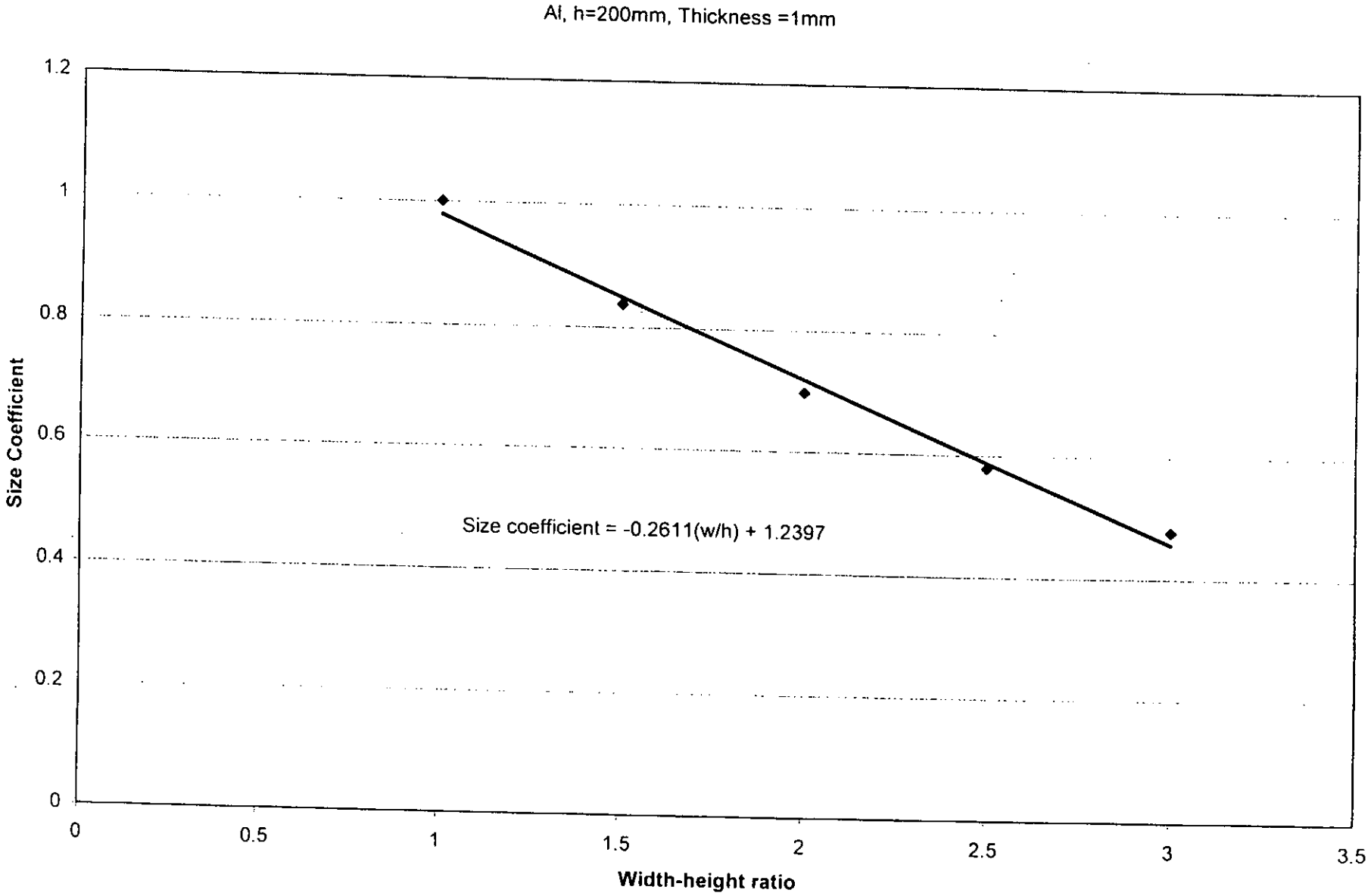
Al, h=200mm, Thickness =1mm
Size Coefficient
1.2
1
0.8
0.6
0.4
0.2
0
Size coefficient = -0.2611(w/h) + 1.2397
0
0.5
1
1.5
2
2.5
3
3.5
Width-height ratio

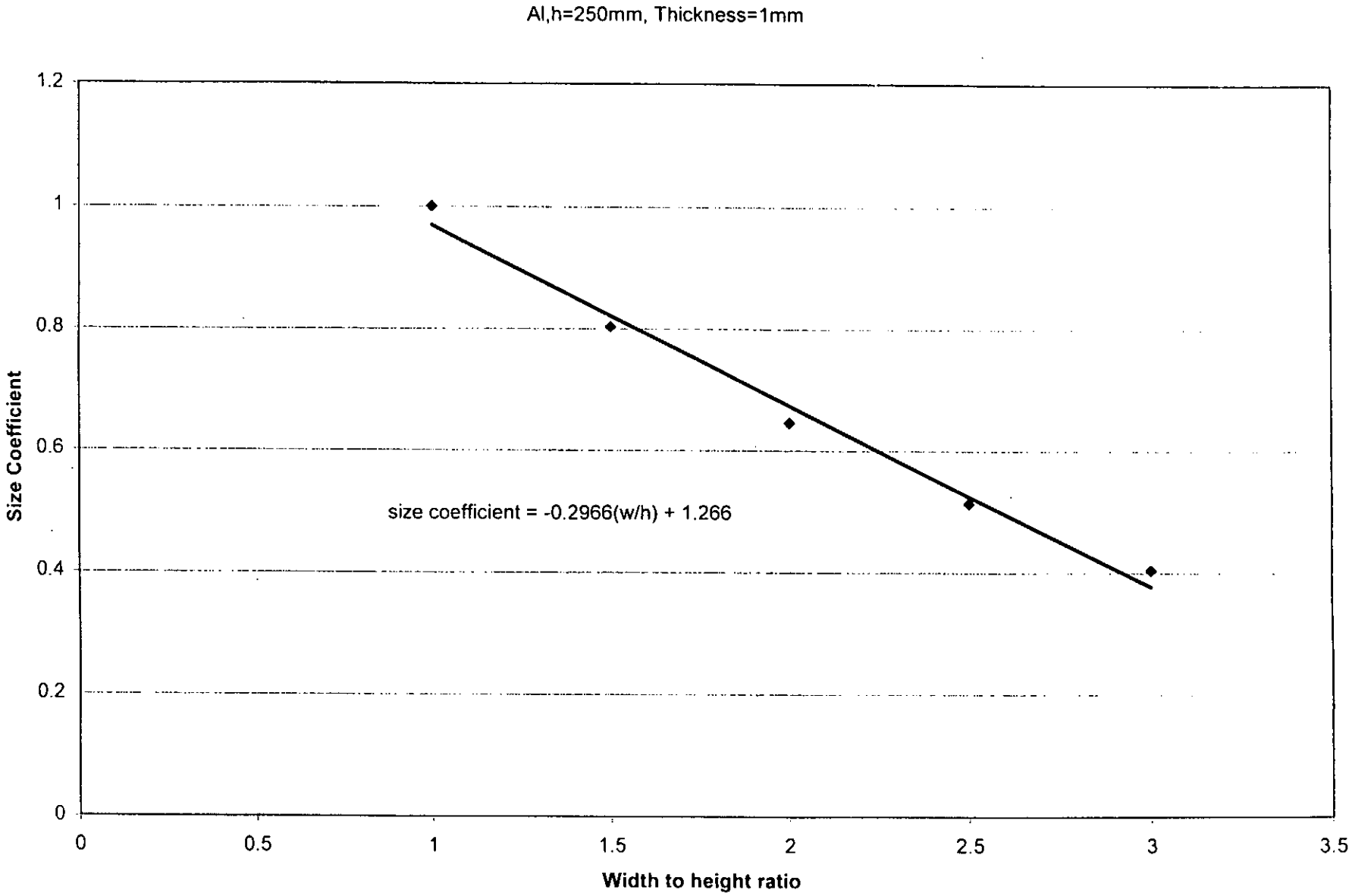
Al,h=250mm, Thickness=1mm
1.2
1
0.8
0.6
0.4
0.2
0
Size Coefficient
size coefficient = -0.2966(w/h) + 1.266
0
0.5
1
1.5
2
2.5
3
3.5
Width to height ratio

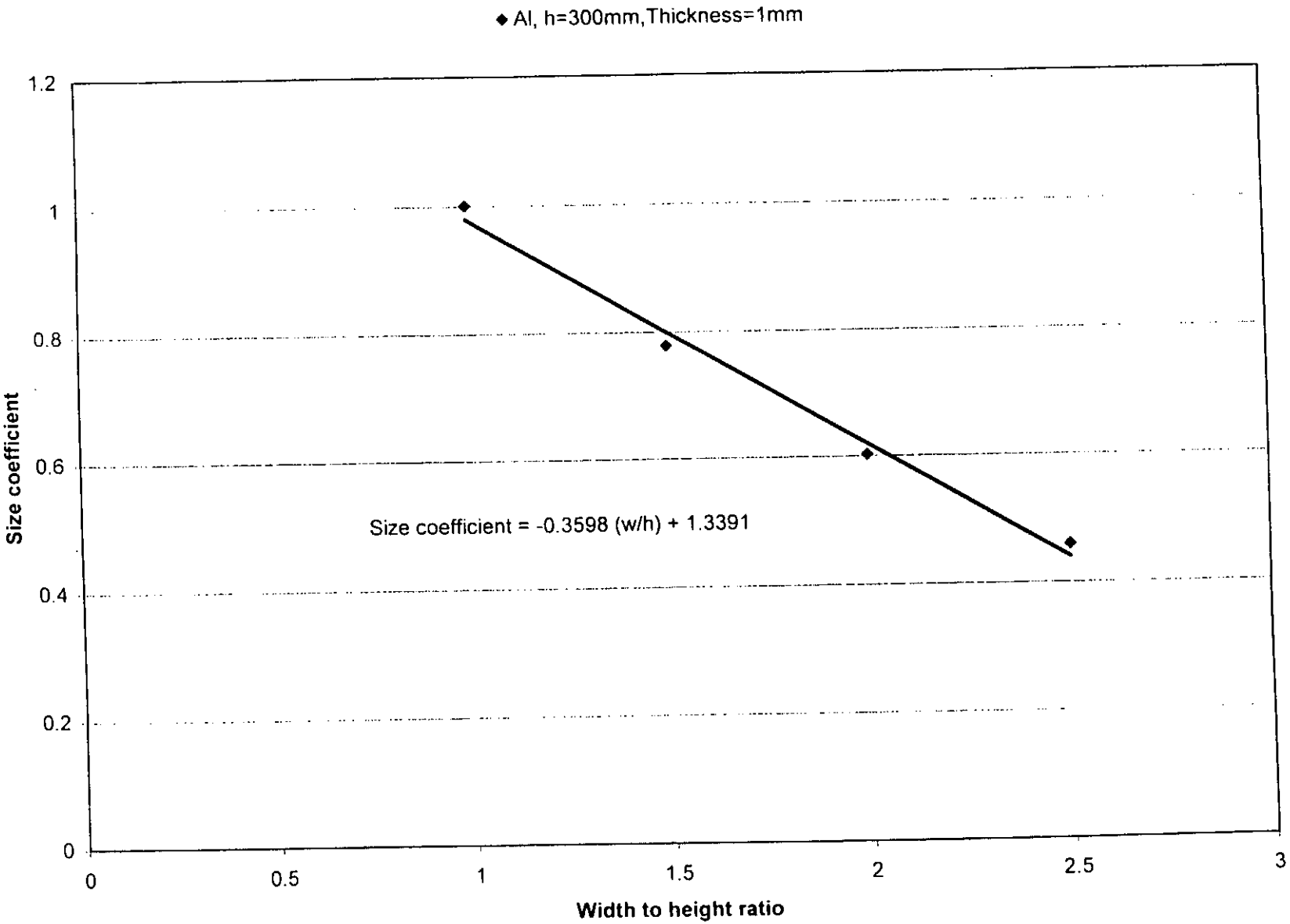
◆ Al, h=300mm,Thickness=1mm
1.2
1
0.8
0.6
0.4
0.2
0
Size coefficient
Size coefficient = -0.3598 (w/h) + 1.3391
0
0.5
1
1.5
2
2.5
3
Width to height ratio

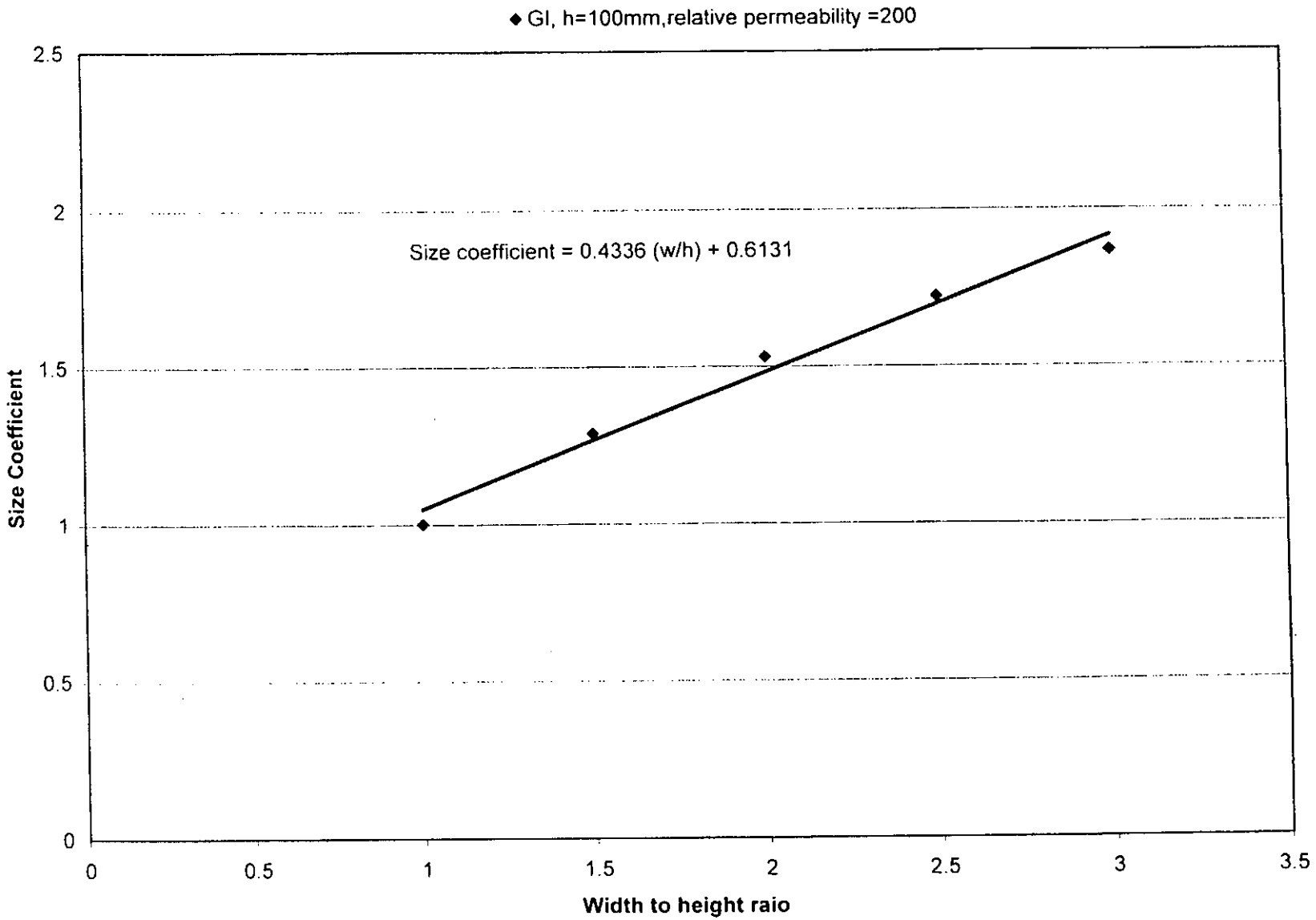
◆ GI, h=100mm,relative permeability =200
Size coefficient = 0.4336 (w/h) + 0.6131
Size Coefficient
Width to height raio
2.5
2
1.5
1
0.5
0
0
0.5
1
1.5
2
2.5
3
3.5

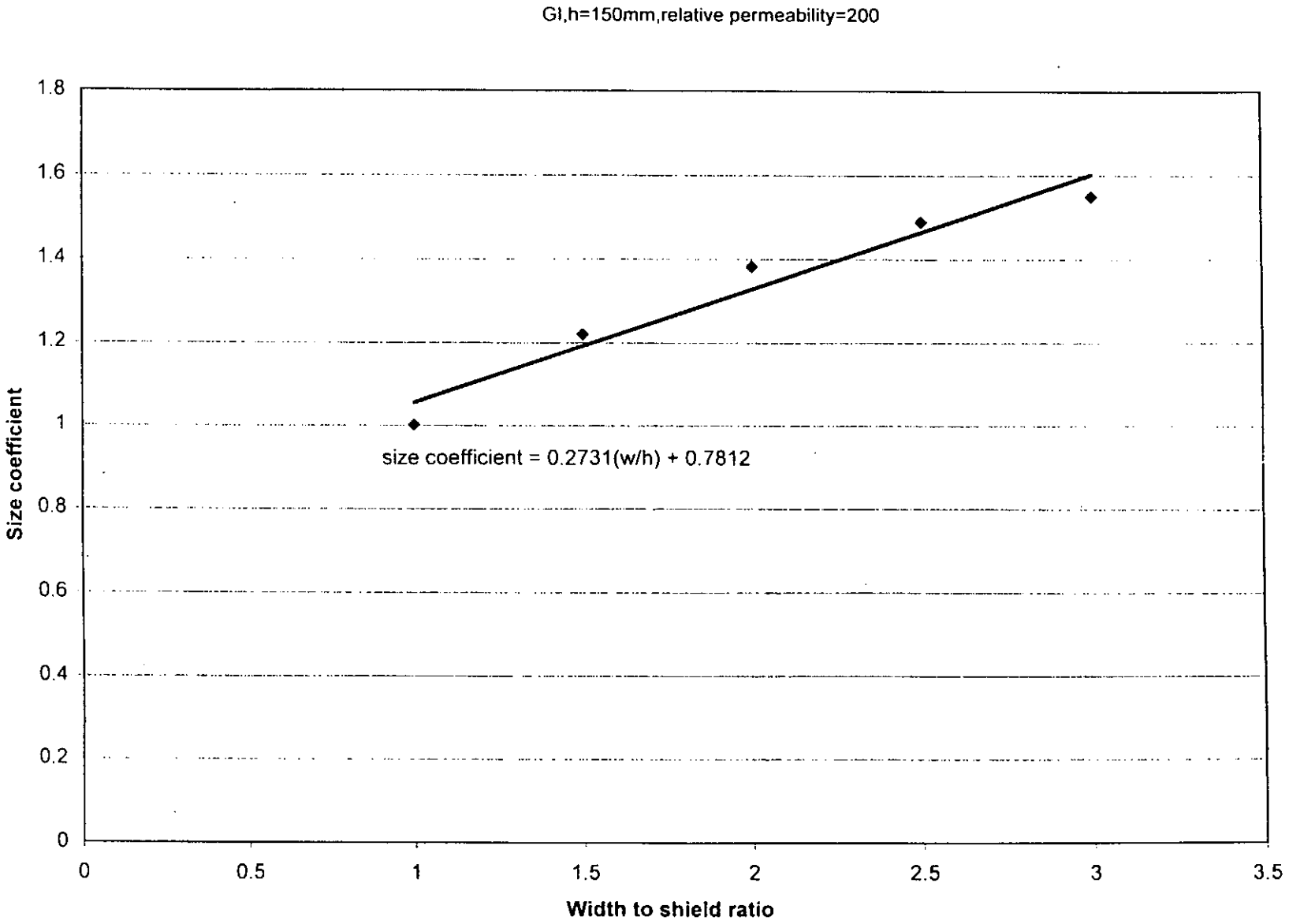
GI,h=150mm,relative permeability=200
size coefficient = 0.2731(w/h) + 0.7812
Size coefficient
Width to shield ratio
0
0.2
0.4
0.6
0.8
1
1.2
1.4
1.6
1.8
0
0.5
1
1.5
2
2.5
3
3.5

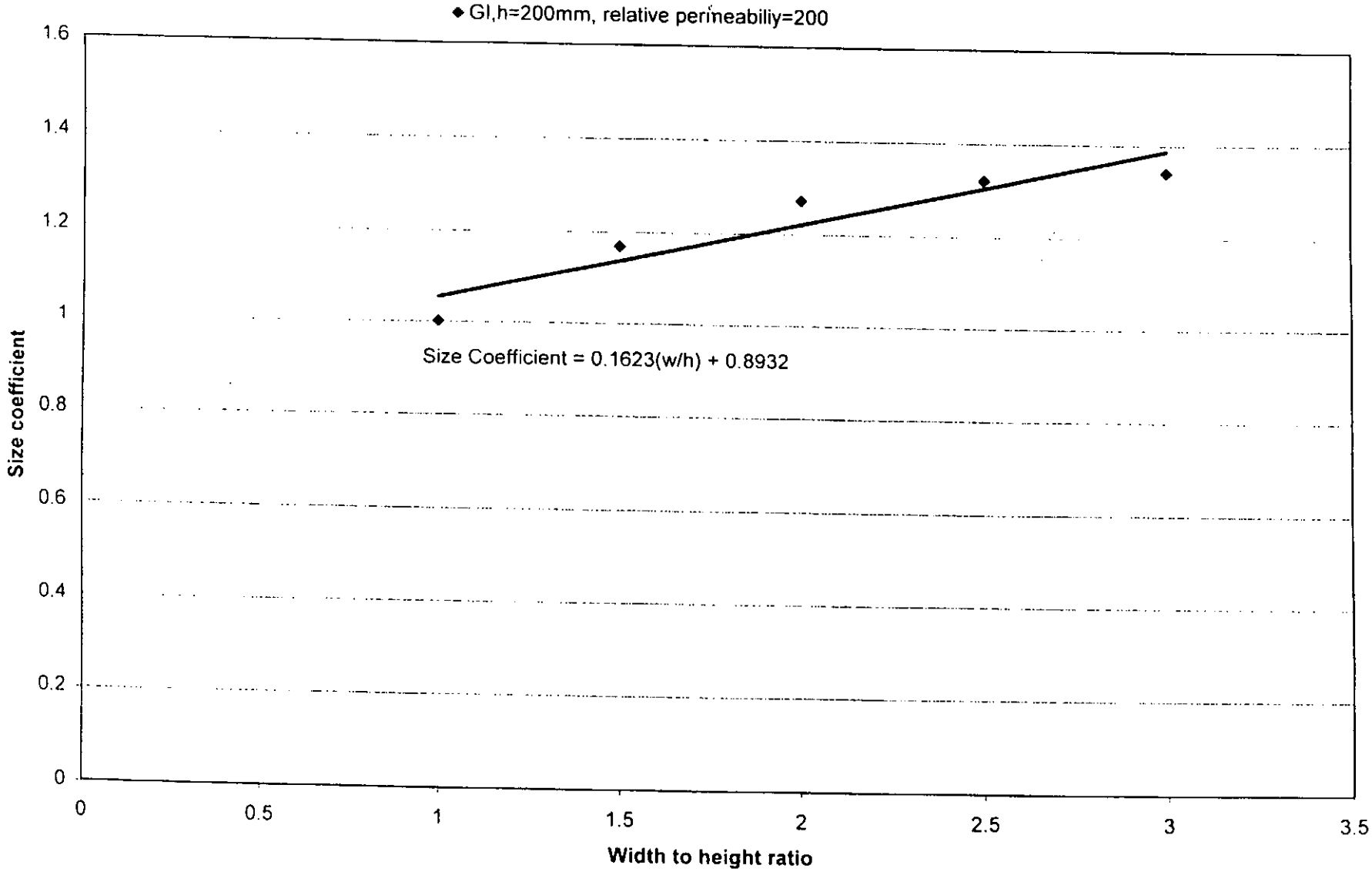
◆ GI,h=200mm, relative perineabiliy=200
Size Coefficient = 0.1623(w/h) + 0.8932
Size coefficient
Width to height ratio
1.6
1.4
1.2
1
0.8
0.6
0.4
0.2
0
0
0.5
1
1.5
2
2.5
3
3.5

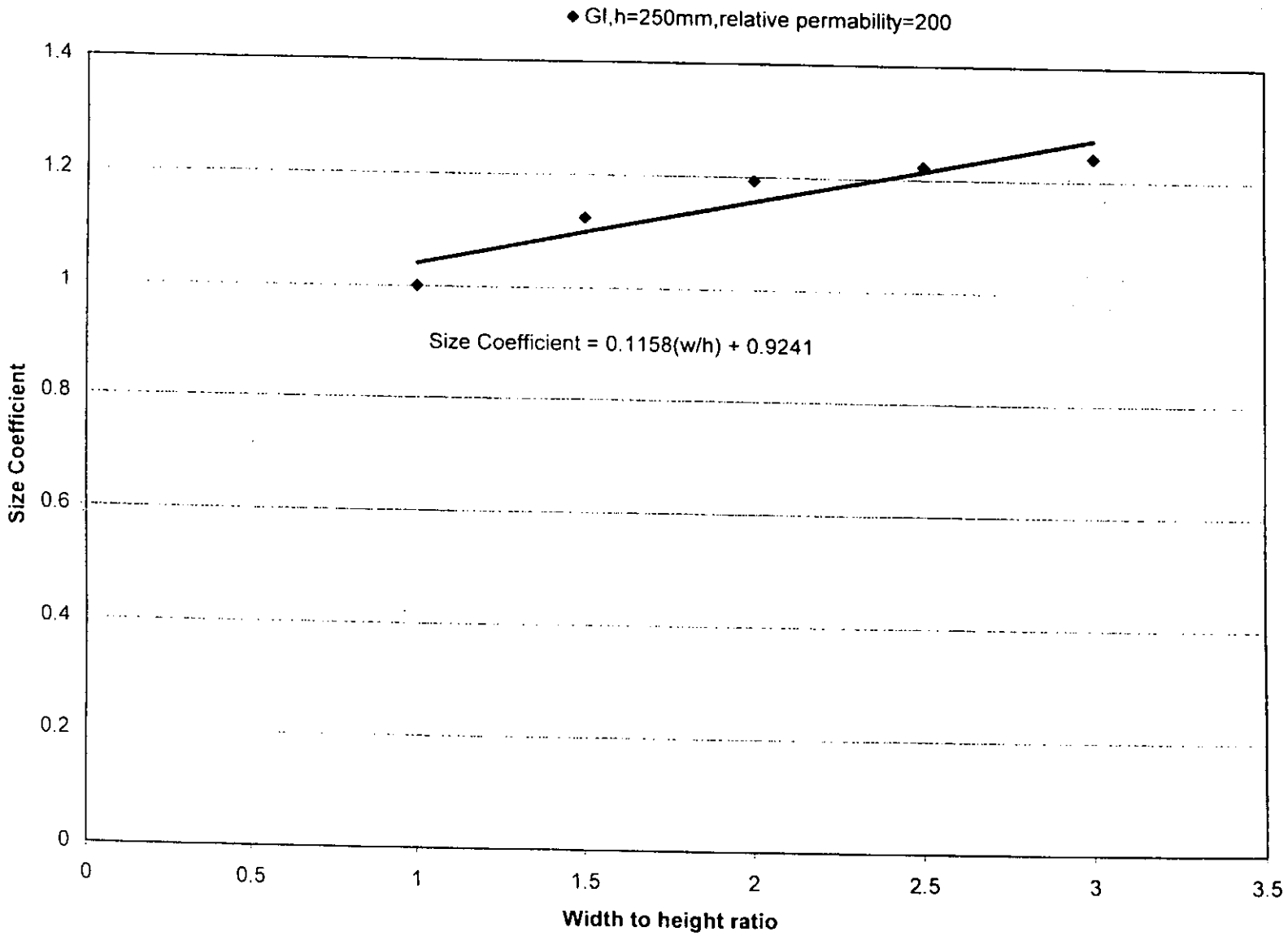
GI,h=250mm,relative permability=200
Size Coefficient = 0.1158(w/h) + 0.9241
Size Coefficient
Width to height ratio
0
0.2
0.4
0.6
0.8
1
1.2
1.4
0
0.5
1
1.5
2
2.5
3
3.5

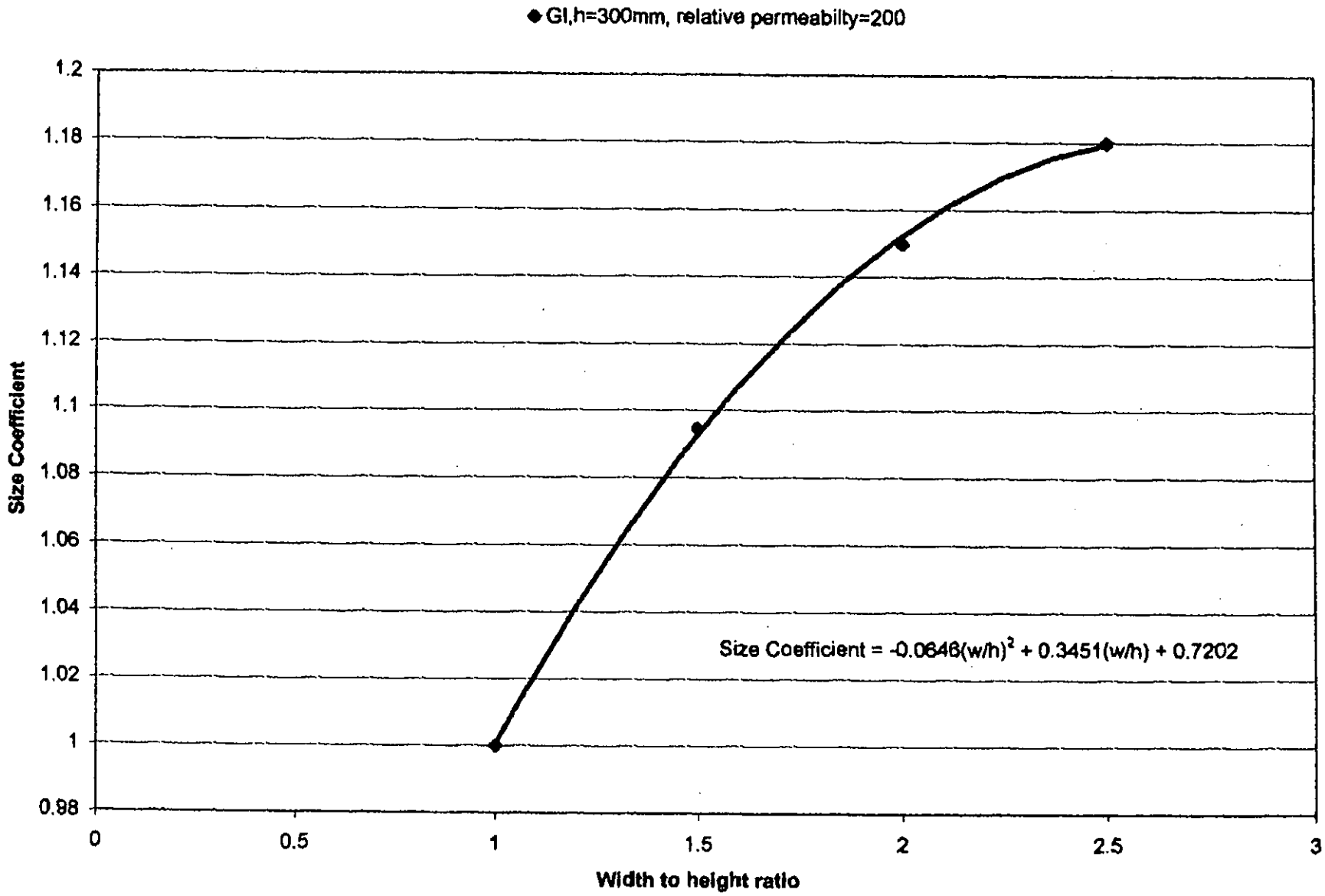
GI,h=300mm, relative permeabilty=200
1.2
1.18
1.16
1.14
1.12
1.1
1.08
1.06
1.04
1.02
1
0.98
Size Coefficient
0
0.5
1
1.5
2
2.5
3
Width to height ratio
Size Coefficient = -0.0646(w/h)² + 0.3451(w/h) + 0.7202

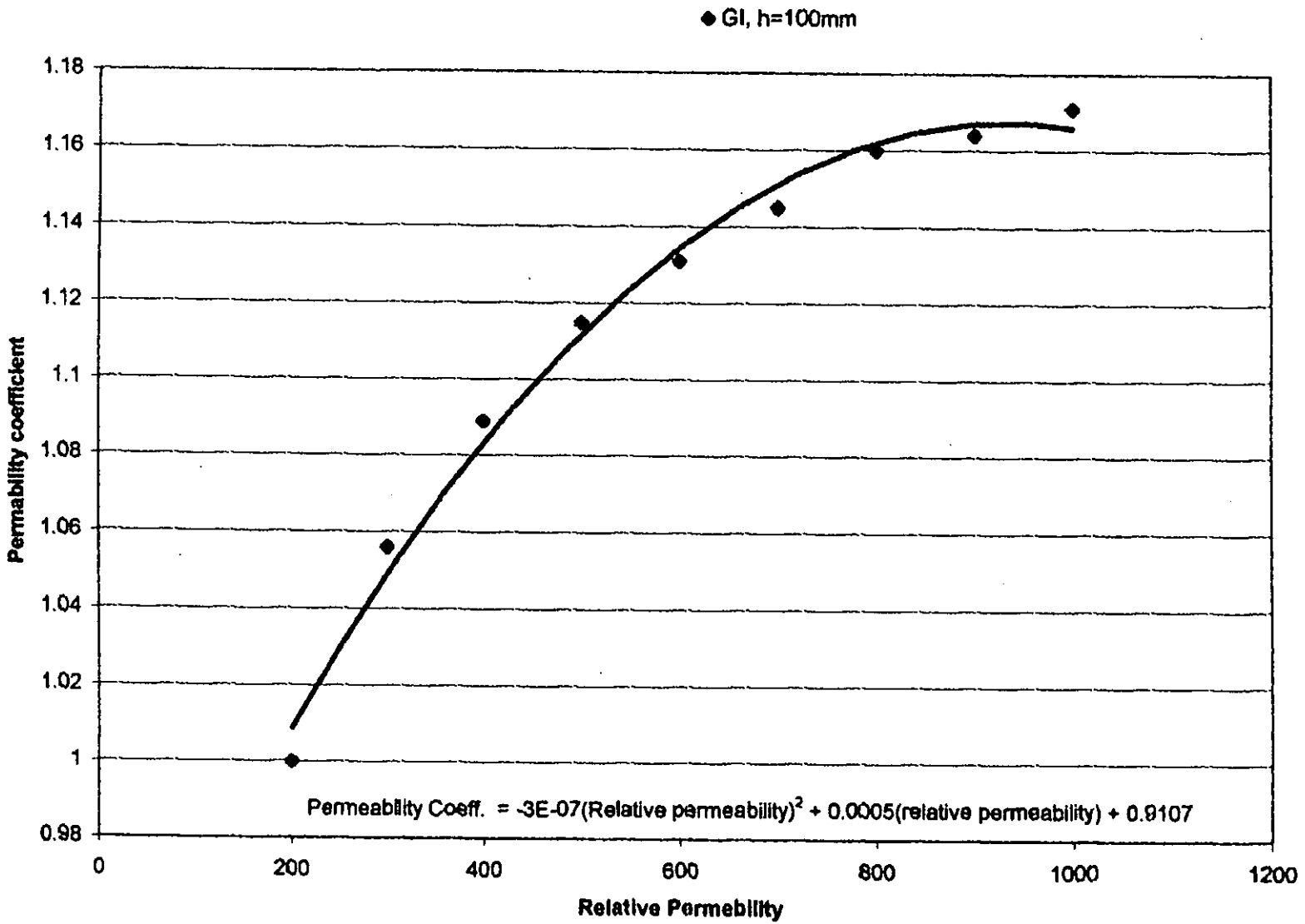
◆ GI, h=100mm
1.18
1.16
1.14
1.12
1.1
1.08
1.06
1.04
1.02
1
0.98
Permability coefficient
0
200
400
600
800
1000
1200
Relative Permebility
Permeability Coeff. = -3E-07(Relative permeability)² + 0.0005(relative permeability) + 0.9107

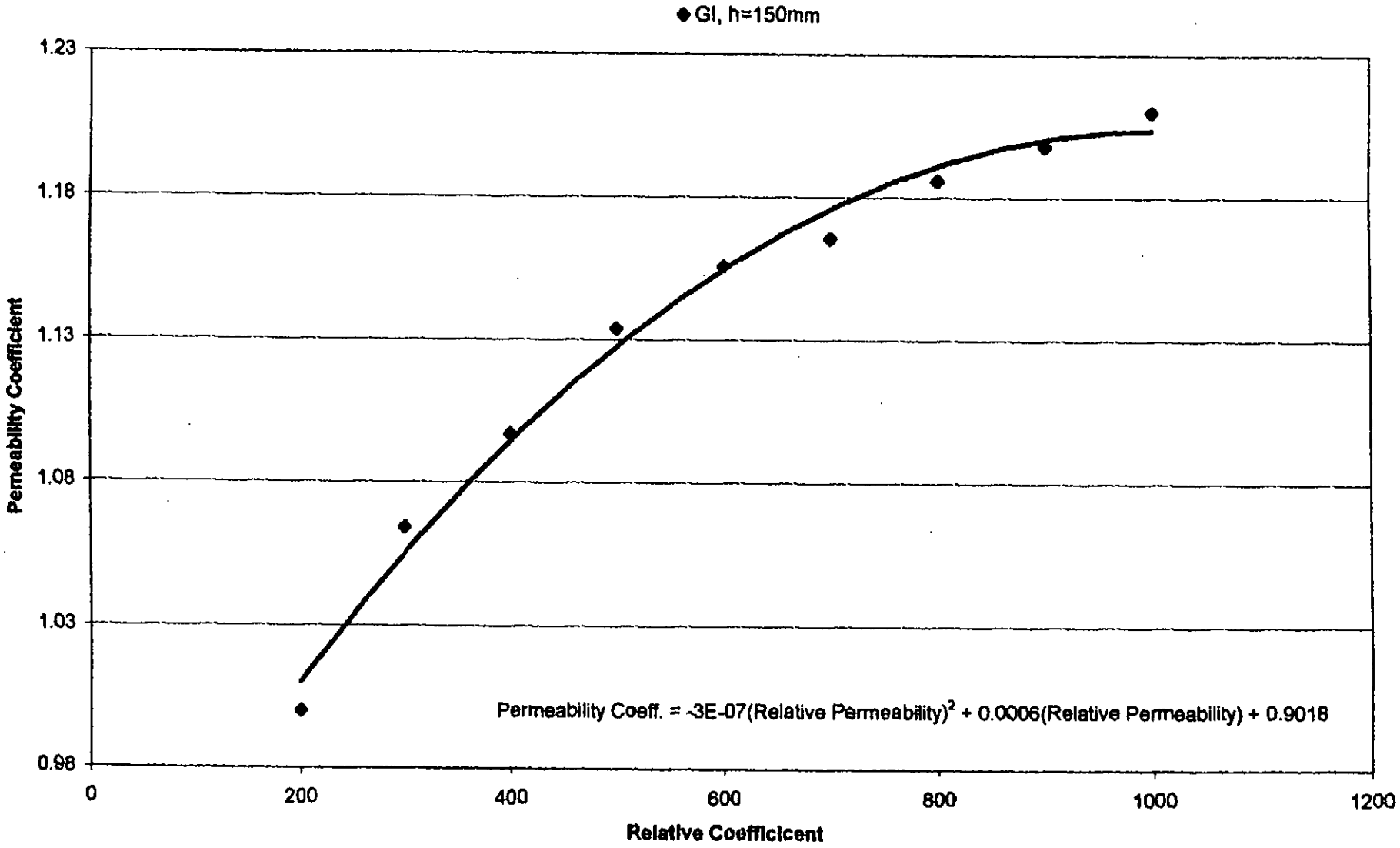
◆ GI, h=150mm
1.23
1.18
1.13
1.08
1.03
0.98
Permeability Coefficient
0
200
400
600
800
1000
1200
Relative Coefficicent
Permeability Coeff. = -3E-07(Relative Permeability)² + 0.0006(Relative Permeability) + 0.9018

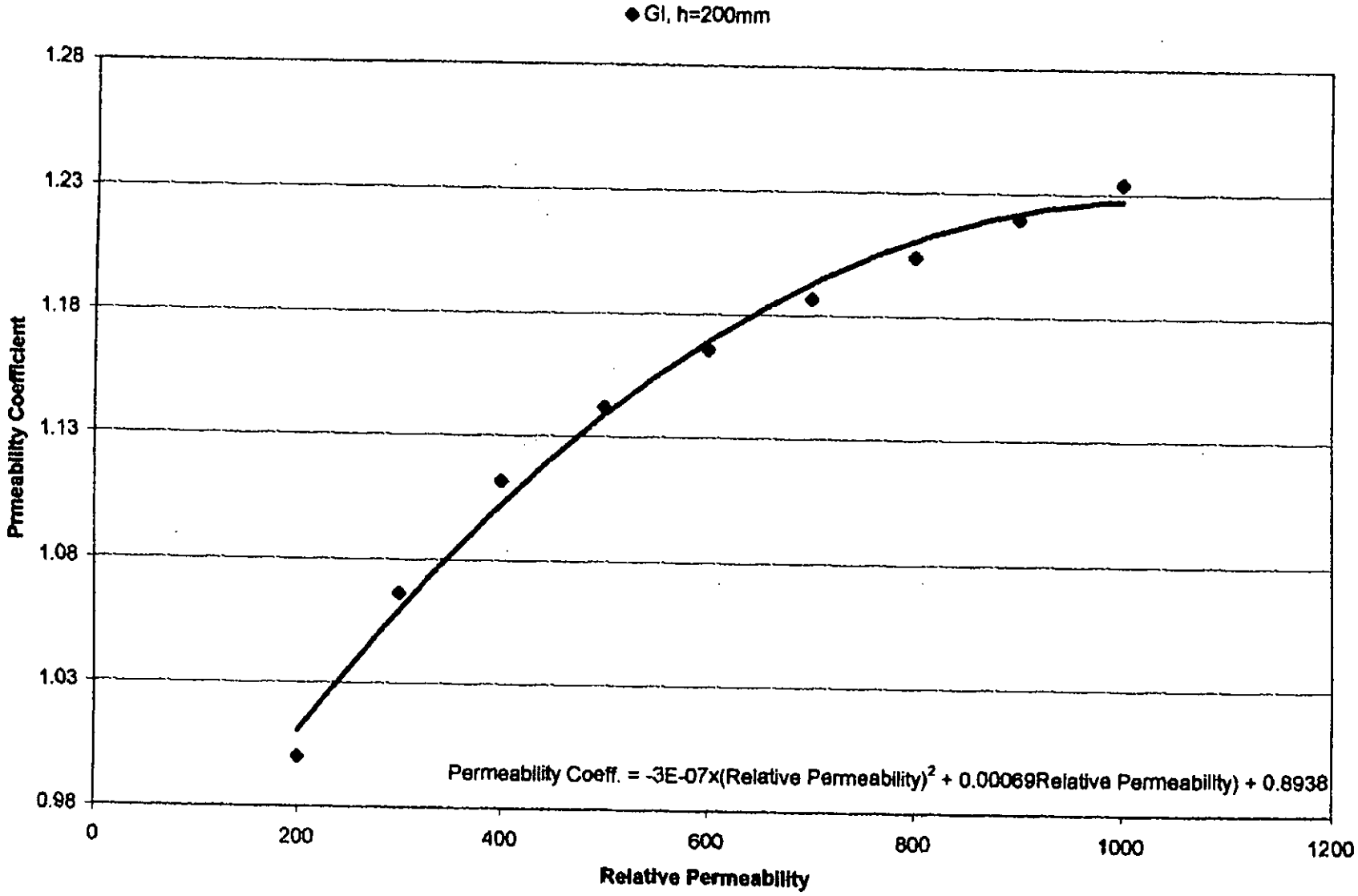
GI, h=200mm
1.28
1.23
1.18
1.13
1.08
1.03
0.98
Prmeability Coefficient
0
200
400
600
800
1000
1200
Relative Permeability
Permeability Coeff. = -3E-07x(Relative Permeability)^2 + 0.00069Relative Permeability) + 0.8938

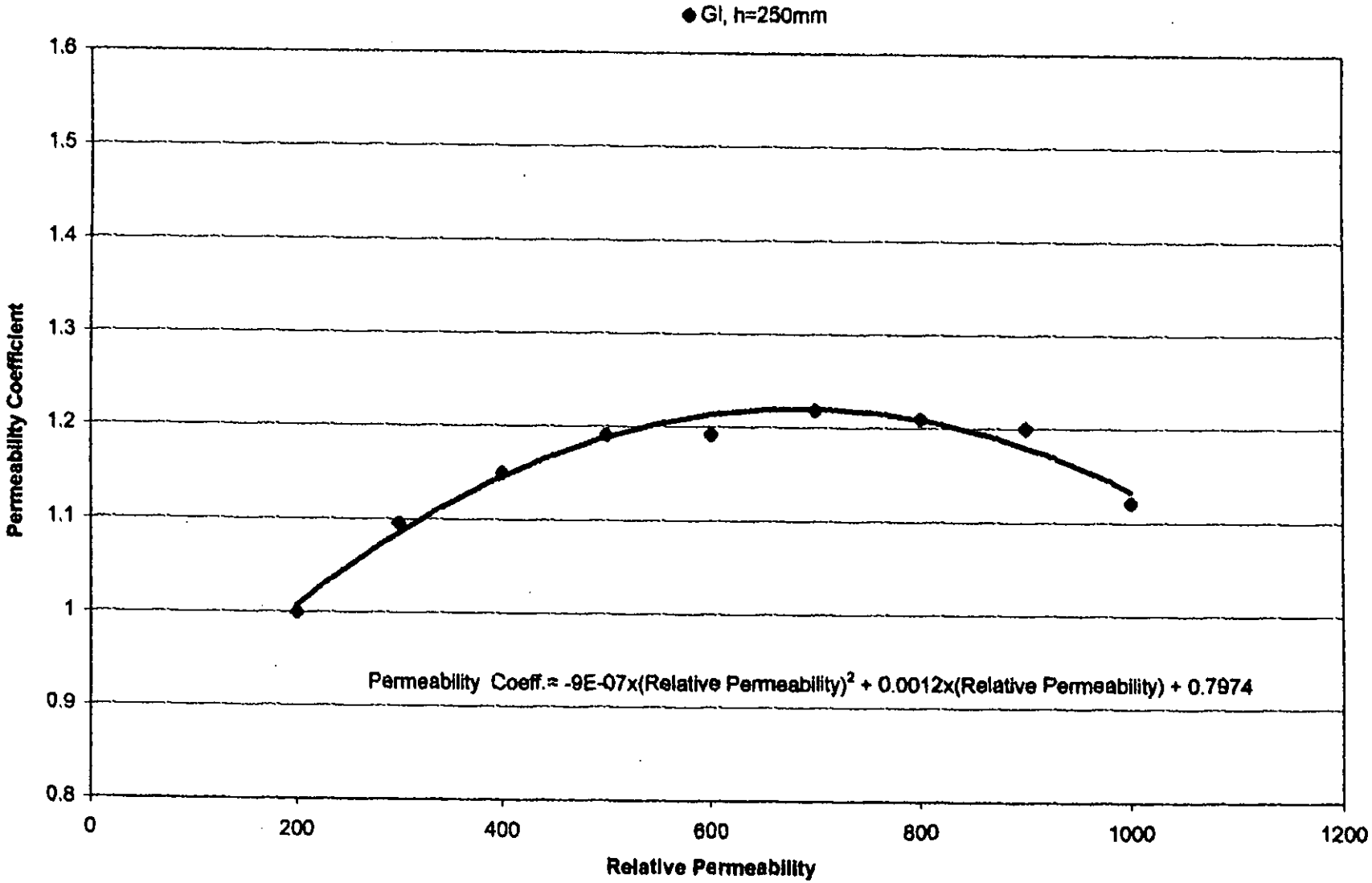
GI, h=250mm
1.6
1.5
1.4
1.3
1.2
1.1
1
0.9
0.8
Permeability Coefficient
0
200
400
600
800
1000
1200
Relative Permeability
Permeability Coeff.= -9E-07x(Relative Permeability)² + 0.0012x(Relative Permeability) + 0.7974

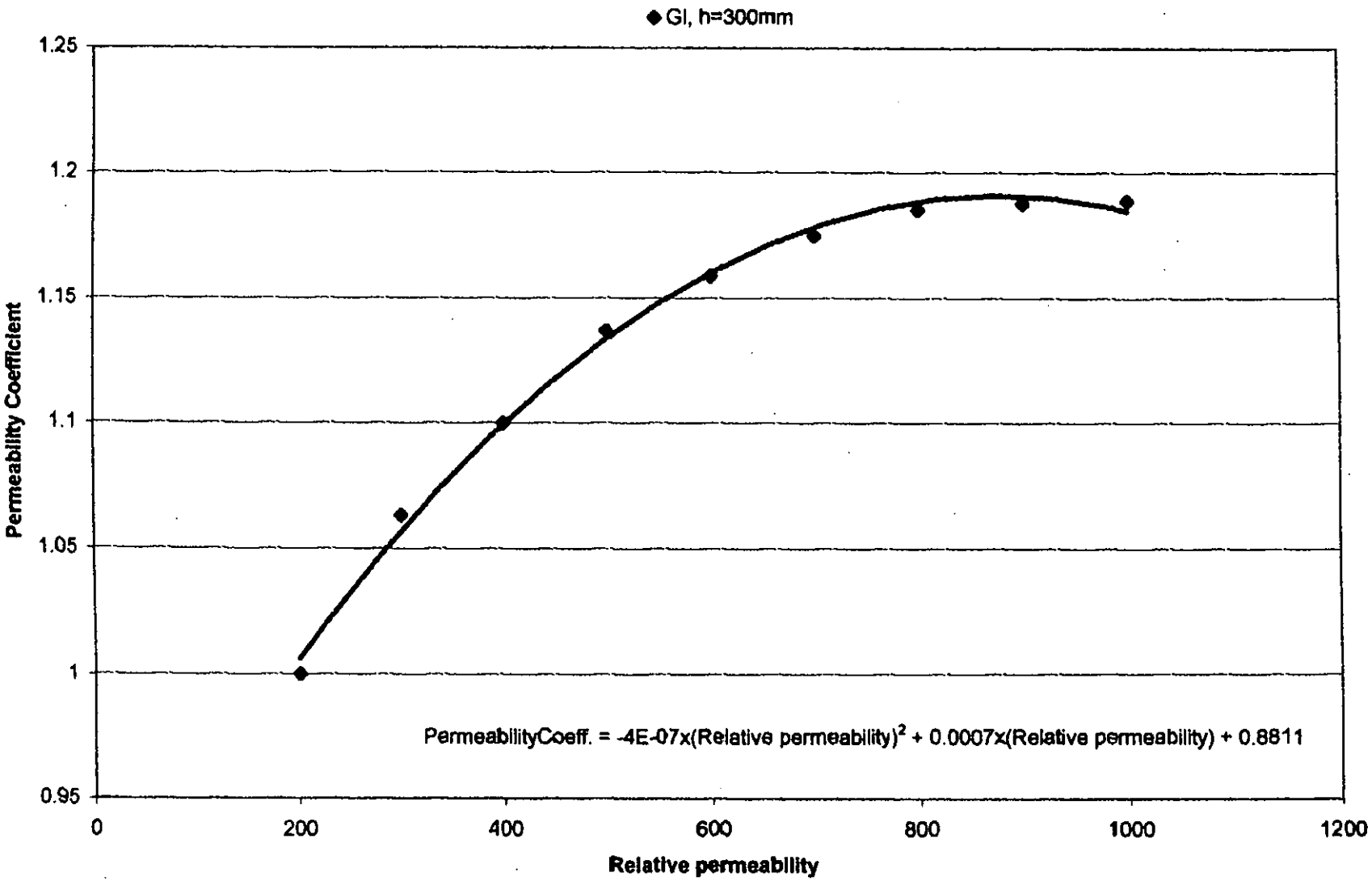
◆ GI, h=300mm
1.25
1.2
1.15
1.1
1.05
1
0.95
Permeability Coefficient
PermeabilityCoeff. = -4E-07x(Relative permeability)² + 0.0007x(Relative permeability) + 0.8811
0
200
400
600
800
1000
1200
Relative permeability

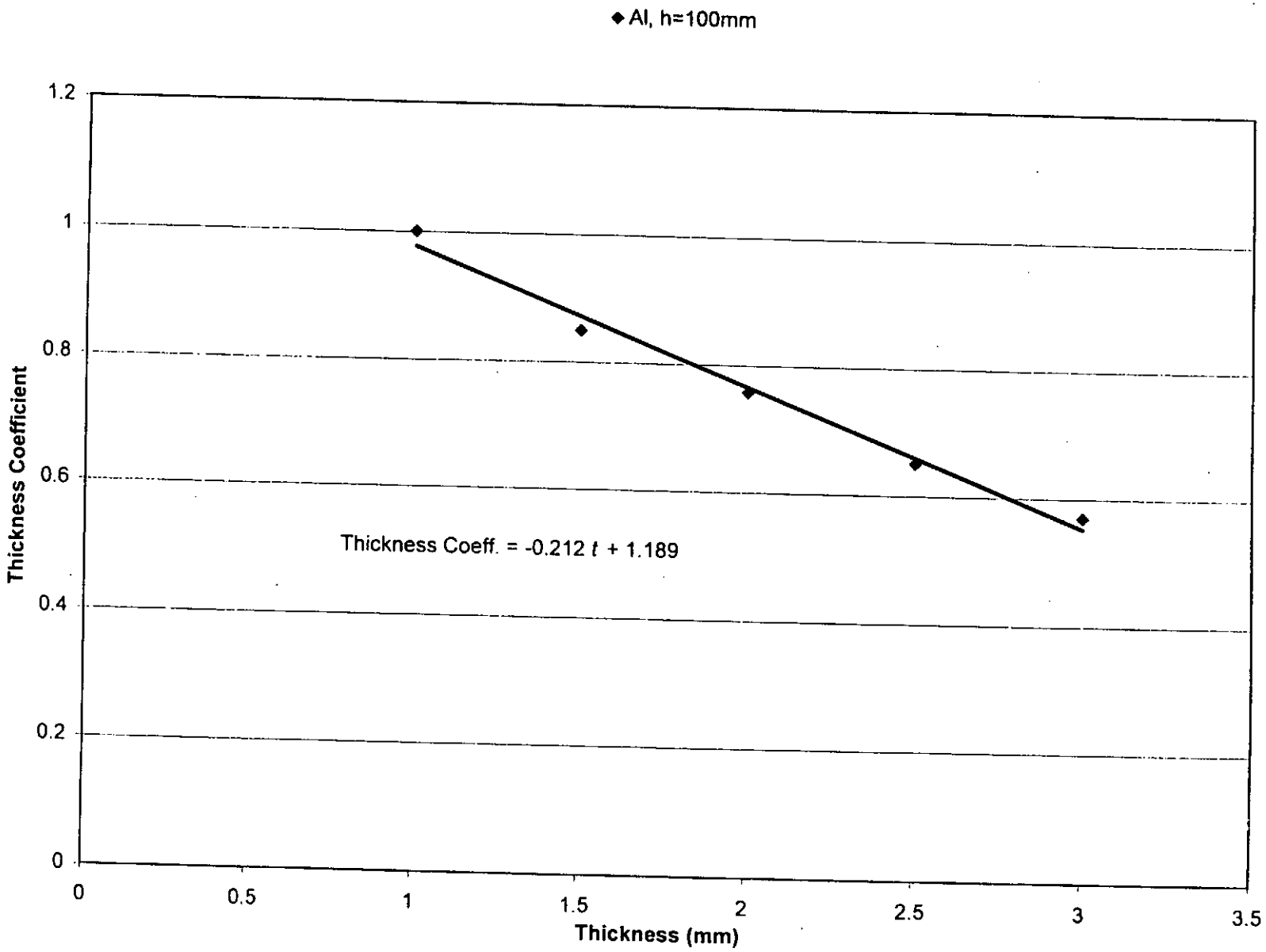
◆ Al, h=100mm
1.2
1
0.8
0.6
0.4
0.2
0
Thickness Coefficient
Thickness Coeff. = -0.212 t + 1.189
0
0.5
1
1.5
2
2.5
3
3.5
Thickness (mm)

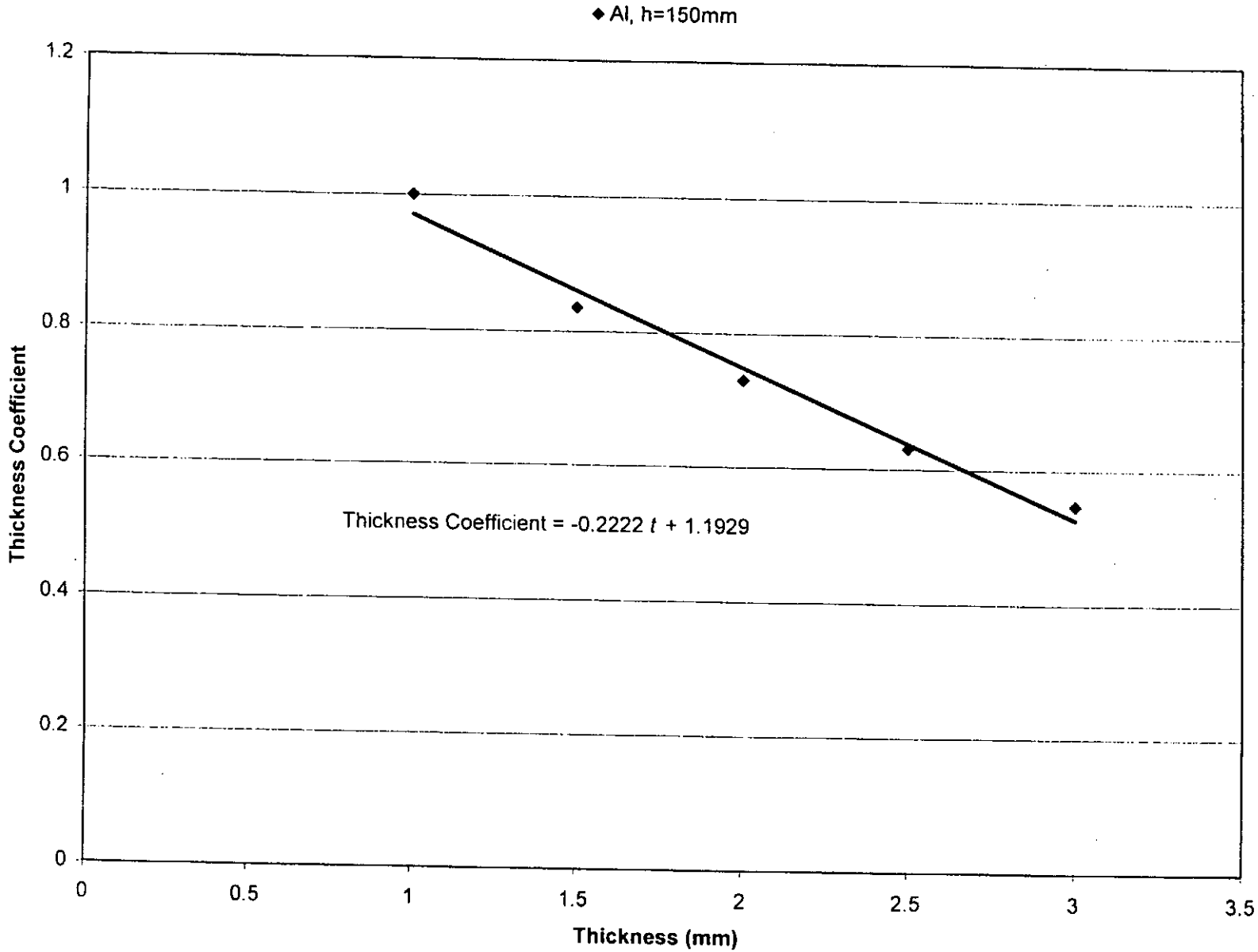
◆ Al, h=150mm
1.2
1
0.8
0.6
0.4
0.2
0
Thickness Coefficient
Thickness Coefficient = -0.2222 t + 1.1929
0
0.5
1
1.5
2
2.5
3
3.5
Thickness (mm)

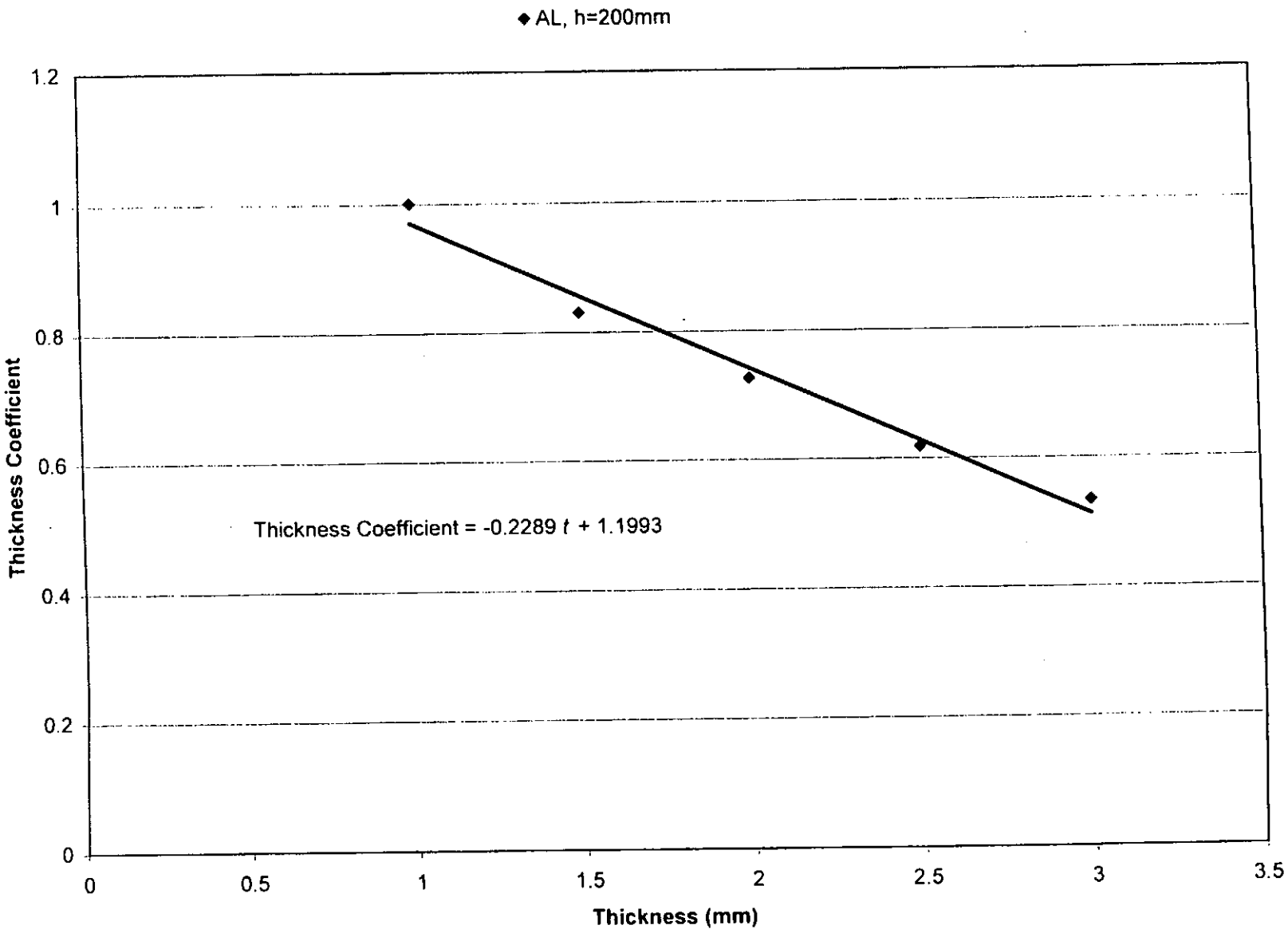
◆ AL, h=200mm
1.2
1
0.8
0.6
0.4
0.2
0
Thickness Coefficient
Thickness Coefficient = -0.2289 t + 1.1993
0
0.5
1
1.5
2
2.5
3
3.5
Thickness (mm)

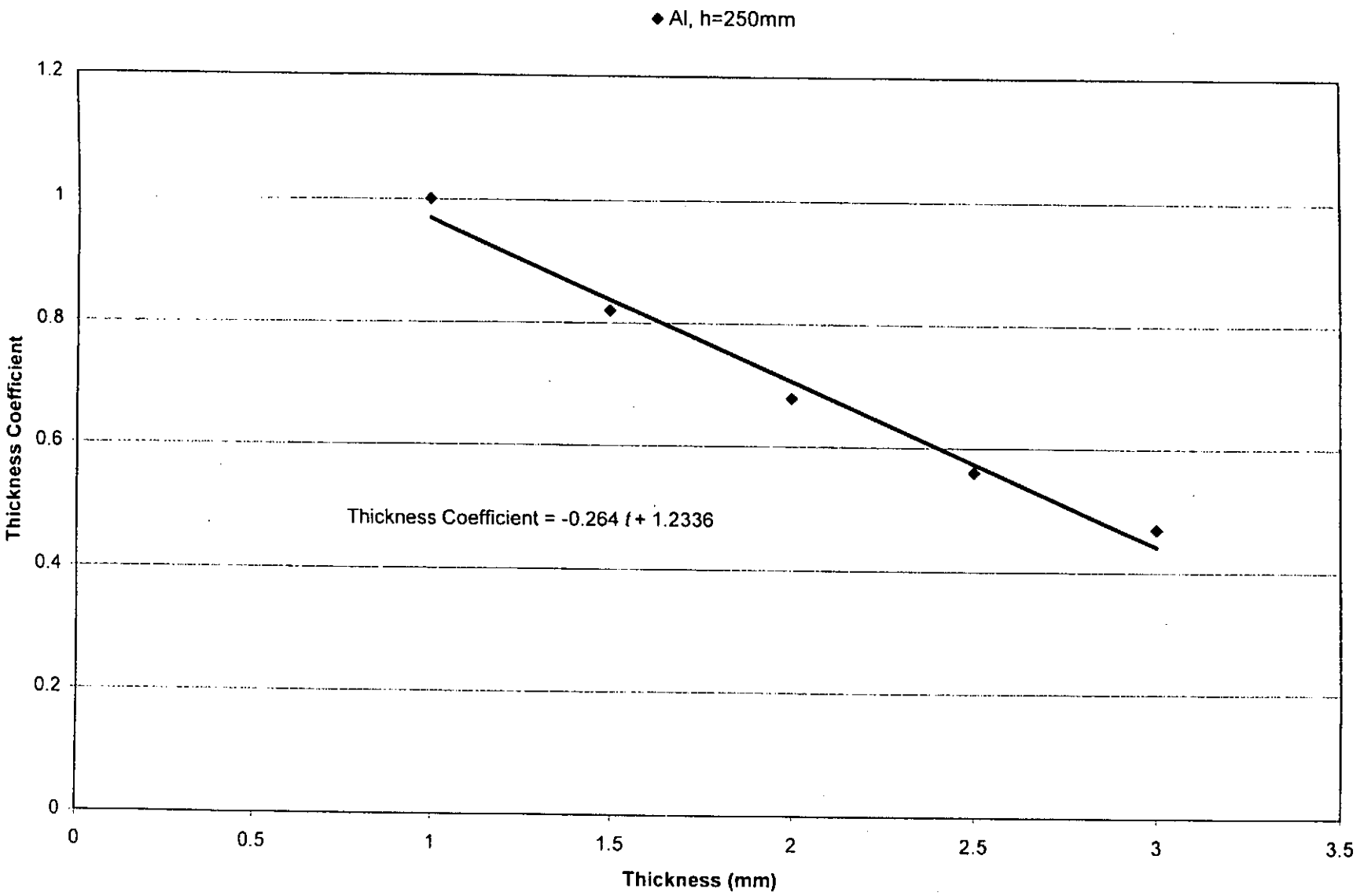
◆ Al, h=250mm
1.2
1
0.8
0.6
0.4
0.2
0
Thickness Coefficient
Thickness Coefficient = -0.264 t + 1.2336
0
0.5
1
1.5
2
2.5
3
3.5
Thickness (mm)

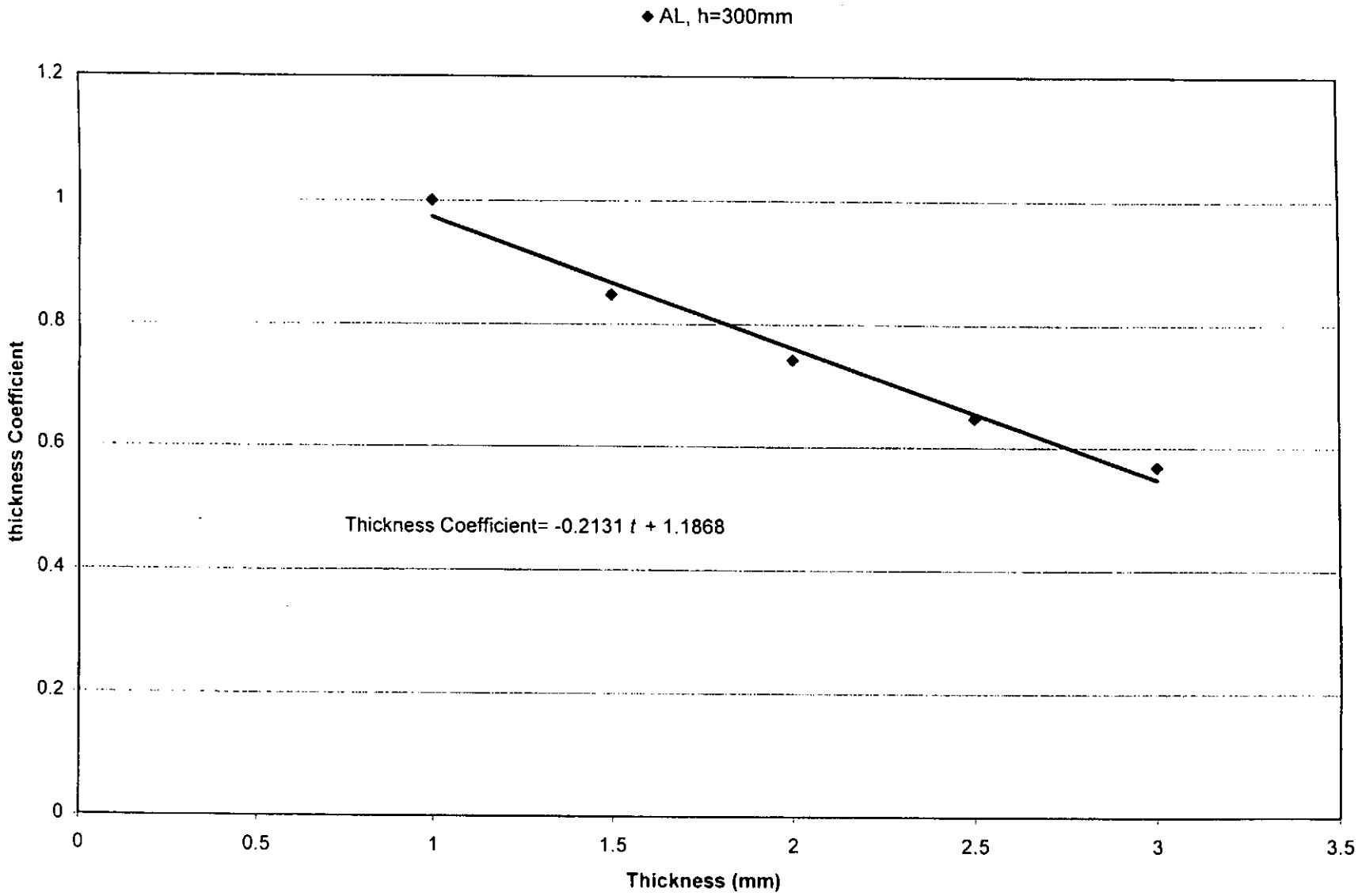
◆ AL, h=300mm
1.2
1
0.8
0.6
0.4
0.2
0
thickness Coefficient
Thickness Coefficient= -0.2131 t + 1.1868
0
0.5
1
1.5
2
2.5
3
3.5
Thickness (mm)

Appendix 2

Simplification of the shielding equation

Simplification of the shielding formulas (4.7) and (4.8)

$$SE = \frac{1}{\cosh(kt) + \frac{1}{2}(K + \frac{1}{K})\sinh(kt)}$$

$$k = \frac{1+j}{\delta}, K = \frac{kr_s}{\mu_r}, \delta = \sqrt{\frac{2}{\omega\mu_0\mu_r\sigma}}$$

For conductive material, $K>>1$, $kt << 1$

$$SE = \frac{1}{1 + \frac{1}{2}(K)(kt)}$$

$$SE = \frac{1}{1 + \frac{1}{2}\frac{r_s(1+j)}{\mu_r\delta}\cdot\frac{t(1+j)}{\delta}}$$

$$SE = \frac{1}{1 + \frac{1}{2}j\omega\mu\sigma t r_s}$$

For permeability material, $K<<1$, $kt \approx 1$

$$SE = \frac{1}{1 + \frac{1}{2K}(kt)}$$

$$SE = \frac{1}{1 + \frac{\mu_r\delta}{2r_s(1+j)}\cdot\frac{t(1+j)}{\delta}}$$

$$SE_{square} = \frac{1}{1 + \frac{\mu_r t}{2r_s}}$$

Appendix 3

Publications

PUBLICATIONS

S. Kong, Y. Du, J. Burnett " Experiment on Finite Width Planar sheets for ELF magnetic Field" *Proc. of IEEE International Symposium on EMC*, May 17-21,1999 Tokyo, Japan, pp 524-527

S. Kong, Y. Du, J. Burnett "Magnetic Shielding Properties of Finite Width Planar Sheets at Extremely Low Frequency", *Proc. of International Conference on Electrical Engineering*, August 16-18 1999 Hong Kong, Vol.1,pp61-64

Y. Du, K. Kong, J. Burnett " Experimental Measurement of ELF Magnetic Fields From Cable Trunking", *Proc. of IEEE International Symposium on EMC*, August 2-6,1999 Seattle, Washington,Vol.1,pp 47-50

Y. Du, K. Kong, J. Burnett " Magnetic Shielding by Ferromagnetic Trunking in Low Voltage Installations", accepted by *HKIE Transaction* for publish